

Elastomeric Bearing Pad
Performance Under
High Stress

A Thesis
in
The Department
of
Engineering

Presented in Partial Fulfillment of the Requirements
for the degree of Master of Engineering at
Concordia University,
Montréal, Québec, Canada

July 1983

© Milind Pimprikar, 1983.

ABSTRACT

ELASTOMERIC BEARING PAD PERFORMANCE
UNDER HIGH STRESS

MILIND S. PIMPRIKAR

The use of elastomeric bearing pads has become common for supporting various structures throughout the world. The survey of literature and existing data revealed that many conflicts exist among various codes and specifications. The difficulty of anomaly of allowable compressive stress limits is critical for designers of these bearing pads.

Principle functions, advantages, and applications of neoprene for supporting or isolation of vibrations in various structures are described. Physical design properties of neoprene pads affecting their behavior in compressions are discussed. The comparative parameters and major differences among design practices followed in different countries and guidelines specified by various codes and standards are discussed with a need for extensive research.

In some instances arises the necessity to strengthen existing structures or applying heavier loads than those adopted in original designs based on allowable stress limits. A research contributing to this area was undertaken at the structures laboratory of Concordia University.

The research includes tests on neoprene pads of 60 Hardness under

compressive stresses up to 20,000 psi., considering different influencing factors such as shape, rate of loading, etc. Also included are tests to study creep behavior under long term compressive stresses of 500 psi. to 3000 psi. Test results are compared with the available values and analysed with respect to the research problem. Results of an experimental study on the effectiveness and behavior of neoprene under higher compressive stresses and for damping and isolation of vibrations are studied in particular. An attempt is made to define failure criterias and ultimate strength of neoprene pads with few recommendations and further need for research.

In memory of my late Grandmother

Smt. Laxmibai and late Uncle

Dadamama.

ACKNOWLEDGEMENTS

I would like to take this opportunity to express my thanks to everybody who encouraged and assisted me in this advanced research study.

First and foremost my very special thanks to Professor Z.A. Zielinski and Professor M.S. Treitsky for providing important guidance, sharing ideas and encouragement throughout this study program. Their keen interest in my work and knowledge in the subject field has directed me from selection of this research topic to its final completion.

Professors of the Engineering Faculty who have provided the elusive quality inspiration and contributed through lecture series as well as other help at many occasions, Mr. Danny Roy, Louis Stankevicius of Structure Laboratory and secretaries of the department through their full cooperation and assistance, have an equal share in the completion of this project.

At this time, I cannot forget the long and hot discussions I frequently had with friends and colleagues from the engineering faculty and outside University. We had a lot to share and learn.

Special thanks to my mother, Mrs. Vina Pimprikar, and family, who not only encouraged me for indepth study of this program, but permitted me to indulge my passion for the long task. Without her support and

patience it was impossible to provide today's shape to this project.

She deserves a major share in this credit.

Although it would be impossible to acknowledge everyone who assisted in this project, and professors and staff of Applied Mechanics Department at Ecole Polytechnic Montréal, and Chemistry Department of McGill University Montreal for their cooperation and assistance in conducting experimental work is deeply acknowledged. Also, I would like to express my gratitude to Professor Newland; Cambridge University, London, Dr. Liquorish; Director of Tico Manufacturers, London; Dr. Müller; Müller-BBM, GMBH, Munich, Mr. Lalancette of ABBDL consulting engineers, Montréal; the publishers of ACI, U.S.A.; Canadian Architect Canada; Maclarin and Sons, London; National Research Council, U.S.A.; Applied Science Publishers, London, for their generous contribution of illustrations and information.

Last, but not least, the financial support provided by the National Sciences and Engineering Research Council of Canada, under Grant No. A1017, by le Gouvernement du Québec, Ministère d'Education, le Programme de Formation de Chercheurs et d'Action Concertée, under Grant No. EQ-1645, and the Scholarship Institutions from India is gratefully acknowledged.

INDEX

	<u>Content</u>	<u>Page No.</u>
(i)	Title Page	(i)
(ii)	Signature Page	(ii)
(iii)	Abstract	(iii)
(iv)	Dedication	(iv)
(v)	Acknowledgements	(v)
(vi)	Table of Contents	(vii)
(vii)	List of Figures	(xii)
(viii)	List of Tables	(xviii)
(ix)	Notations	(xix)
1.	Chapter 1 - Introduction	1
	1.1 Historical Development	2
	1.2 Advantages	2
	1.3 Research Approach	5
	1.3.1 Current Problems	5
	1.3.2 Summary of Previous Research	7
	1.3.3 Research Objectives	10
	1.3.4 Thesis Organization	10
2.	Chapter 2 - Physical Properties, Principal Functions and Applications of Elastomers	13
	2.1 Introduction	14
	2.2 Types of Elastomeric Bearings	14
	2.2.1 Steel Laminated Elastomeric Bearings	15
	2.3 Physical Properties of Elastomers	15
	2.3.1 Hardness	19
	2.3.2 Shape Factor	19

2.3.3	Effective Elastomeric Thickness	21
2.3.4	Requirements According to ASSHTO and German Specifications	23 23
2.4	Principal Functions of Elastomers	
2.5	Applications	26
2.5.1	Buildings	26
2.5.2	Bridges	34
3.	Chapter 3 - Design Practices, Problems and Need for Research	
3.1	Basic Design Requirements	40
3.1.1	Top, Bottom Covers	40
3.1.2	Side Covers	41
3.2	Major Differences and Need for Research	
(a)	Permissible Stress	41
(b)	Type of Elastomeric Bearings	41
(c)	Hardness	45
(d)	Strain Limits	45
(e)	Load-Deflection Behavior	45
(f)	Standard Tests	45
(g)	Rotation	46
(h)	Bearing Dimensions	46
3.7	Problems Encountered in Practice and Initiation of Experimental Study	46 46
	Maximum Permissible Compressive Stresses	47
	Maximum Permissible Shear Stresses	48
	Maximum Permissible Strain Limits	49
	Bearing Dimensions	51

4.	Chapter 4 - Short Term Compression Behavior	55
	4.1 Introduction	56
	4.2 Design Factors Affecting (Influencing) Behavior of Elastomers	57
	4.2.1 Basic Parameters	57
	4.2.2 Effect of Surface Conditions	57
	4.2.3 Relation of the Two Surfaces	58
	4.2.4 Other Factors	62
	4.3 Compression Testing Program	62
	4.3.1 Experimental Program	64
	4.3.2 Testing Arrangement	63
	4.3.3 Testing Procedure	65
	4.3.4 Observations and Analysis	70
5.	Chapter 5 - Creep Behavior Under Compression	84
	5.1 Introduction	85
	5.2 Importance of Tests	85
	5.3 Influencing Factors	85
	5.4 Research Objectives	86
	5.5 Test Program	86
	5.5.1 Testing Arrangement	91
	5.5.2 Testing Procedure	95
	5.5.3 Observations	96
	5.5.4 Comparative Study of Available Creep Test Data	104
6.	Chapter 6 - Vibration Damping and Isolation Properties	105
	6.1 Summary of Previous Research	106
	6.2 Applications	107

	6.3	Vibration Damping	110
	6.3.1	Material Properties for Damping	110
	6.3.2	Damping Capacity of Neoprene	114
	6.3.3	Experimental Results	121
	6.4	Vibration Isolation	122
7.		Chapter 7 - Behavior Under Excessive Compression	124
	7.1	Excessive Compressive Stresses	125
	7.2	Ultimate Strength	125
	7.3	Failure Criteria and Causes	126
	7.4	Predicted Life of Elastomeric Bearings	131
8.		Chapter 8 - General Conclusions and Recommendations	132
	8.1	Conclusions	133
	8.2	Recommendations	134
9.		References	135
		Appendix I - Neoprene Bearings at the Base of the Tower	
		Structure, Olympic Stadium, Montreal	146
	I.1	Description of Structure	147
	.2	Function of Neoprene	150
	.3	Properties of Neoprene and Details	151
	.4	Problems Encountered	152
	.5	Research Requirements	154
	.6	Recommendations	155
	.7	References	157
		Appendix II - Load-Deflection Relation and Critical Load	159
		Appendix III - Measurement of Compressive Creep of Neoprene	
	III.1	Application of Compressive Loading	

(a) Typical Stepped Loading	160
(b) Typical Stepped Loading with Less Time	161
(c) Sudden Loading	162
.2 Typical Compressive Creep Measurement for First 5 Minutes and one Hour	163
.3 Typical Strain Gauge Measurements From Data Acquisition System	165
.4 Typical Compressive Creep Record For First 5 Days for a Test to Verify Existing du-Pont Curve (Including Assumed Initial Deflection)	166

LIST OF FIGURES

- 1.1 Typical steel laminated elastomeric bearing supporting a structure.
- 1.2 Steel laminated elastomeric bearing pads at a Precast-Prestressed T Girder Bridge.
- 1.3 A typical steel laminated bearing pad unit in position.
- 1.4 Various functions of elastomers: (a) absorb vertical forces; (b) horizontal forces; (c) rotational effects.
- 2.1 Bulging and stresses due to vertical load of a single pad.
- 2.2 Different performance of (a) plain and (b) laminated bearing pads.
- 2.3 Effect of laminating steel plates on the compression and shear stiffness of an elastomer.
- 2.4 Splitting of concrete support due to forces produced by excessive bulging of elastomers.
- 2.5 Relationship between shear modulus and hardness, comparative study from literature.
- 2.6 Shape factor of elastomeric pad.
- 2.7 (a) Movement and (b) shear stresses induced due to rotation.
- 2.8 Dubai International Trade Center Tower, floor slab simply supported on elastomeric seatings.
- 2.9 Cross-section of Albany Court, London. 1300 tons of load on 13 mountings of sizes varying 600x500x300 mm.
- 2.10 At Ebury Street, London. (1977), 96 luxury flats structure (24,000 tons) supported on 1400 elastomeric bearings.

- 2.11 103 mm. thick laminated elastomeric bearing in position during construction of luxury flats.
- 2.12 For isolating building from vibrations, flats built on the box within a box principle (a and b). Details of location of pads and their arrangement.
- 2.13 Laminated pads in position to receive structural loads.
- 2.14 Planned structure of the Olympic Stadium and tower in Montreal.
- 2.15 Photograph showing tower structure at present condition (1983). Both front and rear legs are seen.
- 2.16 The tower structure, Fig. 2.14, is supported above the swimming hall.
- 2.17 Junction between Stadium and Tower. Front legs supported on neoprene bearings.
- 2.18 Champlain Bridge during construction. Installation of neoprene pad is underway.
- 2.19 3 km. long Champlain Bridge in Montreal supported on more than 1000 neoprene pads.
- 2.20 Neoprene pads are located between 7 girders which straddle the 50 m. wide bridge and the concrete pillars. Each pad is under a stress of 1350 psi.
- 2.21 Bearings for the Tancarville Bridge across the River Seine, France.
- 3.1 Use of an outer neoprene cover around an elastomeric bearing to reduce the effect of excessive bulging and for uniform compressive stress.

- 3.2 Plan of support bearings at the base of tower structure of Olympic Stadium, Montreal.
- 3.3 Section AA of Fig. 3.2, details of bearing pads and outer cover.
- 4.1 Comparison of compression stress-deflection behavior of neoprene, 60H pads under surface conditions: steel-and-steel, concrete and steel, concrete-and-concrete.
- 4.2 Sandblasting of steel plates, in contact with elastomers, with different adherence characteristics (a) good, (b) poor.
- 4.3 Elastomeric bearings inclined at 2° and loaded at maximum compressive force, induce edge stresses up to 300% of assumed design values.
- 4.4 View of Amsler testing system for compression tests.
- 4.5 Test view of 120,000 lb. loading, Tinus-Olsen compression testing system.
- 4.6 Test specimens for compression tests (a) steel plates larger than sample; (b) steel plates and sample of same size; (c) variation of shape factor.
- 4.7 Sample after unloading under low stress.
- 4.8 Compression of specimen under Amsler testing system at 5000 psi.
- 4.9 Bulging behavior of neoprene under Tinus-Olsen 120,000 lb. loading. Steel plates and neoprene pad of same size.
- 4.10 Force deflection curve for neoprene under compression. For neoprene (65.5mm x 63.5mm x 20mm) and steel plates (101.6mm x 101.6mm x 20mm).

- 4.11 Force-deflection curve for neoprene under compression. For neoprene and steel plates same size (63.5mm x 63.5mm x 20mm).
- 4.12 Force-deflection curve for neoprene under higher compression with reduced shape factor (0.32). For neoprene (25.4mm x 25.4mm x 20mm) and steel plates (63.5mm x 63.5mm x 20mm).
- 4.13 Compressive stress-strain curves for neoprene 60H, S.F. = 0.8, based on load deflection figures 4.10, 4.11.
- 4.14 Compressive stress-strain curves for neoprene 60H, (S.F. = 0.32) and comparison with other two (S.F. = 0.8).
- 4.15 Compressive stress-strain curve for neoprene 60H, (S.F. = 0.8), by du-Pont.
- 4.16 Comparative study of compressive stress-squeeze curves from experimental study and those available from literature.
Neoprene 60H, S.F. = 0.32 to 1.4
- 4.17 Comparison of compressive stress-squeeze behavior of neoprene H60, S.F. = 4 and 200.
- 4.18 Force deflection curve for neoprene under compression. (Test at Tinus-Olsen). (Neoprene pad size 63.5mm x 63.5mm x 20mm and steel plates 101.6mm x 101.6mm x 20mm).
- 4.19 Compressive stress-squeeze curves for neoprene based on Fig. 4.18.
- 4.20 Force-deflection curve for neoprene at Tinus-Olsen machine. For neoprene (63.5mm x 63.5mm x 20mm and steel plates 101.6mm x 101.6mm x 20mm).
- 4.21 Compressive stress-squeeze curve for neoprene under Tinus-Olsen. Neoprene and steel plates of same size (63.5mm x 63.5mm x 20mm).

- 5.1 Schematic of set-up for creep tests on neoprene.
- 5.2 View of testing scheme for creep tests on neoprene.
- 5.3 Deflection measuring arrangements at location 'C' of the loading beam.
- 5.4 (a) Deflection and (b) load, measuring arrangements at location 'B' of the loading beam.
- 5.5 Typical illustration of initial creep under sustained 500 psi. compressive loading.
- 5.6 Short term creep of neoprene 70H within 5 minutes at 2000 psi. (4).
- 5.7 Compressive creep of neoprene under 500 psi. sustained loading.
- 5.8 Compressive creep of neoprene under 500 psi. sustained loading, comparison with du-Pont results.
- 5.9 Variation of total deflection for solid and bonded pads under sustained compressive stress of 500 psi. (77).
- 5.10 Compressive creep of neoprene under varying sustained stresses (800 psi. to 3000 psi.).
- 6.1 Elastomers used for isolation of vibrations at S-Bahn system in Munich.
- 6.2 Installation of multi-layered elastomeric pads before bringing in the ballast.
- 6.3 Schematic representation of the internal damping of rubber. The ellipse surface indicates energy loss.
- 6.4 Energy storage in elastomeric isolator which embodies neoprene in compression (From Fig. 4.10).
- 6.5 Typical test results for measurement of dynamic modulus of elastomer.

- 6.6 Set-up for measuring damping capacity of neoprene under varying high compressive stresses. (a) View; (b) Schematic.
- 6.7 Free-vibration oscillations for neoprene and steel pads under varying high stresses.
- 6.8 Unidirectional transmissibility of a mounting as a function of frequency ratio corresponding to an experimentally found loss factor = 0.095.
- 7.1 Permanent distortion of neoprene pad tested at compressive stress of 18,000 psi. (Principal tear at an angle of 45°.)
- 7.2 Splitting along lateral surfaces due to higher repeated loading.
- 7.3 Bulging along line EF under compression. Tension along points E and F (free sides of pad).
- 7.4 Typical splitting failure due to repeated loading. (From literature).
- A1 Model of Olympic Complex.
- A2 Tower model made of coins.
- A3 The Olympic Stadium and Tower Structure on April 30, 1976.
- A4 Plan and cross-sectional view of Tower with loadings and reactions shown.

LIST OF TABLES

- 2.1 Physical properties of neoprene, 60 hardness used in test program. Requirements according to U.S. and German specifications.
- 3.1 Maximum permissible compressive stress limits by various codes and specifications.
- 3.2 Permissible shear stress according to codes and specifications.
- 3.3 Maximum permissible compressive strain, shear strain and rotation values specified by various codes, specifications and agencies.
- 3.4 Restrictions and limitations concerning bearing dimensions specified by codes, specifications and authorities.
- 4.1 Test program for behavior of neoprene under high compressive stresses.
- 4.2 Experimental program considering various influencing test factors.
- 5.1 Test program for creep test on neoprene pads under different sustained loadings.
- 5.5.4 Comparative study of available test data on neoprene 60H under sustained 500 psi. loading.
- 6.1 Measurement of loss factor for neoprene H60 samples.
- 7.4 Predicted life of elastomeric bearings.
- A1 Total loading at tower base at various construction stages.

NOTATIONS

A	-----	Laminating Steel Plate Area.
A_1	-----	Area of maximum distortion (effective length x effective width at maximum distortion).
b	-----	Width dimension of the pad.
δ_c	-----	Total vertical deflection of the pad.
δ_{long}	-----	Total vertical deflection of the pad under the action of slow load.
δ_{short}	-----	Total vertical deflection of the pad under the action of quick load.
δ_s	-----	Deformation due to shear.
ϵ_b	-----	Maximum shear strain at the edges of the bonds due to compression strain.
ϵ_c	-----	Average Compressive Strain (δ_c/t).
$\epsilon_{max.}$	-----	Maximum shear strain at bond.
$\epsilon_{min.}$	-----	Minimum shear strain at bond.
ϵ_s	-----	Average shear strain.
ϵ_{α}	-----	Maximum shear strain at bond due to angular rotation.
E	-----	Young's modulus for elastomers (in tension).
E_c	-----	Young's modulus for elastomer layer in compression.
F	-----	Safe design factor at the bearing contact surface.
F_{sl}	-----	Safe design factor at the bearing contact surface under the action of slow load.
f_c	-----	Mean compressive stress.
f_{csl}	-----	Mean compressive stress under the action of slow load.
G	-----	Shear modulus of the elastomer.

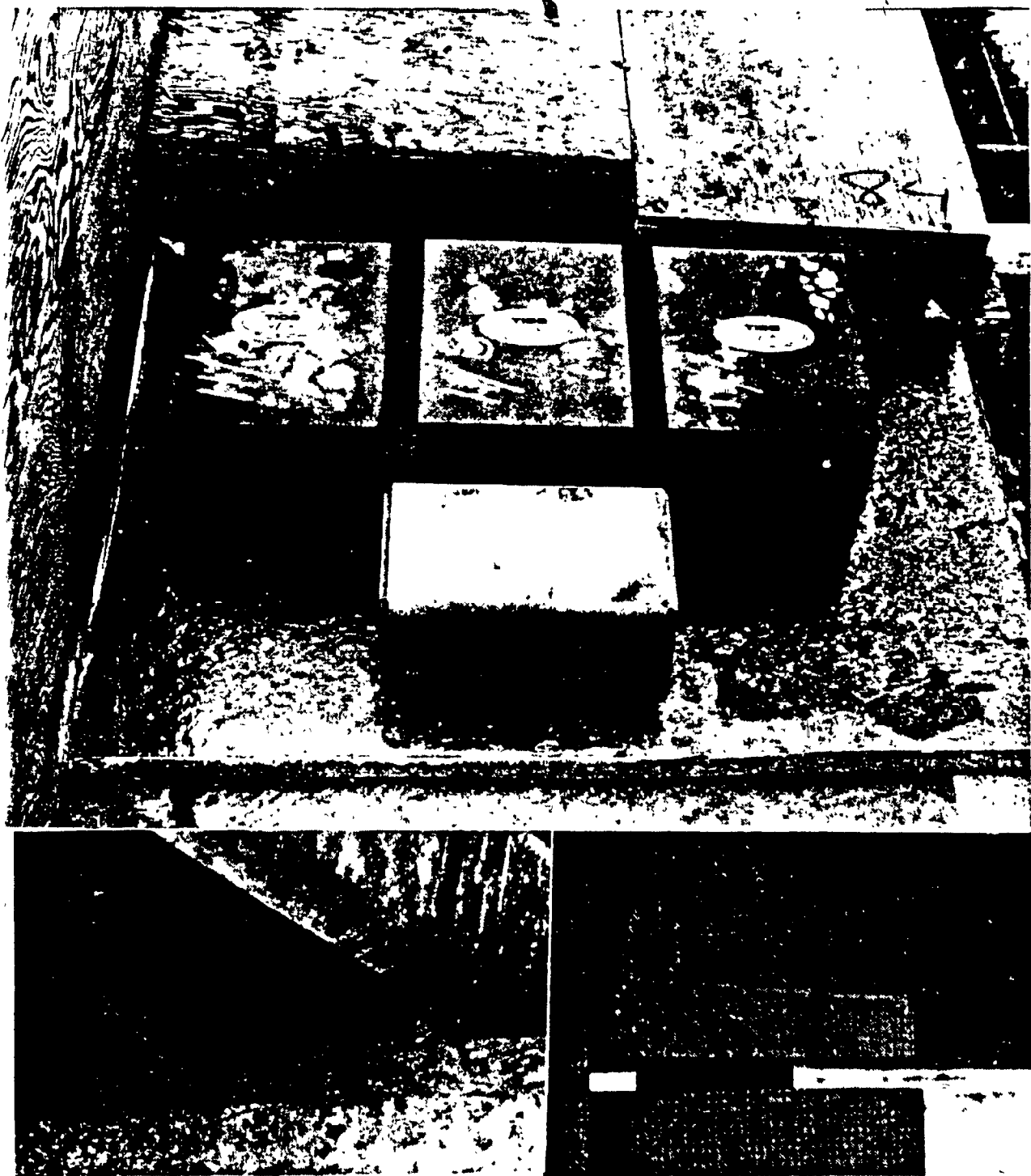
G_D	-----	Dynamic shear modulus.
l	-----	Length dimension of the pad.
α	-----	Rotation in radians at the support section of the structure.
α	-----	Rotation in radians under the effect of slow loads.
α	-----	Rotation in radians under the effect of quick loads.
τ	-----	Shear stress.
τ_H	-----	Mean shear stress due to horizontal forces.
τ_V	-----	Mean shear stress due to vertical force V .
τ_α	-----	Maximum shear stress due to rotation.
G_{ys}	-----	Nominal yield stress of steel.
t	-----	Thickness of one layer of elastomer.
T	-----	Total thickness of elastomer in the bearing.
t_1, t_2	-----	Thicknesses of elastomers for two layers.
t_p	-----	Thickness of steel plate.
G_s	-----	Permissible tensile stress in the steel plates of a laminated bearing.
S	-----	Shape factor = $l.b/2t(l+b)$!
V	-----	Vertical load.
V_{long}	-----	Vertical load acting for long duration (dead load and loads due to shrinkage).
V_{short}	-----	Vertical load acting for short duration (live loads, vehicle, vibrations etc.
C	-----	Compression factor.
S_i	-----	Shape factor of thickest internal layer.
ϵ_{ut}	-----	Ultimate tensile strain.
ϵ_{sc}	-----	Shear strain at edge of bonded surface due to loads normal to bearing surfaces.

ϵ_{sh}

----- Shear strain at edge of bonded surface due to horizontal forces.



C
H
A
P
T
E
R
1



INTRODUCTION

1.1. Historical Development

Natural rubber compression pads (1)* have demonstrated exceptional performance since 1889 (2) as bridge bearing to allow rotation, expansion, or contraction between piers and superstructure without damage to either.

Elastomeric Bearings, Fig. 1.1, (3) have been successfully developed in France since World War II (4) and the Freysinett Company, pioneers in prestressed concrete, did a lot of the original research on the subject. In North America (5), elastomeric pads were first introduced in the late 1950's as a satisfactory bearing device that could accommodate the relatively severe end rotation and translation associated with the prestressed concrete (6) structures, Fig. 1.2, 1.3. Since then elastomeric (neoprene) bearings have given over 25 years of service in field applications (7).

1.2. Advantages

The elastomeric bearings are widely used for both concrete and steel structures (8-17) as bridge bearings (18-28), as antivibration pads for buildings (31-38), for high tower structures (39-42), for railway tracks (43-48) and for earthquake protections (49-50).

* Numbers in parentheses indicate reference numbers.



Fig. 1.1 Typical steel laminated elastomeric bearing supporting a structure.



Fig. 1.2 Steel laminated elastomeric bearing pad at a precast-prestressed T Girder bridge.
(Courtesy of N.R.C. Washington, D.C.)



Fig. 1.3. A typical steel laminated Bearing Pad unit, in position.

The main advantage of these bearings lies in the economy resulting from low materials cost, ease of fabrication and installation, and maintenance free effective operation (51).

Durability is good, there are no exposed metal surfaces to corrode and has proven safe behaviors in fire (52).

Under a compressive load the elastomeric pad absorbs surface irregularities and distributes all forces uniformly (15).

Properly designed and installed (53), elastomeric bearings can supply the required vertical restraint, accommodate horizontal deformation and provide for rotational, transverse and longitudinal movements (Fig. 1.4). For these reasons, these so called, neoprene bearing pads, are being utilized in a growing variety of applications calling for larger sizes, increased shape factors and higher load bearing capacity.

1.3 Research Approach

1.3.1 Current Problems

The survey of literature and available test data revealed that many conflicts exist among current specifications and codes of practices, from different countries, dealing with criteria for design of elastomers in compression and its behavior under short-term and long-term compression creep. Also compression and creep behavior of elastomers under stresses higher than those presently specified by codes and practices is not studied well.

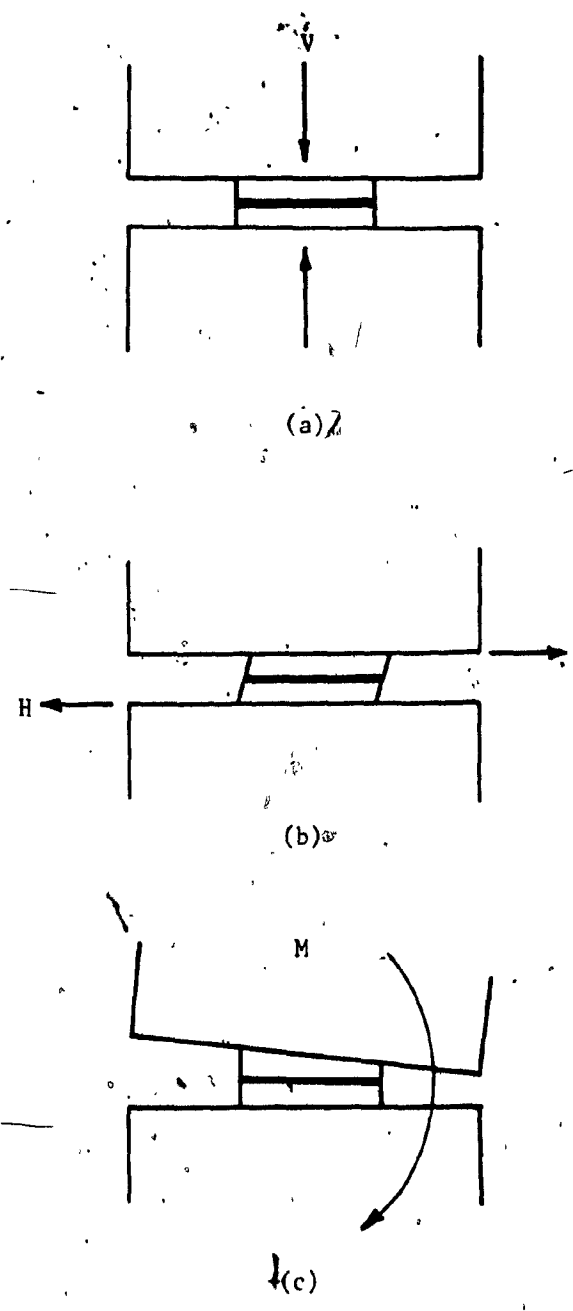


Fig. 1.4 VARIOUS FUNCTIONS OF ELASTOMERS
ABSORB (a) VERTICAL FORCES (b) HORIZONTAL FORCES
(c) ROTATIONAL EFFECTS

In many instances arises the necessity to strengthen existing structures or applying heavier loads than those adopted in original designs based on allowable stress limits (54). Few of such cases are discussed in following chapters.

The problem of overloading of neoprene bearing pads has been encountered at the base of the tower structure of the Olympic Stadium in Montréal. A research contributing to this problem was undertaken at the Structures Laboratory of Concordia University and was partially reported in (54).

1.3.2 Summary of Previous Research

Much of the early works which were concerned with evaluations of physical properties of elastomers and development of design criteria were carried out by Hull (33), Gent (55, 24, 56, 32), Lindley (1, 56, 57, 2), Davey and Payne (17), Grote (52), Eggert (58), Pare and Keiner (4), NCHRP (59), Spitz (8), etc. and few rubber producing companies (60, 61, 29, 7). Based on research, experience and existing codes of practices researchers Beyr et al (22), Topaloff (23), Torr (21), Lee (16), Long (62), Brandt (27), Derek (28), NCHRP (18), Lee (63) and others investigated various aspects of design and use of elastomers as bridge bearings.

Following the experimental developments and widespread use of elastomers, codes of practices and specifications dealing with

materials; design practices, permissible stress-strains, and standards testing procedures were introduced in France (64), U.K. (65, 66, 67, 11), U.S.A. (68, 69, 10) Australia (70), Switzerland (71), Germany (72, 73, 74) and recently in India (75). Design guidelines based on laboratory and field performance of these pads have been prepared by NCHRP (18), Nordlin et al. (6), Eggart (58) and Bell (12). Lucas (76) tested steel laminated elastomeric bearings at temperatures down to -60°F whereas Hirshfield et al. (30) and Aldridge et al. (77), investigated behavior under different bearing contact surfaces including concrete and steel.

Research {(Rivlin 1949, (81), Gent 1956 (55), Treloar (1958 (78), Lindley 1967, 1975 (1, 69)) relating to the basic design formulae and analytical relationship for the complicated compressive stress-strain behavior of elastomers have been under continuous development and there is a wealth of literature in this field extending to high-strain analysis using, finite elements and digital computers. The lack of a commonly accepted basic analytical method for describing the behavior of these materials has resulted in divergent opinions regarding the design criteria that should be applied.

Although elastomers have been effectively used for supporting various prestressed concrete structures (25, 26), the lack of proper

design and performance criteria for these materials has been ranked as 4th most important research need for today's Prestressed Concrete Industry (80).

In summary, the work cited has been concerned with standard load-deformation responses (81, 82) of selected elastomers of varying shape factors, thicknesses and hardness, under influential factors such as temperature, humidity, etc. Considering these parameters, the empirical developments have led to differences among various design limits and criteria.

Purkiss (83) has offered some new design parameters as an improvement in ASTM standards (10), and need and possibility for increasing present stress limits. Whereas Bartendev (84) and Price (85) have made an attempt to study failure performance and behavior of elastomers under abnormal forces, respectively, Bell (12) has recently reported test results for ultimate compressive strength of neoprene bearing pads.

Thus, research is necessary to study the behavior of elastomers under excessive short-term and long-term compression and hence structures resting on these overloaded bearing pads.

1.3.3 Research Objectives

The objective of the research was to study the effectiveness and behavior of neoprene bearing pads under higher compressive stresses and under failures.

Implicit in this objective is the experimental evaluation of compressive behavior of neoprene under high-stresses considering various factors, so that the designer will have both qualitative and quantitative basis to judge the performance of neoprene with respect to overloading of the structure.

Specific objectives in the current research plan include a survey of the literature, study of current design practices and available test data, and (testing) the compressive stress-strain behavior and compressive creep. Also included were the performance evaluation of neoprene under varying stresses as vibration isolator in construction engineering. Several other objectives covered were physical properties and functions of neoprene for various applications followed by its performance in service, failure criteria and some installation and replacement provisions for elastomeric bearings.

1.3.4. Thesis Organization

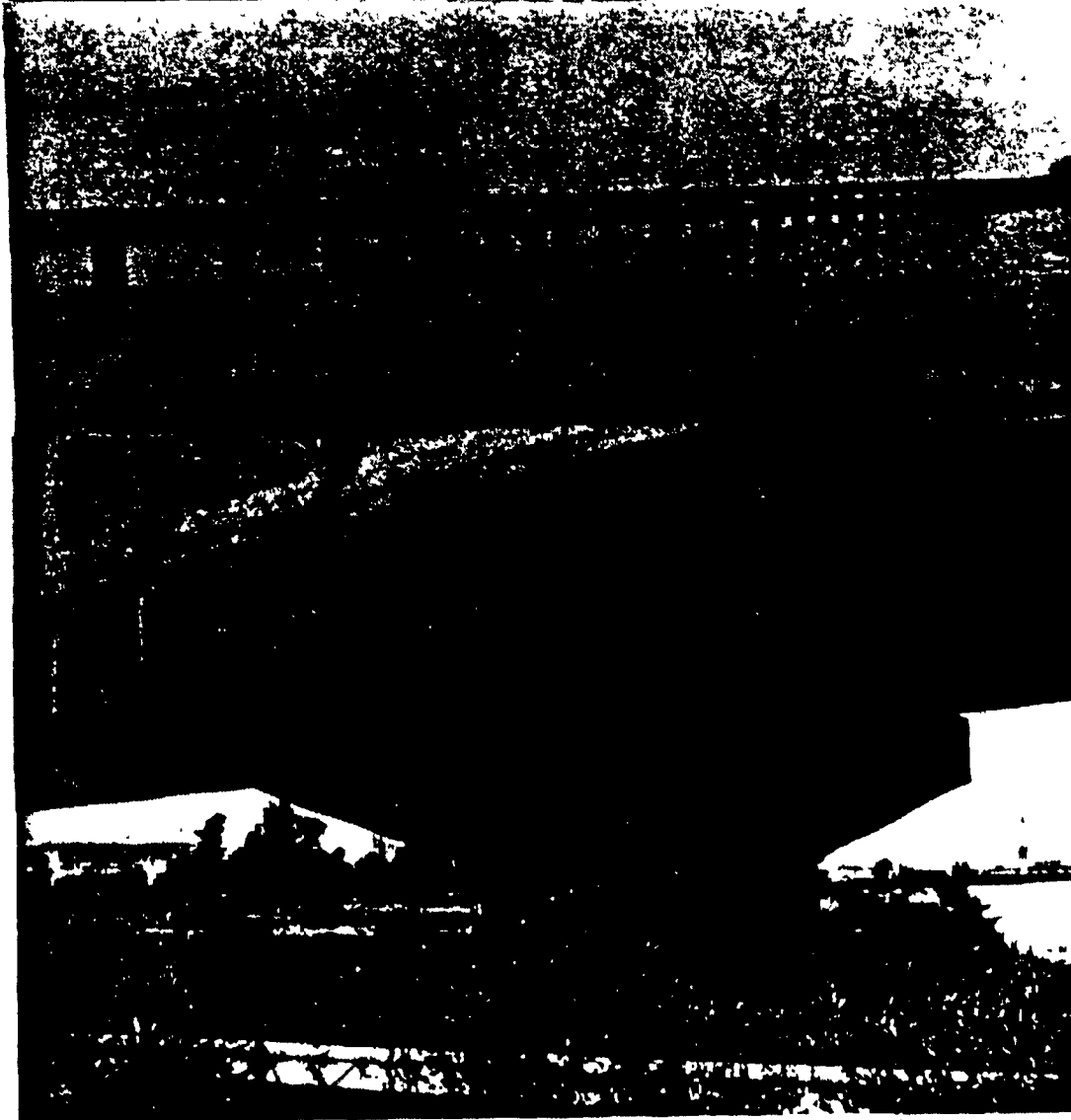
The various objectives investigated in this research plan are discussed earlier and they were reported in earlier publication: (54, 86, 87) elsewhere.

- Different types of elastomeric bearings available today, their basic physical properties and various functions and applicability are discussed in Chapter 2. Examples of structures where neoprene has been used for supporting high stresses are also described.
- In Chapter 3, a comparative study of various Codes Standards and Specifications available throughout the world is prepared in tabular form, pinpointing the anomalies and conflicts among them. Problems encountered in practice are discussed and thus experimental research need is defined.
- Chapter 4 is devoted to study the performance of H60 neoprene pads under instantaneous high compressive stresses (up to 20,000 psi.) considering various influencing factors such as Shape Factor, time and rate of loading, etc. Experimental results are compared with available test data and analysed for higher stress conditions.
- Creep behavior of neoprene under varying high compressive stresses is studied in Chapter 5. Importance of creep behavior and different factors influencing it are described. Experimental results are presented in a comparative form on a logarithmic graph and also, available test data on creep values is given in tabular form.
- A brief description of principles and applications of neoprene for damping and isolation of vibrations, along with results of an experimental study on its effectiveness under higher compressive stresses, for damping and isolation of vibrations are described in Chapter 6.
- Chapter 7 is aimed to describe behavior of neoprene bearing pad under excessive compressive stresses. Based on experimental results and available research data, ultimate strength and potential causes of failure of elastomeric pads are discussed with comments on expected life of

elastomers.

- Lastly, in Chapter 8, on the basis of experimental study and review of available literature, conclusions are drawn on the performance of neoprene under higher compressive stresses. Also, considering the divergence and differences among various design practices and their users, as well as the complex behavior of elastomers in compression, few recommendations are provided for the designer of these pads under the circumstances described.

The test program was limited in scope, mainly to study the behavior of neoprene pads under excessive stresses due to overloading of structures. Variables such as large shape factors, thickness, hardness, etc. have not been included in these studies. Furthermore tests were run at room temperature and thus influence of temperature variation, humidity and presence of deteriorious substances in contact with the neoprene were not studied. Although there may be some question regarding the confidence and validity that may be placed in the experimental findings, due to a limited amount of testing on laboratory scale samples, these findings will prove an up-to-date understanding of neoprene bearing performance under excessive stresses such as encountered at the Olympic Tower structure at Montréal.



C

H

A

P

T

E

R



2

CHAPTER 2

DESIGN PROPERTIES, PRINCIPAL FUNCTIONS AND APPLICATIONS OF ELASTOMERS

2.1 Introduction

Considering the versatility of elastomers, various types of elastomeric bearings are developed. Knowledge of these developments and their requirements is an essential requirement for the designer. Also the designer of elastomeric bearings for buildings and bridges has to know the physical properties of these materials such as shape factor, hardness, effective thickness, etc. Whereas the precise functions of elastomeric pads vary among different structures and depend upon the application, their principal functions with recent applications are to be defined before undertaking the design.

2.2 Types of Elastomeric Bearings

The growing usages of elastomers for the wide range of applications made possible the continuous and rapid development of various types of elastomeric bearing pads. Today there exist five major classes of elastomeric bearings reported being used (88) to satisfy the various requirements of carrying large loads and providing greater movements in long span bridges and heavy structures. Of the five types of elastomeric bearings, namely, plain (unreinforced); steel laminated; fabric laminated; sliding type and pot bearings, steel laminated elastomeric bearings are more commonly used and will be discussed further in this research program.

Steel Laminated Elastomeric Bearings

Under a compressive load the plain (unreinforced) elastomeric pad bulges out along the force-free surfaces, Fig. 2.1 (a). This bulging, relative to the rate of loading, results in shear stresses and strain (1), Fig. 2.1 (b,c). The excessive bulging restricts the use of elastomer for limited load carrying capacity and limited horizontal deformation with smaller thickness of the bearing. Thus in practice, the use of plain elastomeric pads is usually limited to short span, fixed end and free end applications.

Steel laminated elastomeric bearings, pioneered in France (17), are most widely used for supporting large buildings, towers; and long span bridge superstructures. They consist of thin layers of neoprene bonded or placed between steel plates, Fig. 2.2 (b). These laminations provide: (i) an increase in load bearing capacity associated with a possible reduction in area (ii) reduction in vertical deformation Fig. 2.3 and, thus reduction in shape factor (described below) and (iii) reduction in splitting forces exerted on structural elements in contact with the bearing, Fig. 2.4. The provisions and requirements of these laminations have been described by various specifications and are discussed in detail in (11, 12, 18, 52).

2.3. Physical (Design) Properties of Elastomers

Various parameters, affecting the characteristics of neoprene pads itself, need to be considered while designing a neoprene bearing pad

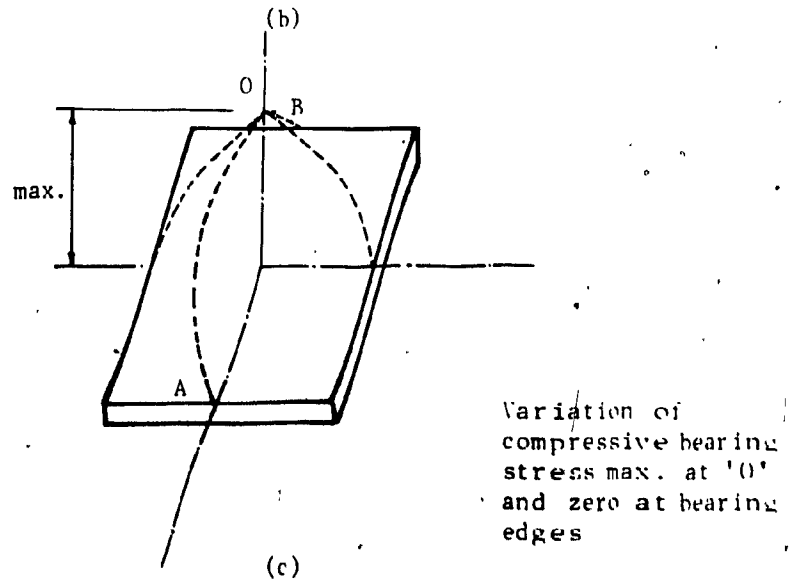
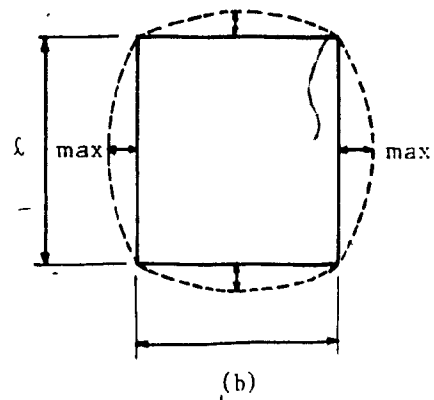
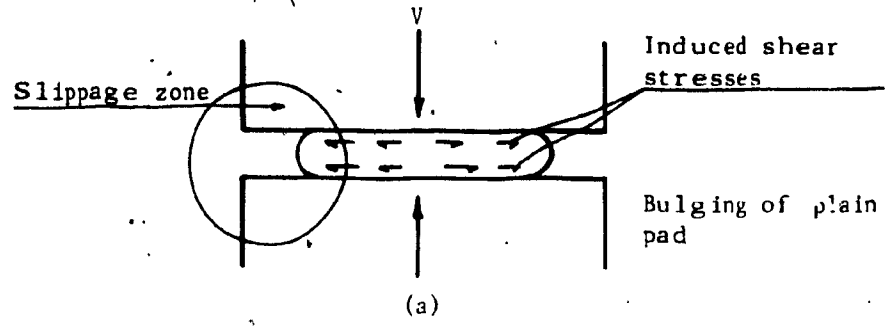
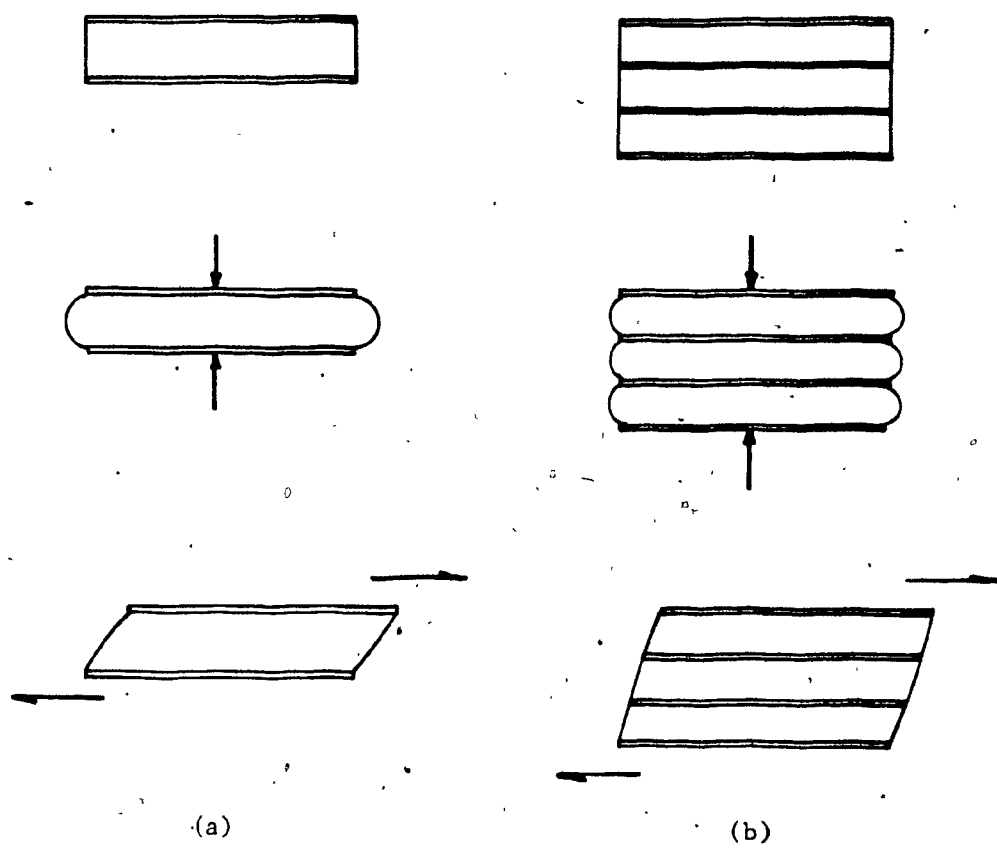


Fig. 2.1 BULGING AND STRESSES DUE TO VERTICAL LOAD OF SINGLE PAD



7 Fig. 2.2 DIFFERENT PERFORMANCE OF (a) PLAIN AND (b) LAMINATED BEARING

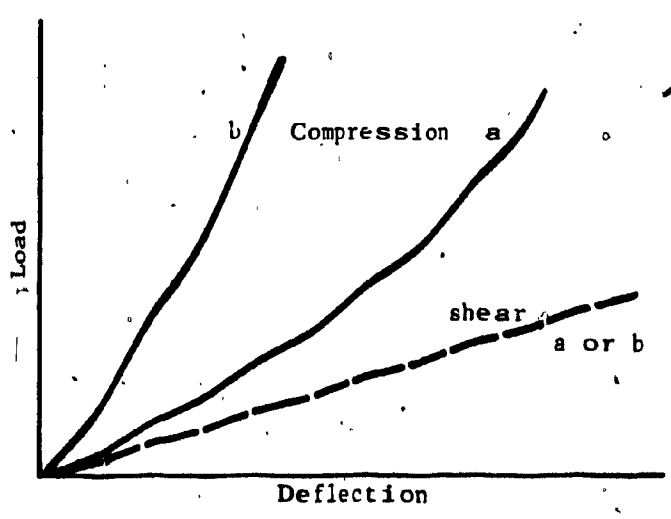


Fig. 2.3 EFFECT OF LAMINATING STEEL PLATES ON THE COMPRESSION AND SHEAR STIFFNESS OF AN ELASTOMER

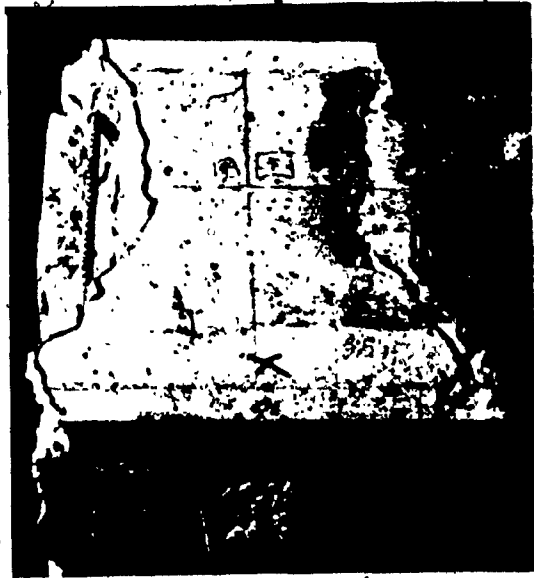


Fig. 2.4 Concrete support split due to forces produced by excessive bulging of elastomers. (Courtesy of ACI (70)).

for a particular application. The stress-strain relationship and stiffness of these bearings both in compression and shear is very much dependent on these main parameters such as shape factor, hardness, thickness and other factors including compounding (manufacture) of elastomers, chemical composition, etc.

2.3.1. Hardness

Elastomers are normally deigned in terms of durometer readings - soft to hard - on a scale of 0 to 100 (4), which is essentially a measurement of reversible elastic penetration produced by a specially-shaped indenter under a specified load (1). Although hardness is a relative [not strictly accurate (8, 89)] measure of the stiffness of the elastomeric bearing both in compression and shear, various publications have reported different values of modulus for same hardness, Fig. 2.5. The property preferred by the designers is stiffness rather than hardness. Neoprene pads, studied in this research program, were of 60 hardness, same as those used for the Olympic Stadium tower in Montréal.

2.3.2. Shape Factor

When elastomers are compressed, due to its high incompressibility, they lose little or no volume, Thus under vertical loading, if the contact surface restrains movement, the area at which bulging can occur is the force-free areas. Shape factor (1, 2, 4, 12, 18, 53) is defined as the ratio of the surface area or plan area of one

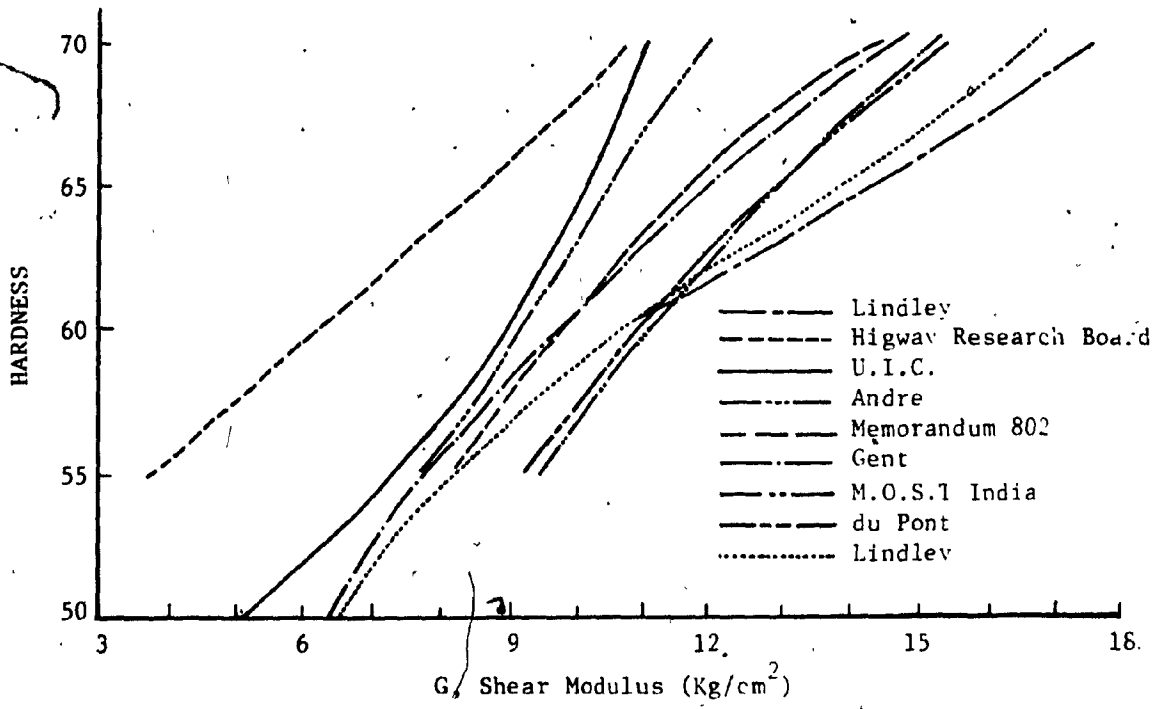


Fig. 2.5 RELATIONSHIP BETWEEN SHEAR MODULUS AND HARDNESS

loaded face to the area free to bulge around the perimeter of the pad, Fig. 2.6. For a rectangular block of length ℓ , width b & thickness h ,

$$\text{Shape factor (S.F.) } S = \frac{\ell b}{2h(\ell + b)}$$

The influence of S.F. on compressive stress-strain is well documented (7, 12, 60, 61) in literature with curves relating stress-strain and S.F. (86). As S.F. increases the amount of deflection in the bearing decreases.

In case of steel laminated elastomeric bearings, (lamination increases S.F.) steel shims are usually surrounded by neoprene along edges as well between laminations for protection against corrosion due to environment. Thus S.F. is based on shim size rather than finished size.

2.3.3. Effective Elastomeric Thickness

The horizontal movement permitted by the bearing depends on the total thickness (T) of elastomer in the bearing (defined as effective elastomeric thickness).

For a shear stress $V_h = G \times \frac{\delta_s}{T}$ (psi), G is shear modulus, δ_s horizontal movements, T - Total thickness of elastomers.

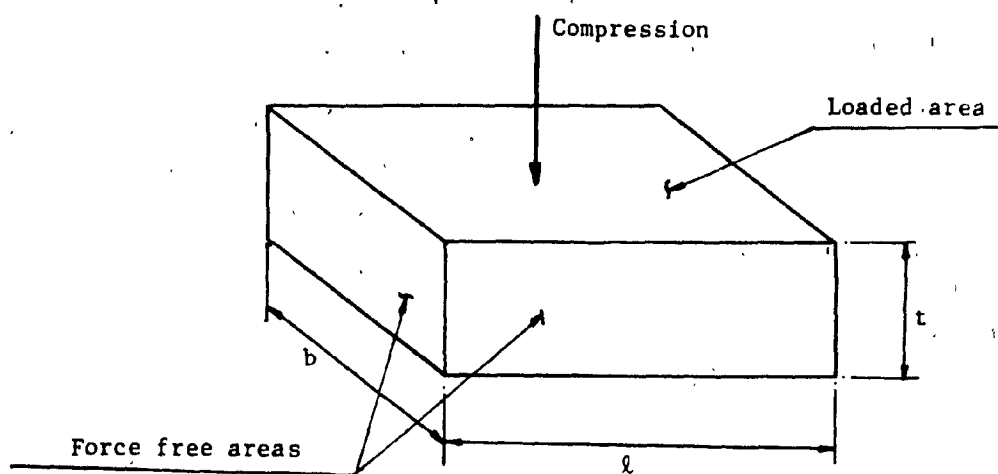


Fig. 2.6

$$\text{SHAPE FACTOR} = \frac{\text{loaded area}}{\text{force-free areas}}$$

2.3.4. Physical properties of neoprene, 60 Hardness, used in test program. Requirements according to U.S.* (68, 69) and German* (73) specifications, (Table 2.1).

* (Since the experimental study was undertaken with respect to the overstressed neoprene bearings at the Olympic Stadium Tower, Montréal, where neoprene bearings were provided by German designers.)

2.4. Principal Functions of Elastomers

Although the precise function of elastomeric bearing pads may vary among various structures, their principal functions are: (i) smooth and uniform transfer of load i.e. Static load distribution (ii) absorption of damageable forces, bending moments, impact and vibration; permitting relative movement of its supporting parts (iii) absorption of movement owing to expansion and contraction occasioned by changing temperatures. The movement can be in the form of translation, rotation or compression, (Fig. 2.1, 2.7).

In prestressed concrete structures, particularly, elastomers should be able to permit both the initial prestressing movements and long term movements. Also, heavy loads can cause high bearing stresses and relatively large rotations at the bearings.

TABLE 2.1

Physical property	Test Designation		AASHTO	Requirements		Mean Average
	ASTM	DIN		German approval 1980 Specified		
Durometer Hardness	D 2240	53 505	60 ± 5	60 ± 5	61	
Tensile Strength minimum psi (N/mm ²)	D 412	53 504 RI	2 500 (17 000)	17 000	19 200	
Ultimate Elongation minimum %		53 504 RI	350	450	483	
Compression set	D 395 method B	53 517				
22 hrs/158°F (70°C)			25	15	11	
22 hrs/212°F (100°C)			35	-	-	
28d/72°F (22°C)				-	14	
Tear Test (minimum)	D 624-Die (C)	53 515	250 psi	20 N/mm	20 N.MM	

Thus, the basic and important requirements for elastomers is that they must be able to accommodate dimensional changes in the superstructure or relative parts of the structure, such as those due to temperature; prestress; creep and shrinkage, without undue strain i.e. without overstraining the bearings or overloading the support or bridge deck. At the same time it must be able to carry the forces due to erection, gravity, braking, centrifugal effects, and wind without undue deflection (11).

Specific functions of elastomers for buildings and bridges are dis-

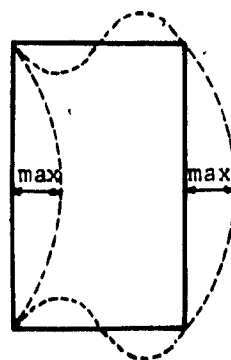
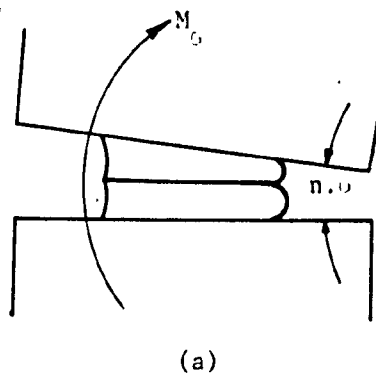


Fig. 2.7

(b)

(a) MOVEMENT AND (b) SHEAR STRESSES INDUCED DUE TO ROTATION

cussed further with few selected applications including those where neoprene bearings are subjected to forces in excess of design limitations.

2.5. Applications

Today the elastomeric bearings are widely used for both concrete and steel structures throughout the world. As mentioned earlier, their versatility and widespread applications have been illustrated as bridge bearings, antivibration mountings for buildings, at marine piers, reservoirs, causeways, elevated walkways and approach ramps, for rail track suspension and earthquake protections; mounting heavy machinery; construction equipment; harbor cranes, etc.

2.5.1. Buildings

In building construction elastomer pads have been used in a variety of ways (12) including: (i) supporting cast-in-place and precast prestressed beams and slabs (ii) at expansion joints (iii) absorbing movements of concrete slabs resting on brickwork or masonry walls (iv) insulation of structure borne and paraseismic vibrations, (v) column to footing isolation (vi) protection of structures against earthquake movements (vii) accoustical insulation between floors and noise control at studios and laboratories, etc.

In all these applications, elastomers have two main functions, i.e. to absorb various movements and to eliminate high stresses at

junctions between adjacent supporting structural members.

Various early examples of building structures supported on elastomers and performance of these pads have been discussed in detail by (40, 90). Few of the recent structures which have made extensive use of elastomeric pads are:

(i) The 34 storey reinforced concrete tower of the Dubai International Trade and Exhibition Center (91) Fig. 2.8, has been designed using the elastomeric seatings to withstand compressive stress of 8.5 MN/m^2 . Also the differential vertical movements of $\pm 40 \text{ mm}$ between the outer and inner columns of the building due to temperature changes is accommodated successfully.

(ii) At the Albany Court flats, 13 rubber mountings of size (600 x 500 x 300 mm) are used below the reinforced concrete foundation beams to carry the total load of 1,300t. (each unit carries around 60 t. to 200 t. of load). The bearings are designed to prevent the transmission of low frequency railway vibrations (46). In between the pads, Fig. 2.9, are reinforced concrete shoulders designed to carry the entire load of the building in the case of failure of elastomeric pads.

(iii) The 24,000 ton luxury flats structure on Ebury Street in London, (41, 42), Fig. 2.10, is supported on 1,400 elastomeric bearings 103 mm thick, Fig. 2.11. The complete building separated from its foundation, Fig. 2.12, by these bearings is designed to prevent the transmission of vibration and noise from the tube train passing beneath. Although the bearings, Fig. 2.13, are de-

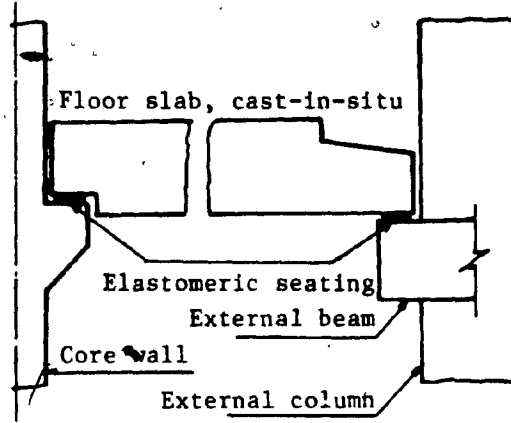


Fig. 2.8

DUBAI TOWER BLOCK FLOOR SLAB,
SIMPLY SUPPORTED ON ELASTOMERIC SEATINGS

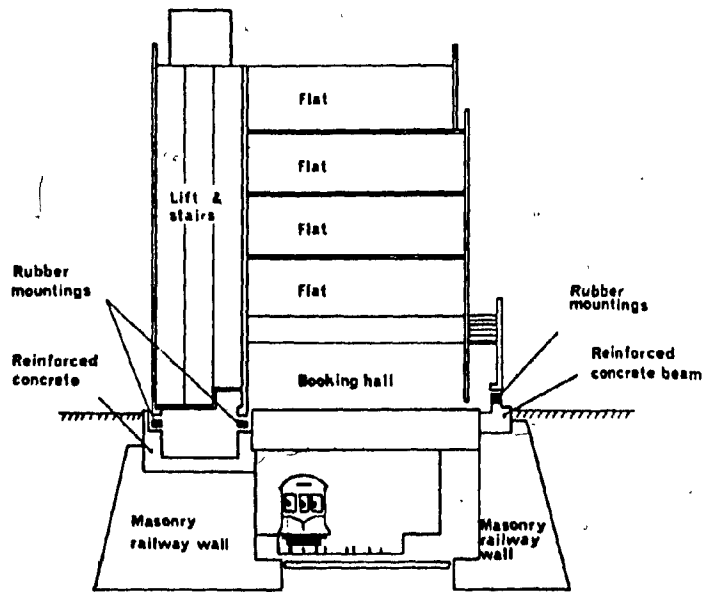


Fig. 2.9 Cross-section of Albany Court, London,
(1300 tons of load on 13 mountings of sizes
varying 600 x 500 x 300 mm.)



Fig. 2.10 At Ebury Street, London (1977). 96 Luxury Flats structure (24,000 tons) supported on 1400 elastomeric bearings (Courtesy of Liquorish A.D., Director Tico Manufacturing Ltd.)

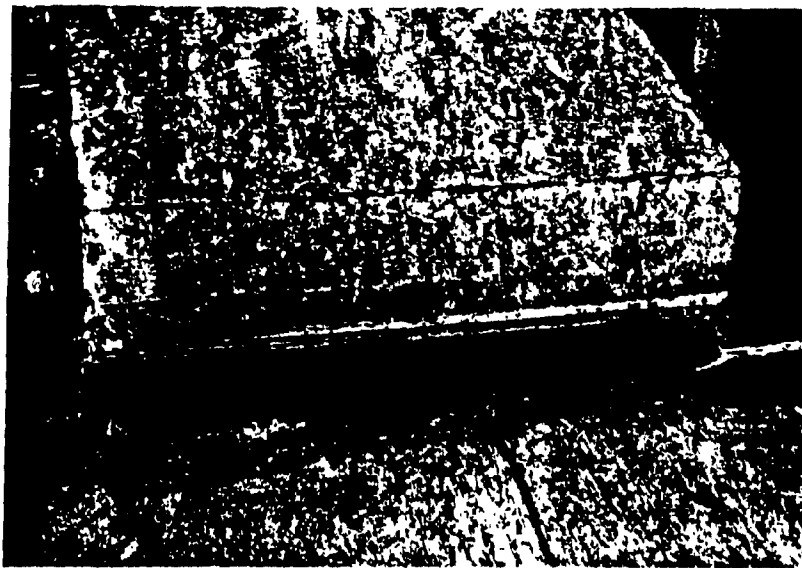
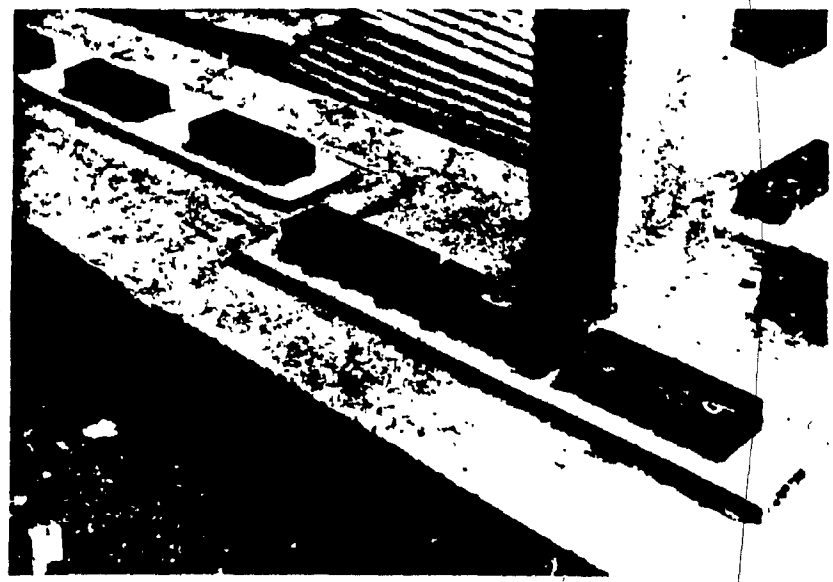


Fig. 2.11 103 mm. thick bearings in position during construction of luxury flats (courtesy of Prof. Newland, Cambridge University, London).



(a)



(b)

Fig. 2.12 For isolating building from vibrations, flats build on the box within a box principle, (a and b). Details of location of pads and their arrangement.

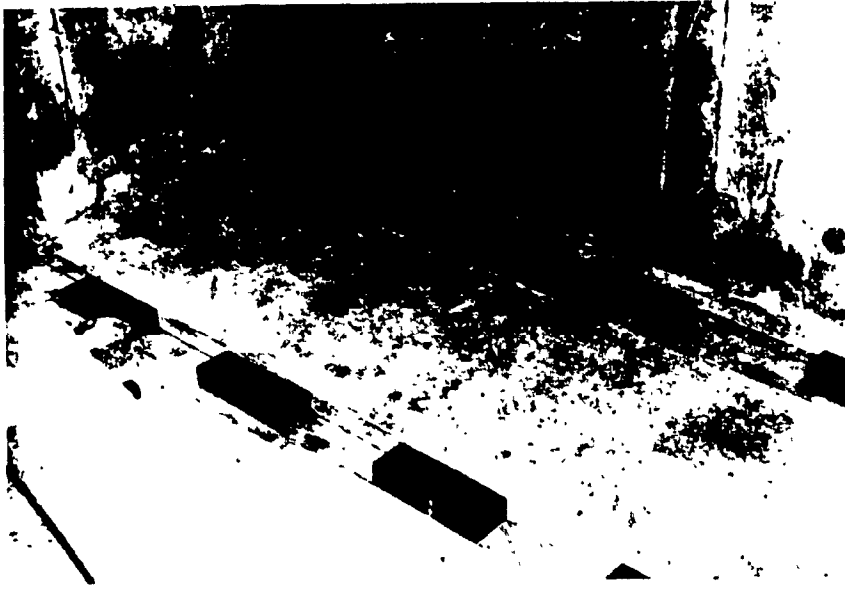


Fig. 2.13 Laminated Pads in position to receive structural loads.
(Ebury Street London).

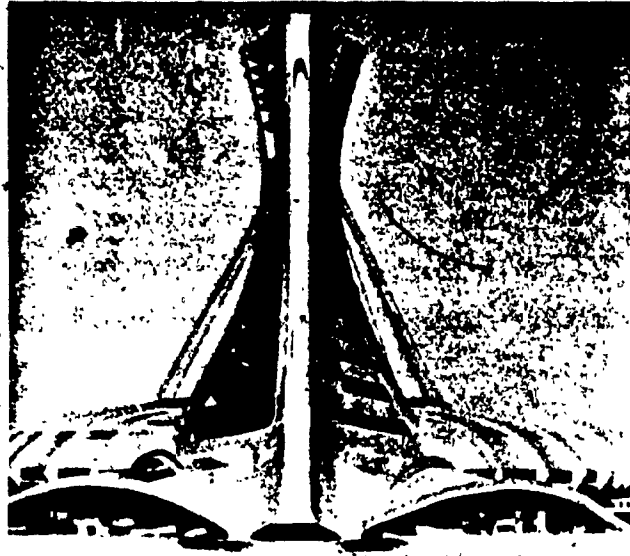


Fig. 2.14 Planned structure of the Olympic Stadium and tower in Montreal. (Courtesy of Southam Communications Ltd.)

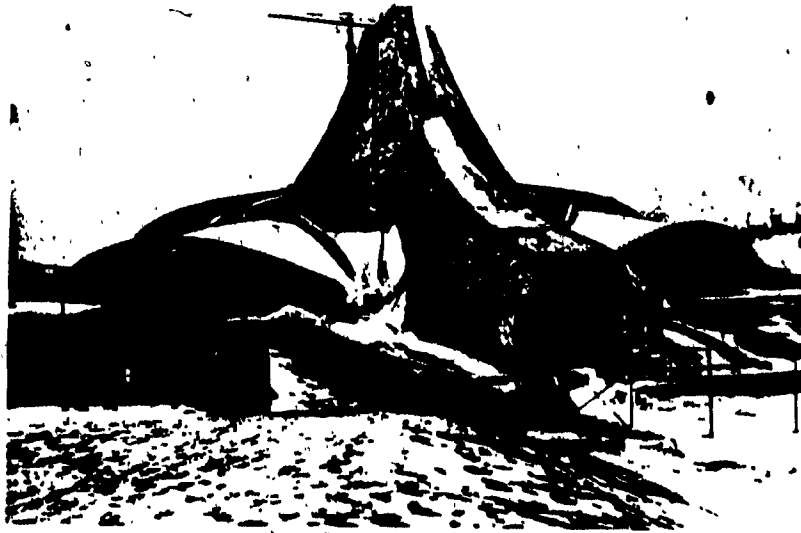


Fig. 2.15 Photograph showing tower structure at present condition (1983)
Both front and rear legs are seen.



Fig. 2.16 The tower structure is supported above the swimming hall.

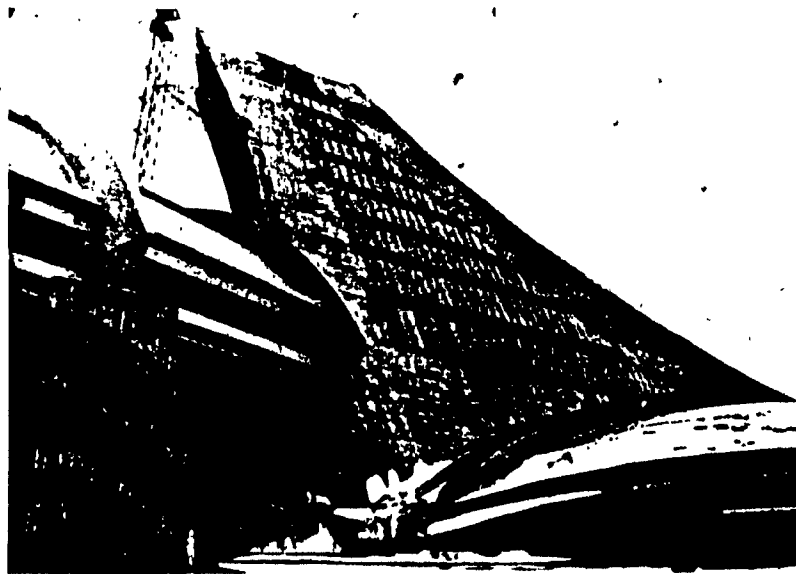


Fig. 2.17 Junction between stadium and tower. Front legs supported on neoprene bearings.

signed for stresses greater than operating conditions, fail-safe devices have been incorporated according to standards (65) with provisions of replacements.

(iv) The 552 foot high prestressed concrete tower structure of the Olympic complex in Montréal, (54), under construction, Fig. 2.14-2.17, is resting on (2 x 36 - 900 x 900 x 185 mm) steel laminated neoprene bearing pads. The bearings, designed to provide horizontal movements of the order of ± 60 mm will be carrying a load of 66,000 tons at (7,000 psi) (AI). Details of these bearings and tower structure are given in Appendix I and Chapter 3.

2.4.2. Bridges

The continuous development (13) and widespread use of elastomers (neoprene) in bridge engineering has been illustrated through numerous publications (7, 12, 21, 4, 26, 2, 17). As bridge bearings, of types mentioned in 2.1, elastomers are designed to maintain a specified vertical load while allowing movements due to thermal expansion and contraction of the span as well as angular rotation at the supports due to bending of the beams under self and traffic load.

Elastomeric bearings placed between the deck and its fixed supports have to satisfy: (i) to support the load (D.L.) of the bridge deck with a minimum deflection under live and traffic loadings given in (15, 62, 28) (ii) to accommodate the slope and change in slope of the deck caused by bending with minimum possible increase

in compressive stress (iii) to accommodate change in length of the deck due to temperature, shrinkage, etc.

A brief description of few of the selected applications include:

(i) Neoprene bearing pads under stress of 1,350 psi (17), are supporting (Fig. 2.18) the 3 km long Champlain bridge (Fig. 2.20) across St-Lawrence River in Montreal.

More than 1,000 pads, each (300 mm wide x 600 mm long x 36 mm thick) consist of 3 layers of neoprene bonded with 1 mm thick galvanized metal sheets. The pads are located between the 7 girders which straddle the 50 m. wide bridge and the concrete pillars, (Fig. 2.20). Each of the pads carrying 171 tons of weight are performing satisfactorily over last two decades.

(ii) A (2,000 mm wide x 3,600 mm long x 95 mm high) steel laminated concave shaped neoprene bearings located at the left bank of the 960 m long Tancarville bridge in France is shown in Fig. 2.21. The bearings supporting loads up to 16,000 tons, provide horizontal displacement of ± 4 cm and rotation of $\pm 4^\circ$.

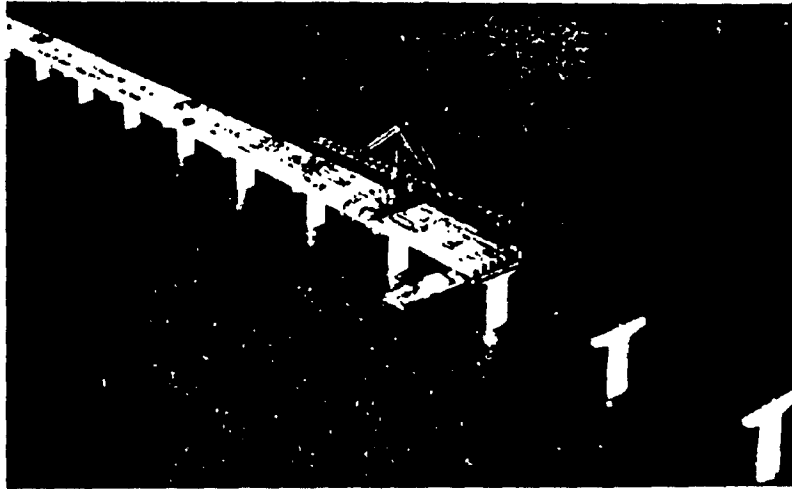


Fig. 2.18 Bridge during construction. Installation of neoprene pads underway. (Courtesy of Prof. Davey and Prof. Payne, Ref. 17).



Fig. 2.20 Neoprene pads are located between 7 Girders which straddle the 50m. wide bridge and the concrete pillars. Each pad is under a stress of 1350 psi.



(a)



(b)

Fig. 2.19 3 km. long Champlain Bridge in Montreal supported on more than 1000 neoprene pads.

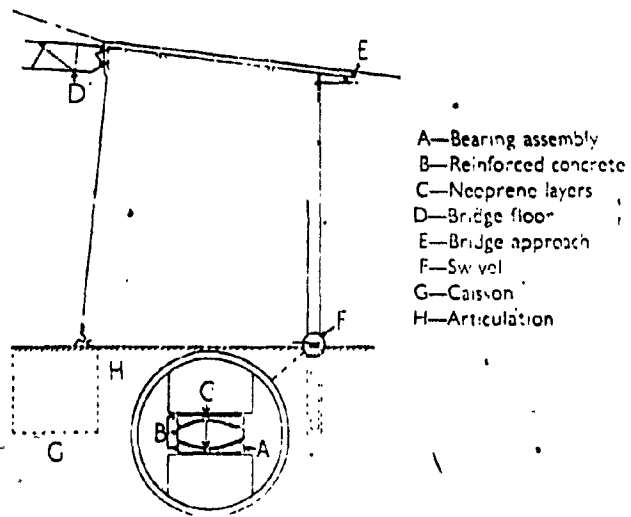
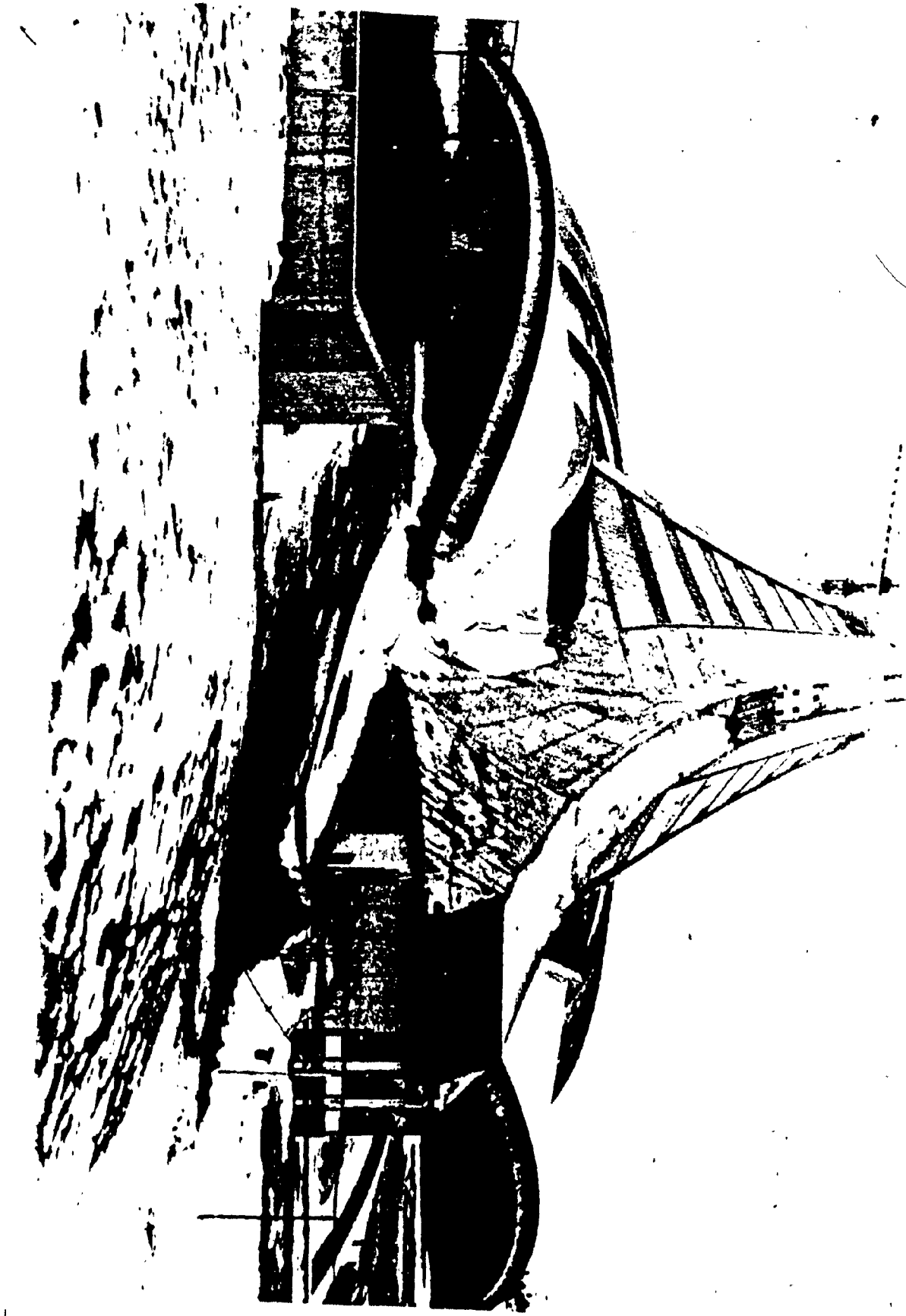


Fig. 2.21 Bearings for the Tancarville Bridge across the River Seine, France.



C
H
A
P
T
E
R
3

CHAPTER 3

DESIGN PRACTICES, PROBLEMS AND NEED FOR RESEARCH

The study of available literature and referred Standards revealed that many conflicts exist among current Specifications and Codes of Practices, dealing with elastomeric properties and criteria for design in different countries. Thus, a thorough analysis of these codes {U.S. (10, 68, 69) B.S. (11, 65, 66, 67), UIC France (64), Germany (72, 73, 74), Australia (70), India (75)} , and research reports {Lindley (1, 2, 56, 57), du Pont 7, 9), Goodyear (60, 61), PCI (3), NCHRP (59)}, is necessary.

The comparative parameters such as maximum permissible compressive and shear stress and strain limits as well as other basic design requirements specified by various Codes and Agencies are presented in Table 3.1, 3.2, 3.3, 3.4. Major differences are discussed at the end of the study with a clear outline of need for research.

3.1 Design Requirements

3.1.1 Top, Bottom Covers: Most of the specifications recommend minimum thickness of about 2mm for top and bottom covers to accommodate irregularities in the contact surfaces.

3.1.2. Side Covers: The side covers protect the steel plates and lamination bonds from environment as well as reduce the surface strain caused by compressive loading. 3 to 6mm thick neoprene or rubber sheets are provided as acceptable side covers. Fig. 3.3, shows the 1/16" thick cover used for bearings used at Olympic Stadium Tower base. Fig. 3.1, shows a bearing under uniform compressive stress illustrating the use of an outer neoprene cover to reduce the bulging effect.

3.2 Major Differences and Need for Research

While studying the available Codes and Specifications dealing with design of elastomeric pads, it has been observed that most of the design practices are based on either stress limitations or strain limitations (no consistency). Few of these major differences are summarized as follows:

(a) Permissible Stress: In North America (7, 68, 69), the elastomeric bearings are designed for 500 psi. (4.45 MPa) and 800 psi, (5.5 MPa) compressive stress which is well below the allowable stress values permitted by other countries and authorities (Table 3.1). Permissible stress limits according to German specifications, are much as 300% higher than those by AASHTO. The advantage of high working stresses result in a considerable reduction of bearing area and proportionally reduced stiffnesses.

(b) Type of Elastomeric Bearings: Whereas few specifications including UIC make distinction between plain and reinforced (laminated pads, AASHTO and others design limitations are based on

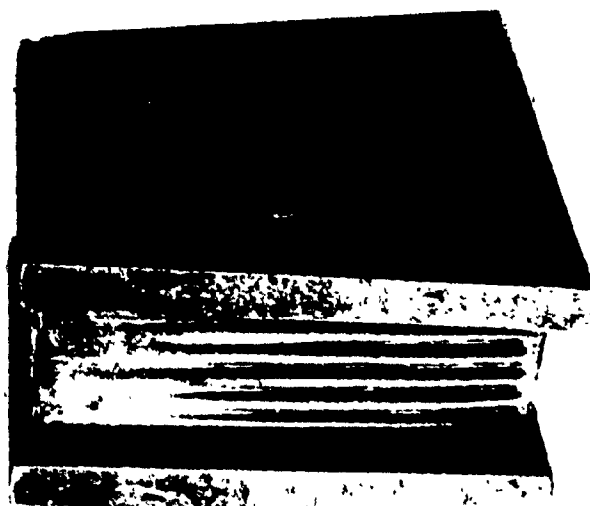
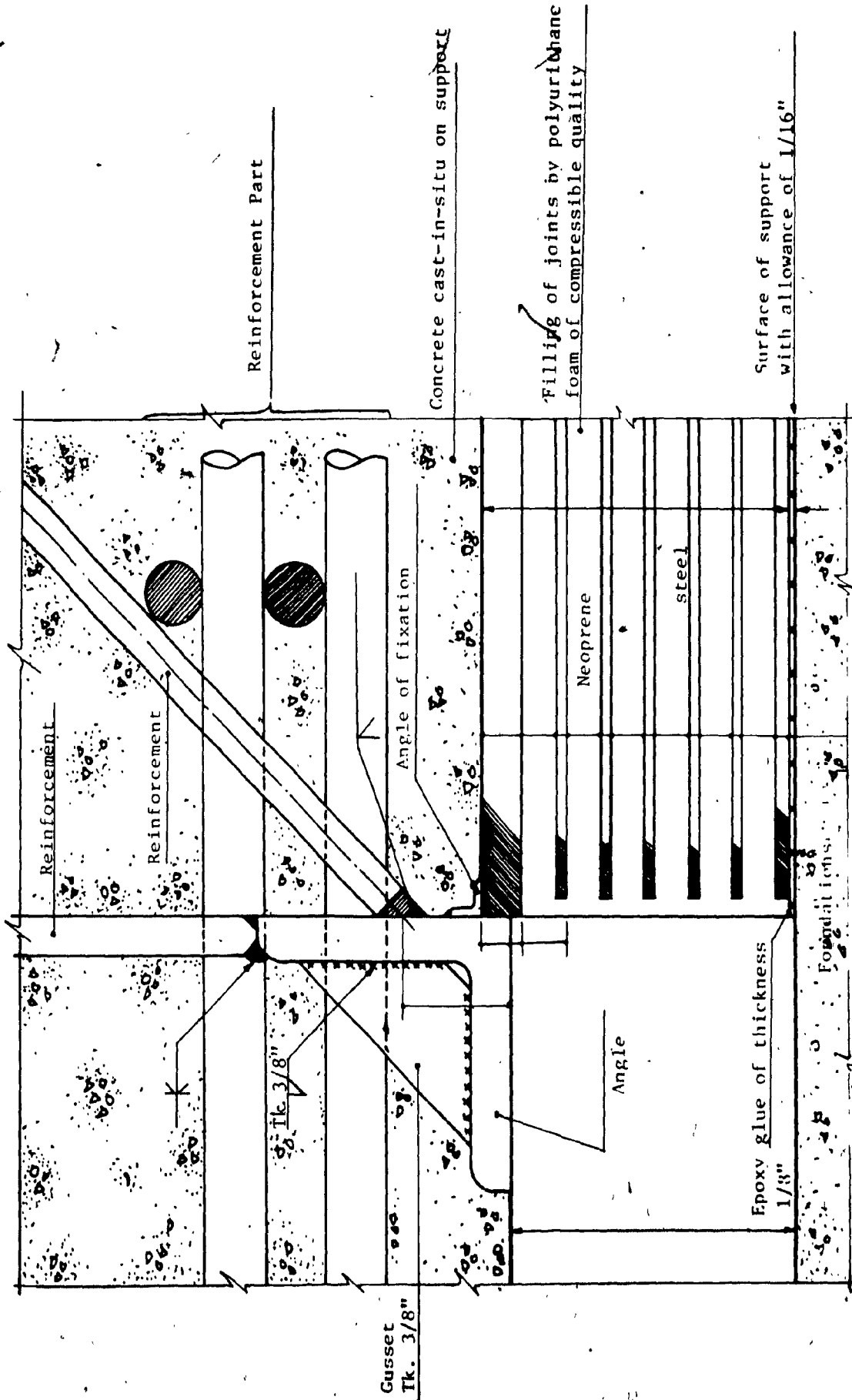


Fig. 3.1 An outer neoprene cover around an elastomeric bearing to reduce the effect of excessive bulging and for uniform compressive stress. Also protection of steel plates from corrosion. (For details see Fig. 3.3, p. 43, Chapter 3, Neoprene bearings details at Olympic tower structure.)



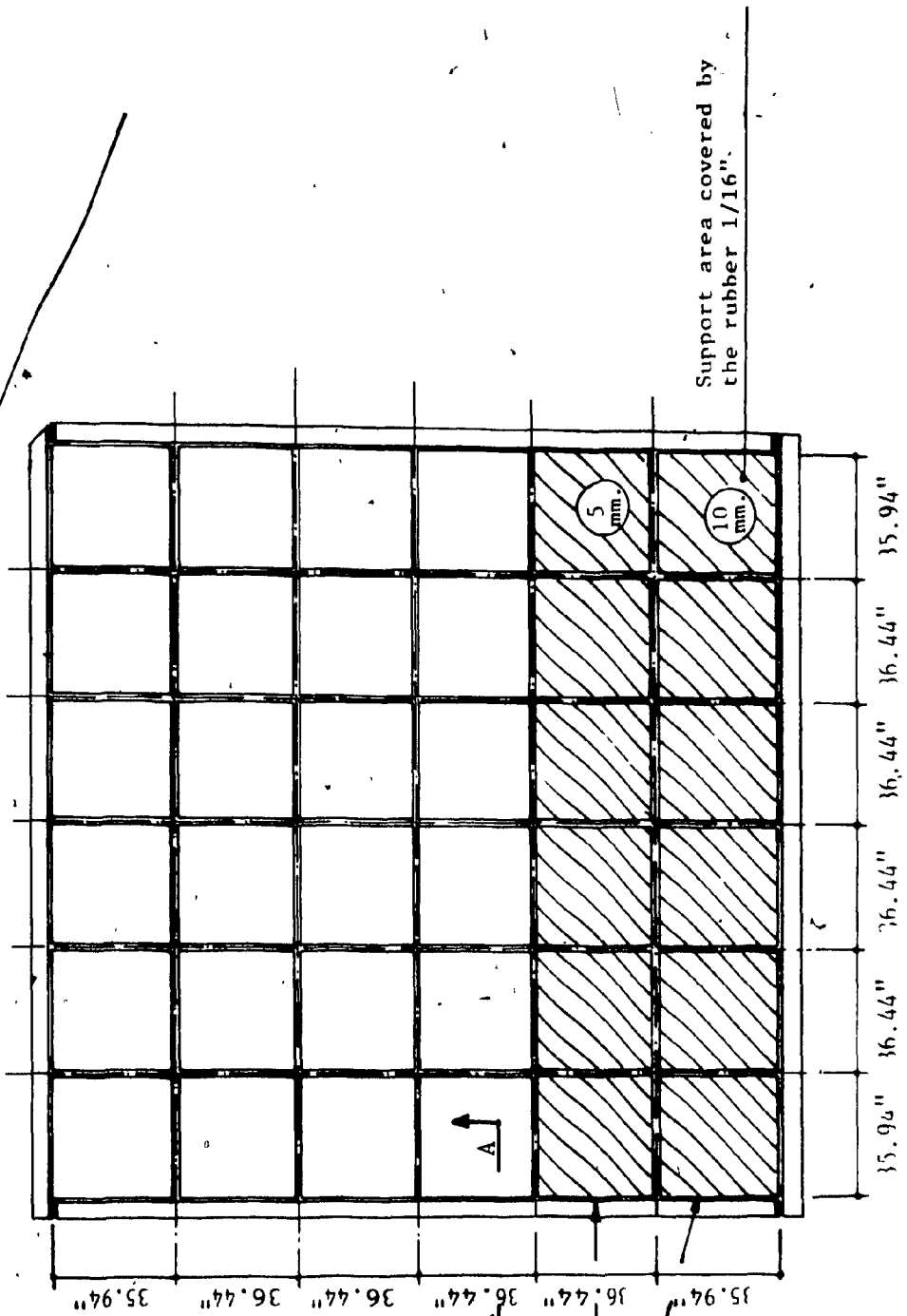
All dimensions in mm.

FIG. 3.3 SECTION AA

P

lateral face of the tower

Front face of the tower



6 Rubber plates thickness 5 mm.

6 Rubber plates thickness 10 mm.

PLAN OF SUPPORT BEARINGS

FIG. 3.2 TOTAL NO. OF BEARINGS AT EACH SUPPORT: 36

plain pads only, irrespective of laminations.

(c) Hardness: According to British Specifications, vertical load carrying capacity decreases with increase in hardness whereas Europeans follow inverse of that: i.e. increase in load carrying capacity with corresponding increase in hardness. The proposed ASTM Standard (1982), is an important contribution concerning this dispute and hardness related properties. In this proposal (10), hardness has been replaced by designation of shear modulus of elastomers.

(d) Strain Limits: There is no consistency of values for both compressive and shear strain limits (Table 3.3).

(e) Load-Deflection Behavior: Whereas the Europeans and others consider nonlinearity of load deflection behavior of elastomer which occurs at higher compressive stresses or strain exceeding 10%, Britain does not take into account the nonlinearity of load deflection behavior considering it as linear only. (The load deflection relationship under higher stress is given in Appendix II).

(f) Standard Tests: Most of the specifications and standards (including recently proposed ASTM) specify series of compression tests for evaluating the performance of elastomeric bearings, but, there is no uniformity in these test procedures. Different rates of loading and varying time for load application make it difficult to compare test results.

(g) Rotation: Elastomeric bearings undergo rotation due to - either construction tolerances, tilt between faces of bearings etc. or vertical gradients and deflections of the supported span under live load in case of bridges. In the European specifications these rotational effects are taken into consideration whereas in Britain rotation is not taken into account. According to ASTM (83), rotational effects on bearings are not yet clearly understood.

(h) Bearing Dimensions: Specification (75) imposes a restriction on size of bearings because of limitations on thickness based on plane dimension. The easy solution is adopted by German standards, standard sizes and thicknesses for elastometer pads provided in tabulated form for all users. Also, the formula for computing thickness of steel plates, provided by British and European Specifications (64, 67) is considered as wrong by Spitz (8) with large variations. Again, in this respect, the Approval Rules by German standards can be considered as most convenient and well suited, satisfying the need of the designer.

In summary, a concentrated effort is needed to resolve the conflicts and divergence of limitations among various codes and specifications and thus pinpoint the various problems the designer is faced with.

3.7. Problems Encountered in Practice and Initiation of Experimental Study

Recent trends to increase the design compressive stress as demonstrated in table 3.1, and few examples illustrated in Chapter 1,

TABLE 3.1 MAXIMUM PERMISSIBLE COMPRESSIVE STRESS

1. AASHTO 1.12.2	5.5 MPa (800 psi), dead load and live load) minimum psi: 200 psi (1.4 MPa) 3.4 MPa (500 psi), dead load only)
2. Dutch & French	15 MPa (2200 psi)
3. Australia	15 MPa [used up to 23 MPa (3370 psi)]
4. German	Less permissible stresses for small bearings compared to large ones 10.00 MPa (1465 psi) for areas $A < 200 \times 250 \text{ mm}$ 12.50 MPa (1840 psi) for $200 \times 250 \text{ mm} < A < 250 \times 400 \text{ mm}$ 15.00 MPa (2200 psi) for $A > 300 \times 400 \text{ mm}$
5. Bejcha (PCI)	7 MPa (1025 psi)
6. UIC	Max. compressible stress allowing for horizontal movement for plain elastomer pads = 2GS for laminated elastomer bearings = $\frac{2IGS}{3I}$, f_{caf} (1.4b2) MPa to prevent slip due to bulging for laminated but unbonded $f_{caL} > 2MPa$
7. NEPRA	Max. comp. stress - 1.15 MPa (S = Shape factor)
8. MOT 802	-- (strain limits) $E_c = E(1 + 2CS^2)$
9. BE 1/76	-- (strain limits) but considers bearing surface in contact conditions*
10. Long	Load - 3000 kN

* ratio of minimum compressive force on bearing to maximum horizontal shear force applied for elastomer on concrete = 3 safe design factor F = 0.33

UIC Max shear stress in the thickest layer of elastomeric bearings

$$\tau_u + \tau_u + \tau_\alpha < 5G$$

AASHTO 1.11.2 Shear force = $\frac{\text{modulus} \times \text{area} \times \text{movement}}{\text{pad thickness}}$ $\frac{1}{5}$ dead load

BE 1/76 Strain limits

MOT 802 Strain limits

Germans Strain limits

TABLE 3.2 SHEAR STRESS

3.3 MAXIMUM PERMISSIBLE LIMITS

	Comp. Strain	Shear Strain	Rotation
MASHRO	Max. initial vertical deflection including rotational effects - 1% uncompressed thickness		
UIC	15%	70% G dynamic loading = 2G static loading	For reinforced pads $a \text{ long} < \frac{26 \text{ long}}{b}$ $a \text{ long} + 1.5 a \text{ short} < \frac{26c}{b}$ For reinforced pads $a \text{ long} < \frac{66 \text{ long}}{b}$ $a \text{ long} + 1.5 a \text{ short} < \frac{66c}{b}$
BE 1/76	10%	50%	For no tension $\delta c > \frac{ab}{2}$ Values not mentioned
BS 5400	Combined compression shear and rotation Average strains $\epsilon_g < 0.7$ $\epsilon_g < 0.5$	$\epsilon_{\max} = \epsilon_b + \epsilon_s + \epsilon_\theta < 5$ $\epsilon_{\min} = \epsilon_b - \epsilon_s - \epsilon_\theta > 0$ - 50 hardness $\epsilon_c < 0.1$ - 70 hardness	Not available
German	Stress Limit	$\tan \delta_s = 0.7$ for $T \leq 1/5$ of width $\tan \delta_s = 0.6$ for $T < \frac{1}{3.33}$ of width	Maximum permissible values are given in tabular form corresponding to plane dimensions

3.3 MAXIMUM PERMISSIBLE LIMITS

2/2

	Comp. Strain	Shear Strain	Rotation
NRPPRA	15% (including bulk comp. effects)	50% — 70 hardness 60% — 60 hardness 70% — 50 hardness	Maximum tensile stress for no uplift $\delta = \frac{E(s-1)}{2S}$
Lindley	15%	60%	Values given corresponding to maximum shear strain
India	Not available	$E_{sc} + E_{sh} < 0.33 E_{ut}$ $E_{sc} + E_{sh} + E_{\alpha} < 0.55 E_{ut}$	$\delta_c > \frac{\alpha L}{2}$
Long	—	Maximum horizontal movement from all causes = 70 mm	Max. 0.02 radian for rotation @ horizontal axis
MOR 802	—	$E_b = 6S E_c$	$\alpha < \frac{2\delta c}{L}$
Du-pont	10%	50%	Not available

3.4 BEARING DIMENSIONS

1/2

Bearing Dimensions	AASHTO 1.11.2	German	BE 1/76	Memo HQT 802	UIC	India
Elastomer layer thickness (t)		1/10 of shorter plane dimensions (minimum)	10 mm (min.) 25 mm (max.) $\frac{1}{4}$ of least plane dimension (mm.)	5 mm (min.) 25 mm (max.)	8 mm (min.)	12 mm (max.)
Total elastomer thickness in (T) bearing	$\frac{1}{5}$ of width of plain bearing (maximum) $\frac{1}{3}$ of width of laminated bearing (maximum)	1/5 of shorter plane dimension (maximum) Improved to 1/3.33 recently (maximum)	1.0 times least plain dimension (maximum)	Maximum	Max. $\frac{1}{5}$ of shorter plain dimension for plain bearings $f_c < \frac{2b}{3T}$ GS for reinforced bearings	$T > \frac{Sla}{E_{ac}}$
Size restrictions	Minimum pad thickness = 2 times the total horizontal movement or 1 in. (25 mm)					Largest size of bearing 2592 cm ² .

3.4 BEARING DIMENSIONS

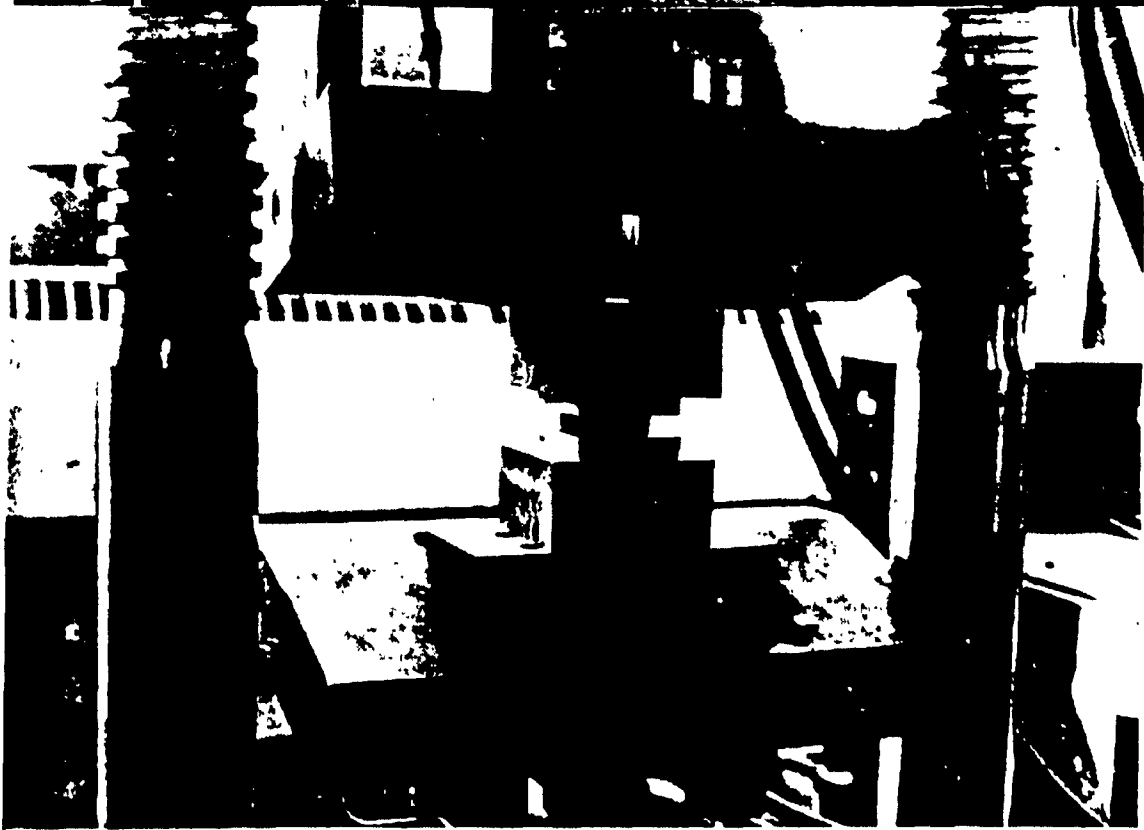
Bearing Dimensions	AASHTO 1.11.2	German	BE 1/76	BS 5400	UIC	India
Reinforcing steel shims (laminated) Minimum thickness	Proposed ASTM 1.5 mm - for cross sectional dimensions not exceeding 450 mm 2.0 mm - for all other cases		$\frac{2(f_1 + f_2)}{A_1 \times 65} V$ 3 mm for outer plates 1.5 mm for inner plates	Max. tensile stress in the steel plates: $s = 1.5V \sqrt{A_1 P}$ min. 2 mm and $\sigma_s < 0.58$ ys or 158 MPa (24000 psi) whichever is less	$\frac{2(f_1 + f_2)}{A_1 \times 65} (V_{avg} + 1.5 V_{min})$ For L.L. apply factor of safety	

originates the need to study the behavior of neoprene bearing pads under stresses higher than those currently accepted as design stress limits.

Also, there exist situations in structures, where elastomeric bearings are being subjected to forces in excess of design limitations due to: - either, strengthening of existing structure, excessive settlements, underestimation of movements due to temperature; shrinkage, etc., or in case warped or misaligned beams of bridges.

In many instances the necessary arises for applying heavier loads than those adopted in original designs. For example, neoprene bearing pads at the base of Tower Structure of the Olympic Stadium in Montreal, are currently under a compression of 4700 psi. which is much above allowable by any standards, and the maximum pressure expected when the tower structure is completed is in the order of 7000 psi. The neoprene bearing pads of 60 H are 900mm x 900mm x 18.5mm in size, 2 x 36 in numbers, Fig. 3.2. The required functions of these neoprene bearing pads, their properties, and applied loadings are given in Appendix I. The neoprene pads have bulges at observable edges which indicate overstress or ruptures in it. Thus, neoprene pads are stressed under excessively high stresses than the stress limits adopted by international codes and criteria.

The experimental program was initiated considering the above mentioned problems. Test program includes study of ultimate strength and performance under higher compressive stresses. Also included were, long term creep behavior of neoprene under long term sustained loading stresses of the order twice than those encountered in practice.



C
H
A
P
T
E
R
V
4

CHAPTER 4

SHORT TERM COMPRESSION BEHAVIOR

4.1. Introduction

Experimental study was undertaken to study the compressive behavior of elastomeric pads under instantaneous loading higher than those specified by current design limits. Various factors influencing test behavior and interpretation of results are defined. Other factors such as surface conditions of elastomer in contact, relation of the two bearing surfaces etc. are described with test results available from different sources. Complete test program, testing arrangement, testing procedure and sources of errors are discussed in the following paragraphs.

The designer of elastomeric bearing has to consider (i) load deflection characteristics under compression and (ii) the long term creep behavior (continued deflection under sustained loading). The behavior of elastomer in compression itself is complex and thus predicting how it will perform in service is a difficult task.

It is very difficult to correlate much data from various research results. For example two sets of data for 60H, neoprene, bonded single pads with the same shape factor, as studied in this experimental program, give significantly different compressive load deflection curves. The difference in data can be due to several factors.

4.2. Design Factors Affecting Behavior of Elastomers

The various design and construction factors affecting behavior of elastomers in compression are: (i) hardness and shape factor (ii) bearing surface contact conditions (iii) relation of the two bearing surfaces (iv) rate of loading (testing rate) (v) previous deformation history of the sample (vi) temperature fluctuation, etc. Also in the laboratory testing program factors such as different loading (testing) equipment, inconsistency in recording and interpretation of test results, may produce significant variation in the compressive deflection curves.

4.2.1. Hardness

Hardness measurement is not highly accurate. As mentioned earlier, 2.2, according to specifications a 60H material must demonstrate 60 ± 5 hardness i.e. a considerable difference in compression and creep performance as well as variation in shear modulus is also imminent. Effect of shape factor is discussed in the testing program.

4.2.2. Effects of Surface Conditions

When the elastomeric pad is placed between parallel steel plates and subjected to a compressive load, under laboratory conditions, the elastomer slips to a certain extent upon the metal surfaces, particularly near the outer free surface of the sample. There are two extreme possibilities of contact surfaces (smooth or rough, glued,

or unglued) in compression loading. (1) the surfaces of elastomers in contact with the compressing area can slide along the compressing faces with negligible friction by employing polished steel plates or (2) movement may be restrained almost completely by roughed surfaces of the plates i.e. relatively fixed, Fig. 4.1.

Also sandblasting of the steel plates may even result in different adherence between the elastomer and steel, depending on the surfaces (52). Photographs, Fig. 4.2 (a) and (b), show different surface conditions. Larger deflections occur for pads between steel and steel surfaces and even much larger when lubricated polished plates are used, Fig. 4.1. It is important that the exposed surfaces of the pads be free of cuts or imperfections which will cause the pads to tear when they bulge under the load.

4.2.3. Relation of the Two Surfaces

A distinctive factor in the application of elastomeric bearings is the relation of the two bearing surfaces. With inclination of one surface with respect to the other, one edge of the elastomer is subjected to high unit compression giving non-uniform distribution of strain over the loaded surfaces. Research results, Fig. 4.3, (85) have shown that inclinations varying from 0° to 5° produce compressive edge stress in excess of 700% of maximum design stress.

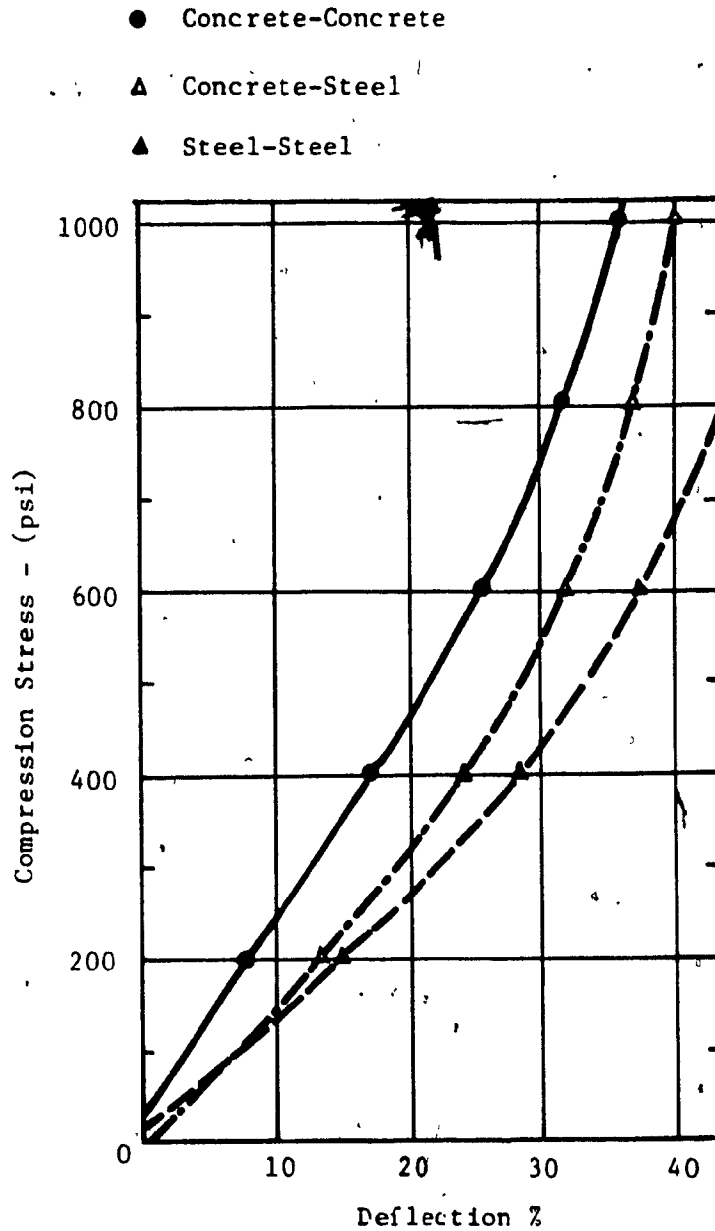
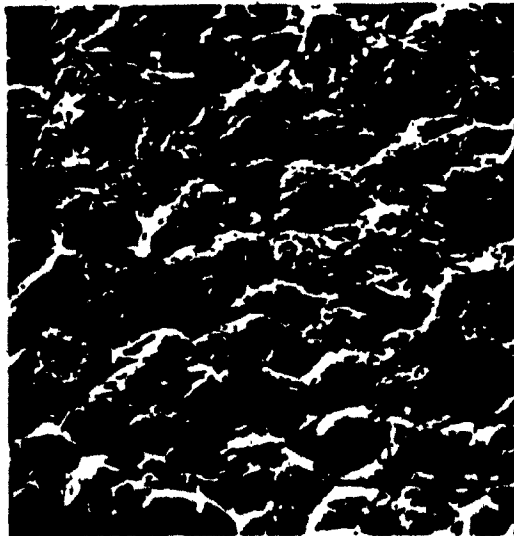


Fig. 4.1 COMPARISON OF COMPRESSION STRESS-DEFLECTION BEHAVIOR OF NEOPRENE PADS 60H FOR SURFACE CONDITIONS: STEEL-AND-STEEL, CONCRETE-AND-STEEL, CONCRETE-AND-CONCRETE.



(a)
Good



(b)
Poor

Fig. 4.2 Sandblasting of steel plates in contact with elastomers, with different adherence characteristics (a) Good, (b) Poor.

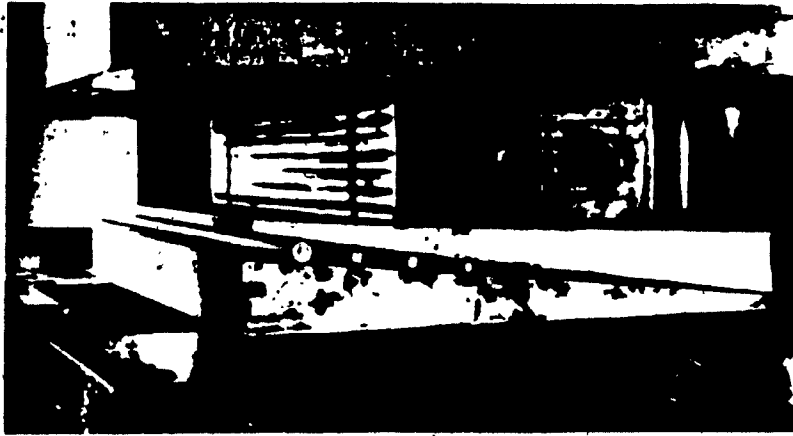


Fig. 4.3 Elastomeric bearings inclined at 2° and loaded at maximum compressive force, induce edge stresses up to 300% of assumed design values, i.e. overloading 3 times right from initial installation. (Courtesy of Transportation Road Research Laboratory, London).

4.2.4. Other Factors

From the experimental study it has been learned that the parameters that also affect the load deformation curve is the rate of loading the test specimen. Considering its softness compared to support surface there are substantial changes in the vicinity of the load interfaces. Elastomers under strain always show some permanent set and thus compressive curves are dependent on the previous compressive history of the sample. Some information on the behavior of the pads at severe temperatures, as presented by recent reports (6) indicate that temperatures as low as -40°F will not adversely affect its performance.

4.3. Compression Testing

4.3.1. Test program: Tests described in this study were performed on neoprene pads of 60 hardness and 20 mm thick. The test program is shown in Table 4.1. The test program was limited in scope without variables such as hardness, thickness, bearing surfaces in contact, etc. All tests were done at room temperature. Considering the time dependence behavior of elastomers, large variations in load-deformation readings are obtained. Furthermore, there is no international standard for compressive stress-strain tests. BS 903 Part 9A, 1973 specifies rate of compression of $12 \pm 2 \text{ mm/min.}$, and that sand paper be used between test piece and plattens to approximate to non-slip conditions. ASTM D 575 follows same as BS but gives two methods namely force at given deflection and deflection at given force.

Table 4.1 Test program for behavior under high compressive stresses

Test	Load in psi (MPa)	Remarks/Purpose
1	800 (5.1)	To verify. Present AASHTO limits.
2	1,800 (7.0)	To verify. Current practices.
3	2,000 (14.0)	To verify. Proposed design curves.
4	5,000 (34.45)	Equivalent to average concrete bearing strength. Approx. present loading at Olympic Tower.
5	7,000 (49.0)	Expected max. stress at Olympic Tower.
6	10,000 (68.9)	Under higher compression.
7	20,000 (137.8)	Maximum strength possible.

4.3.2 Testing Arrangement

Considering the high compressive stress and different rate of loading considered in the test program as listed in Table 4.2, three different testing machines were used. Tinius-Olsen Compression-tension testing machines with the capacities of 60,000 lbs. and 120,000 lbs. with varying load ranges, were used for first two series, Fig. 4.5. The one with 60,000 lbs. capacity is equipped with load deflection recorder which records the relative deflection of the test sample correspondent to a particular load. Four dial gauges, one on each side, of the pad were used to measure the deflection readings. The average of the readings on the dial gauges on the opposite sides of

TABLE 4.2 EXPERIMENTAL PROGRAM*

Testing Equipment	Maximum Stress Pat.	Comp. Mpa.	Test conditions		Time for loading & unloading	Rate of loading Pat./sec	Kpa/sec	S.F.	Fig. #	
			Sample /	Size of Neoprene pad mm.						
Amster	5110	35	2	63.5 x 63.5 x 20	101.6 x 101.6 x 20	100 sec. each	50	344.75	0.8	4.10
Amster	5110	35	3	63.5 x 63.5 x 20	63.5 x 63.5 x 20	100 sec. each	50	344.75	0.8	4.11
Amster	20000	137.8	4	25.4 x 25.4 x 20	63.5 x 63.5 x 20	400 sec. each	50	344.75	0.32	4.12
Tinus-Olsen	1460	10	5	101.6 x 101.6 x 20	101.6 x 101.6 x 20	-	-	-	1.4	4.16
Tinus-Olsen	6000	41	6	63.5 x 63.5 x 20	101.6 x 101.6 x 20	180 sec.	-	-	0.8	4.18
Tinus-Olsen	9600	65.5	7	63.5 x 63.5 x 20	101.6 x 101.6 x 20	300 sec.	-	-	0.8	4.20
Tinus-Olsen	19200	130	8	63.5 x 63.5 x 20	101.6 x 101.6 x 20	300 sec.	-	-	0.8	4.21

* Load deflection curves obtained were average of five experiments
 ** Surface of steel plates was neither polished nor sandblasted

each pad was taken as compressed thickness of the pad.

The Amsler testing machine with the capacity of 200,000 lbs. facilitates loading of samples at predetermined rate of loading within a specified time. The unit was attached to a load deflection recorder. The horizontal and vertical (x and Y axes) pen movements were controlled by voltages proportional to compressive load and deflection respectively. (e.g. Amsler F - 45,000 lbs. 10V,
 $Y = 0.5V/cm, x = 0.25 V/cm$)

The testing system for both above machines is shown in Fig. 4.4.

4.3.3. Testing Procedure

The basic test factors considered in the test program are given in Table 4.2. Neoprene test samples of different shape factors were used. The elastomer pads were placed between two steel plates for two cases (i) Steel plates projecting from the faces in contact with the elastomers i.e. the size of steel plates were more than that of the elastomer so that part of the elastomer projected beyond their edges when maximum deflections were expected (ii) steel plates and neoprene sample of same sizes to allow free lateral area for bulging on all four sides.

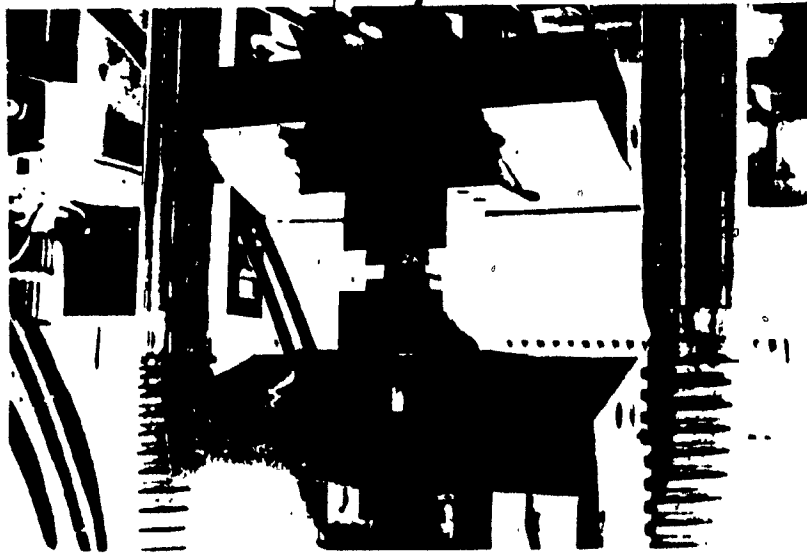
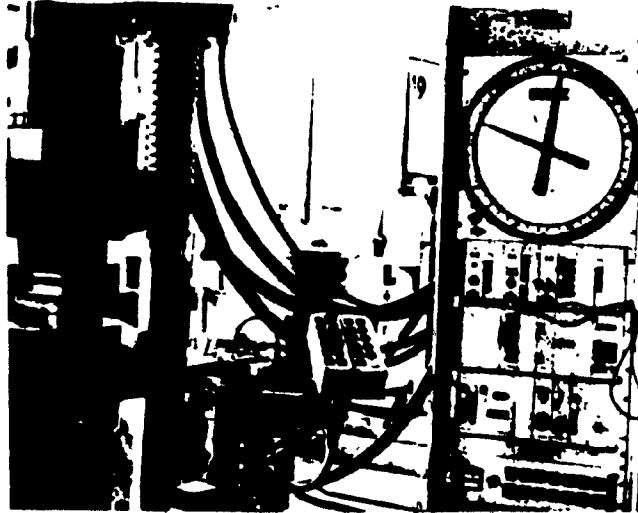


Fig. 4.4 View of Amsler Testing System for Compression Tests.



Fig. 4.5 Test view of 120,000 lb. compression loading Tinus-Olsen machine.

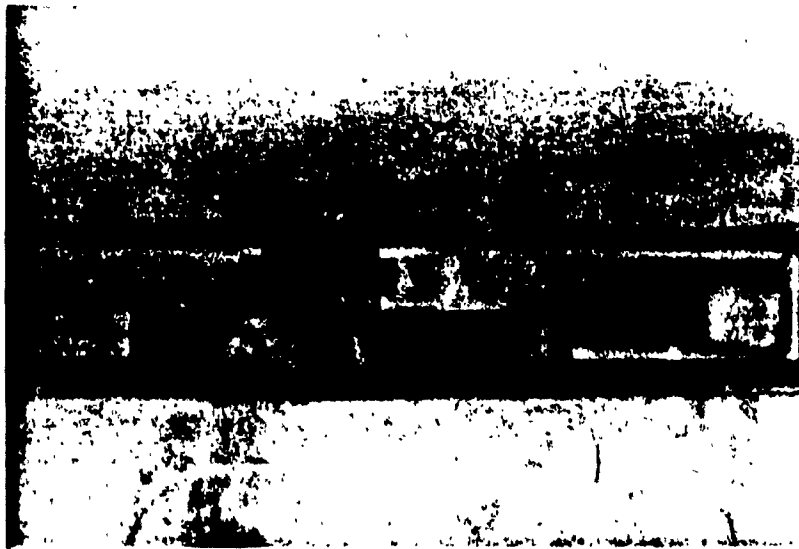


Fig. 4.9 Bulging behavior under Tinus-Olsen 120,000 lb. loading. Steel plates and neoprene pad of same size.

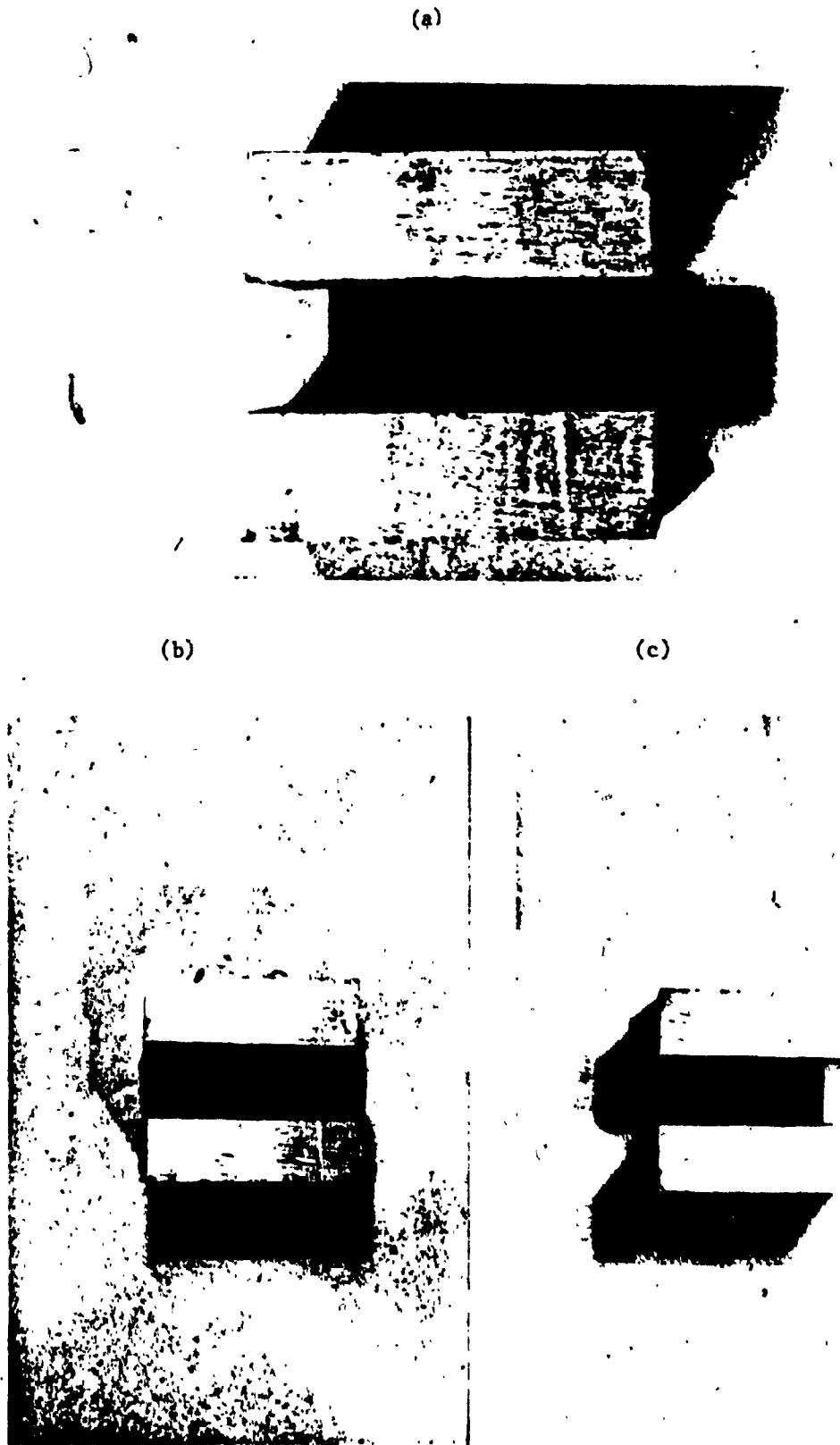


Fig. 4.5 Test Specimens for compression tests, (a) steel plates larger than sample (b) steel plates and sample same size (c) variation of shape factor.

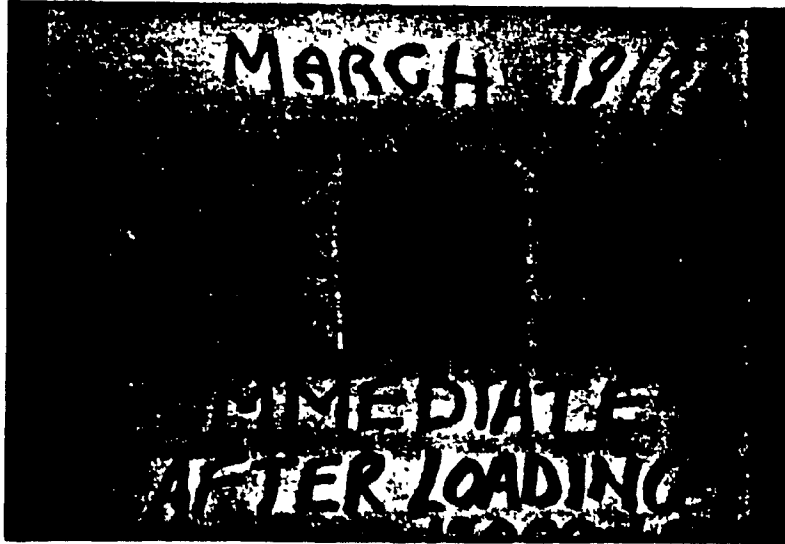


Fig. 4.7 Sample after unloading under lower stress.

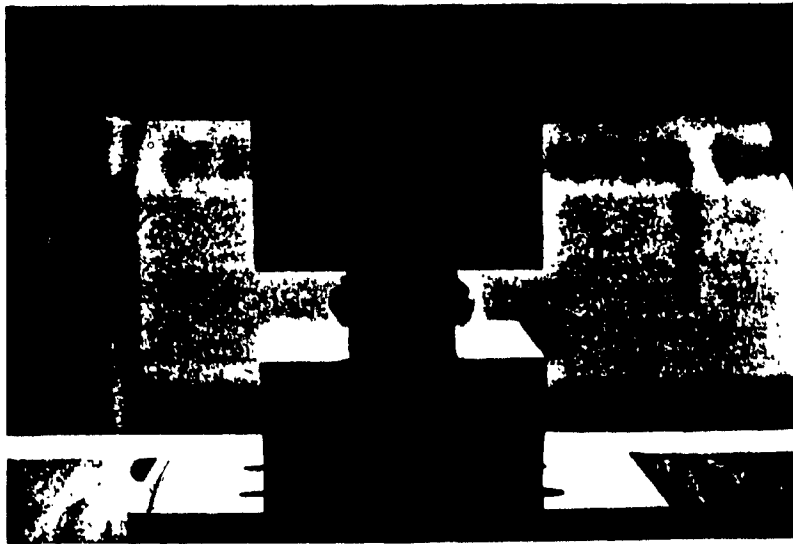


Fig. 4.8 Compression of specimen under Amsler testing system.

For tests conducted on Timus-Olsen machine, a nearly constant rate of loading was selected. At each specified increment of load, the specimens were held at that load so that all four deflection gauges were read simultaneously. Testing was performed in step-by-step manner i.e. hold for specified increment, take deflection reading, load again and so on. At the maximum loading level, the pad was held for 1 to 2 minutes. The pad was then unloaded with load-deflections recording in the same manner. Simultaneous recording was obtained on the automatic load-deflection graph recorder. Changes in the pad dimension were measured immediately after the sample was unloaded, and after an interval of 5 minutes.

In case of Amsler testing machine, two parameters, namely percentage of maximum load on the loading scale and rate of loading for the required time for loading were determined before starting a test. Tests on different sizes of samples at varying loading rate, were performed (Table 4.2).

On all cases five samples were tested for each condition.

4.3.4. Observation and analysis

Compressive load deflection curves were plotted as shown in Fig. 4.10, 4.11, 4.12, 4.18, 4.20, 4.21. Each curve has been taken as an average of five experimental test curves. The comparable stress-squeeze curves based on test results of Fig. 4.10 and Fig. 4.11 are shown in Fig. 4.13. It is evident from Fig. 4.13 that, by allowing less free area for expansion, the squeeze is reduced by almost

25% corresponding to a compressive stress of 35 MPa. Compressive stress-squeeze curves, Fig. 4.16, plotted against those provided by Dupont, Fig. 4.15, and others (4, 19, 18) show overall good agreement. When the S.F. is reduced to as much as 0.32 total compressive squeeze ranges to 100% to 120% at a stress of 20,000 psi Fig. 4.14. Neoprene pad of low shape factor of 0.32 (Fig. 4.14) when stressed produces a squeeze of 40 to 45% under a compressive stress of 4,000 psi. Load deflection curves for larger shape factors varying from 4 to 200 provided by NCHRP and Lindley is shown in Fig. 4.17. While comparing these curves, it is found that an equal compressive squeeze of less than 5% is obtained for shape factors of 16 (2) and 160 (18) under a same compressive stress of 2,000 psi. Also considering the compressive strain limit of 10%, most of the test results agree with S.F.=4 corresponding to loading limits of 800 to 1,000 psi. Variations in the compressive squeeze due to different surface conditions in contact with the bearings are shown in Fig. 4.1. Thus for the same stress and S.F. it can be observed that pads between concrete-concrete and steel-steel surface conditions show differences of more than 40%.

Plain, unreinforced H60 neoprene of very low S.F. (0.8) at stress approximately 5000 psi. shows signs of deformation whereas at a higher stress of more than 20,000 psi. with reduced S.F. (0.30) it exhibit set behavior. Performance of neoprene for stresses higher than above mentioned and failure criteria are discussed in Chapter 8.

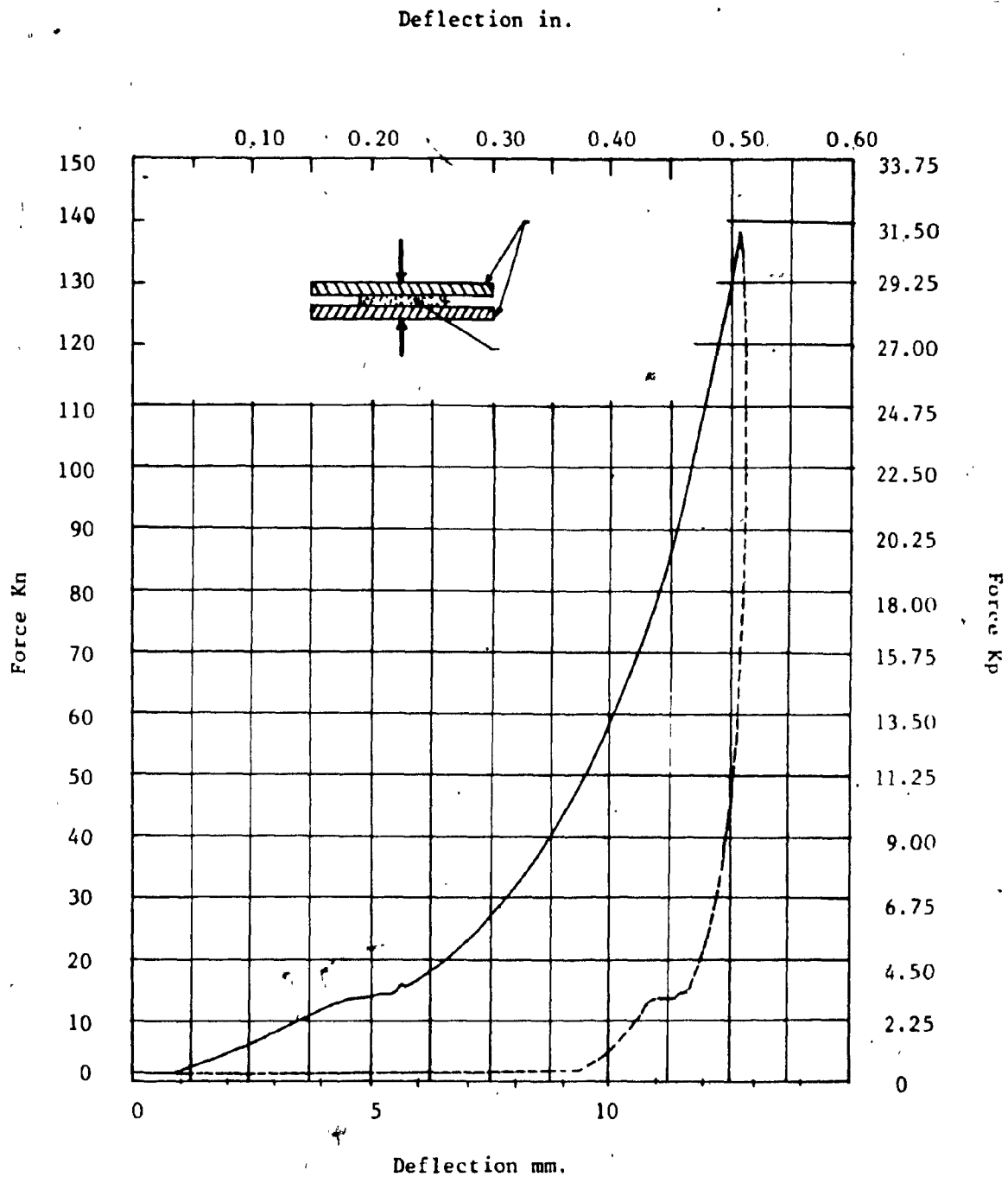


Fig. 4.10 Force-deflection curve for neoprene under compression.
For neoprene (63.5 mm x 63.5 mm x 20 mm) and steel
plates (101.6 mm x 101.6 mm x 20 mm).

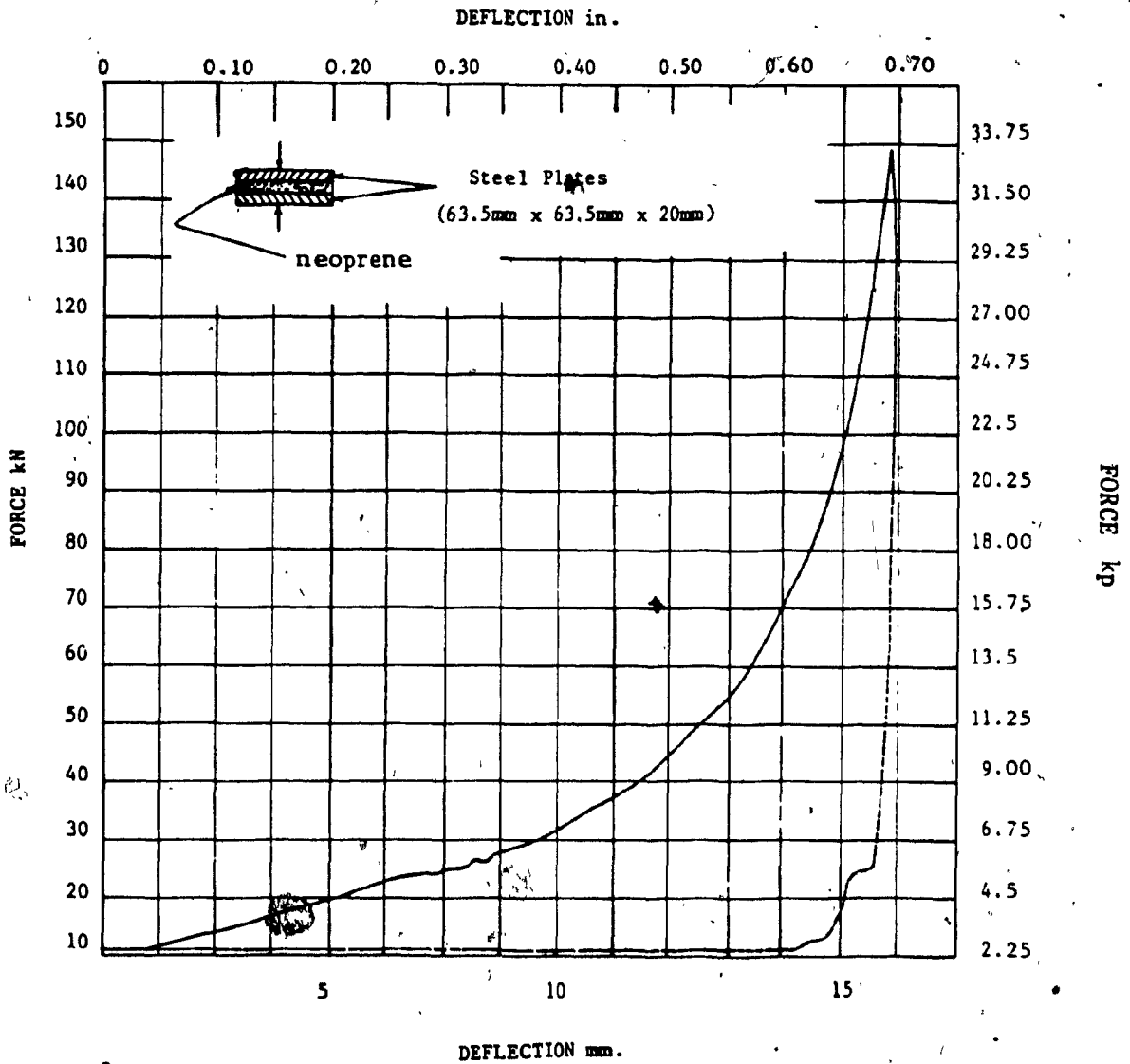


Fig. 4.11 Force-deflection curve for neoprene under compression.
For neoprene & steel plates same size (63.5mm x 63.5mm x 20mm).

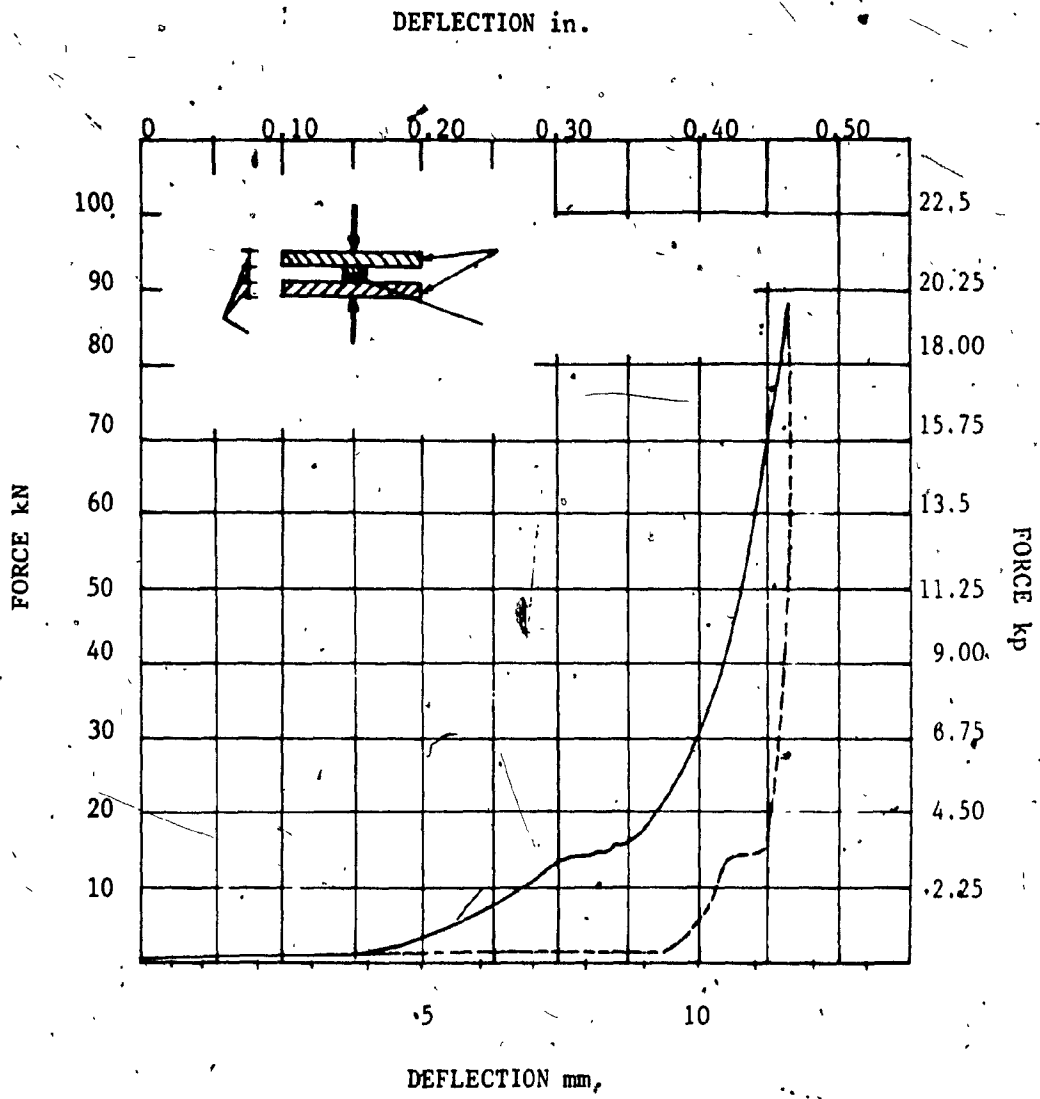


Fig. 4.12 Force-deflection curve for neoprene under higher compression with reduced shape factor (0.32) for neoprene (25.4mm x 25.4mm x 20mm) and steel plates (63.5mm x 63.5mm x 20mm).

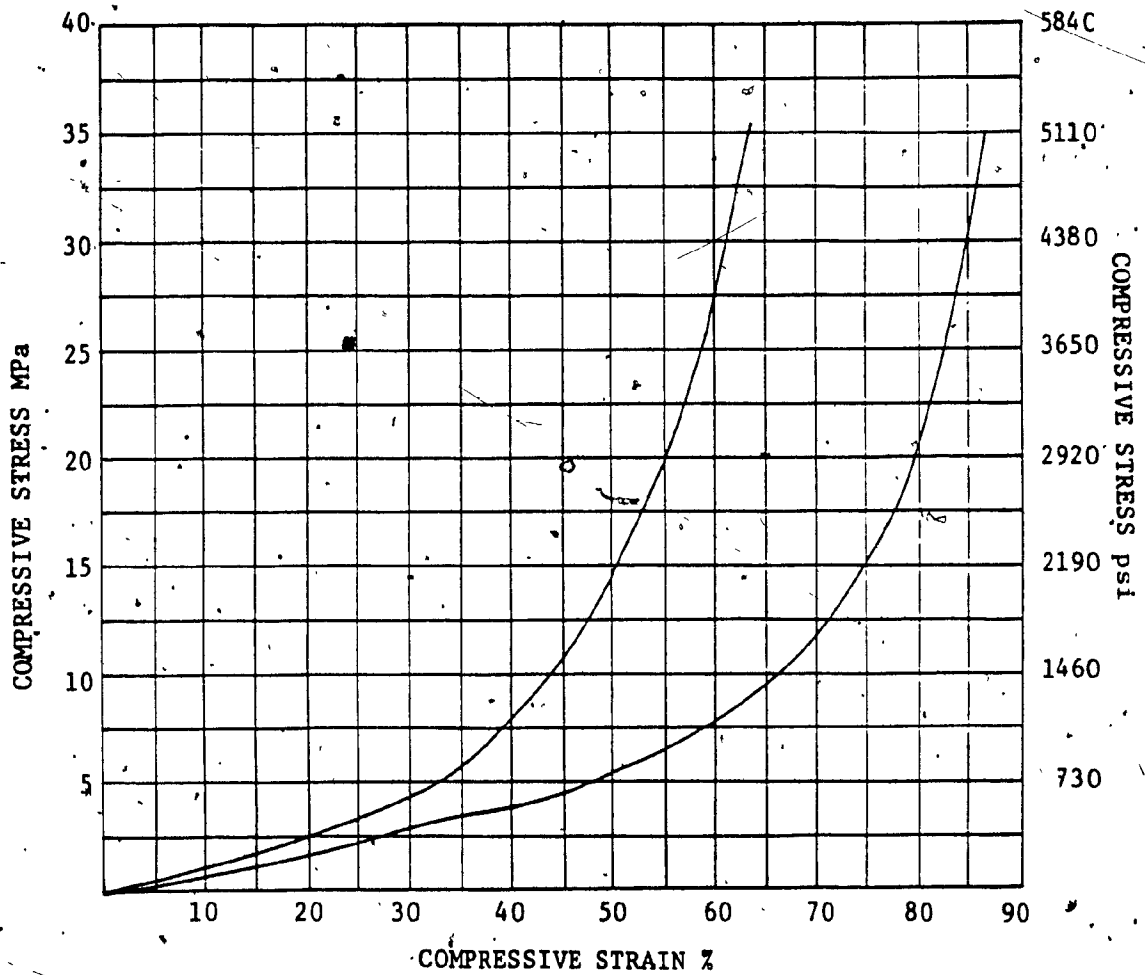


Fig. 4.13 Compressive stress-strain curves for neoprene 60H, S.F. = 0.8, based on load-deformation figures 4.10, 4.11.

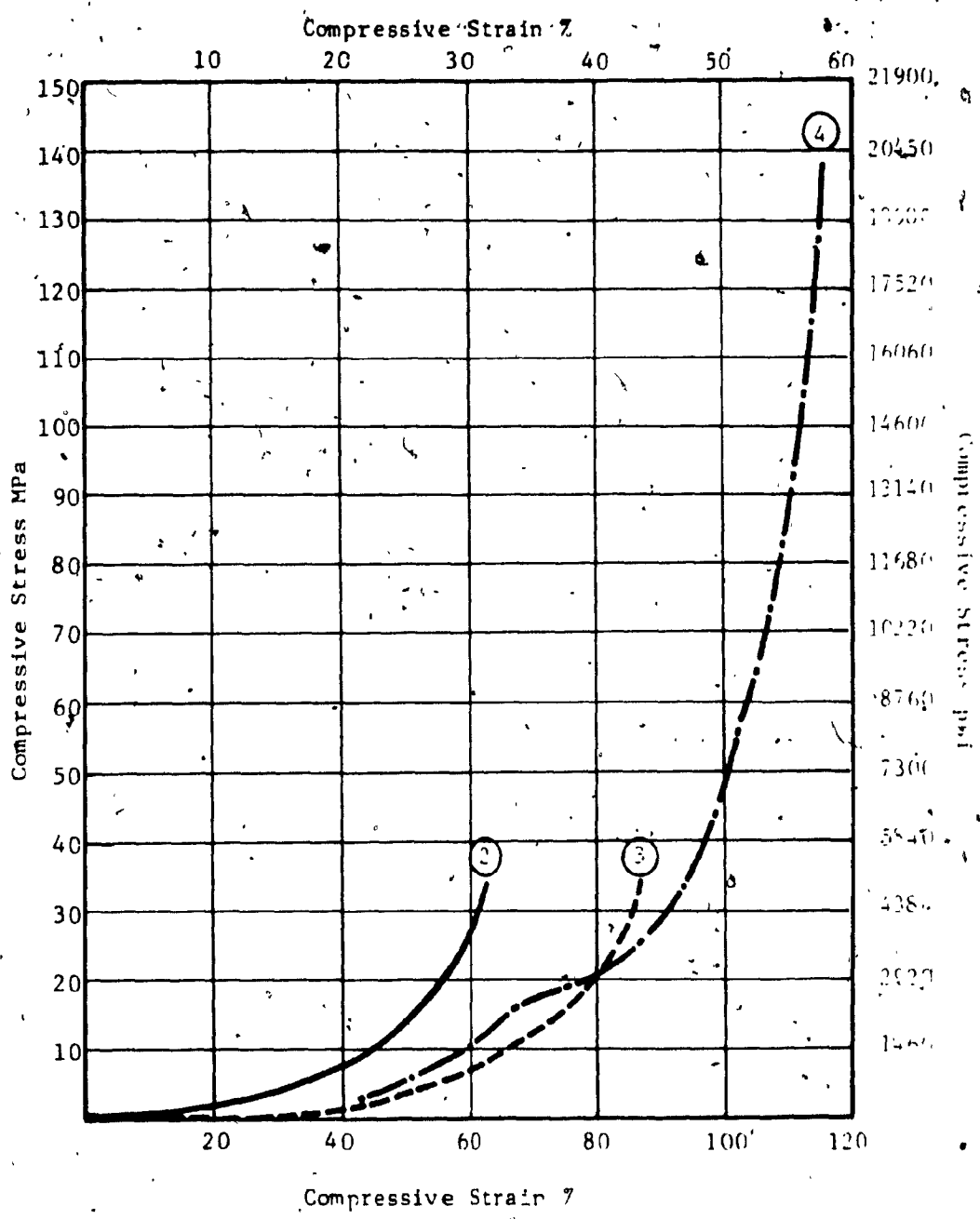


Fig. 4.14 COMPRESSIVE STRESS-STRAIN CURVES FOR NEOPRENE 60H (S.F. = 0.32)
AND COMPARISON WITH OTHER TWO (S.F. = 0.8)
[ALL TEST RESULTS FROM TESTING ON AMSLER SYSTEM]

- (2) - Steel plate larger than neoprene
- (3) - Neoprene and steel plates same size
- (4) - Neoprene with reduced shape factor (0.32)

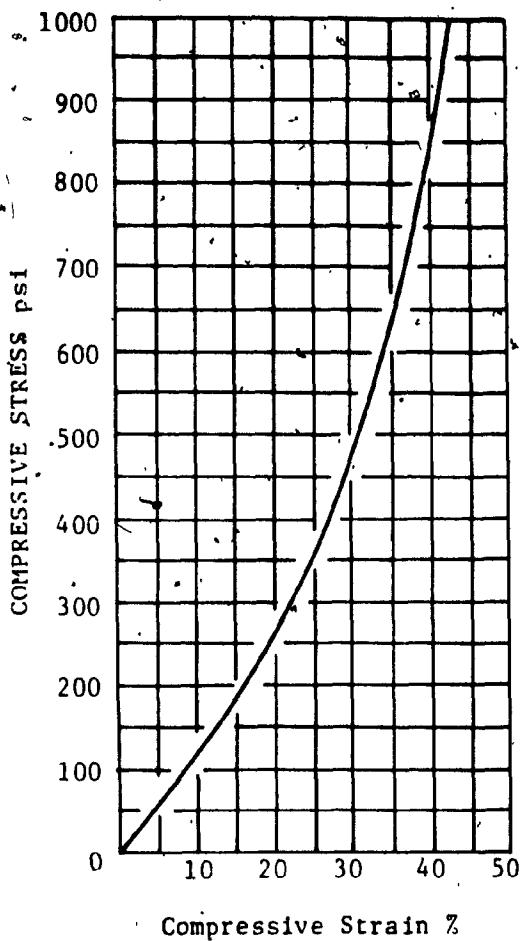


Fig. 4.15 COMPRESSIVE STRESS-STRAIN CURVE FOR NEOPRENE BY DU-PONT (S.F. = 0.8)

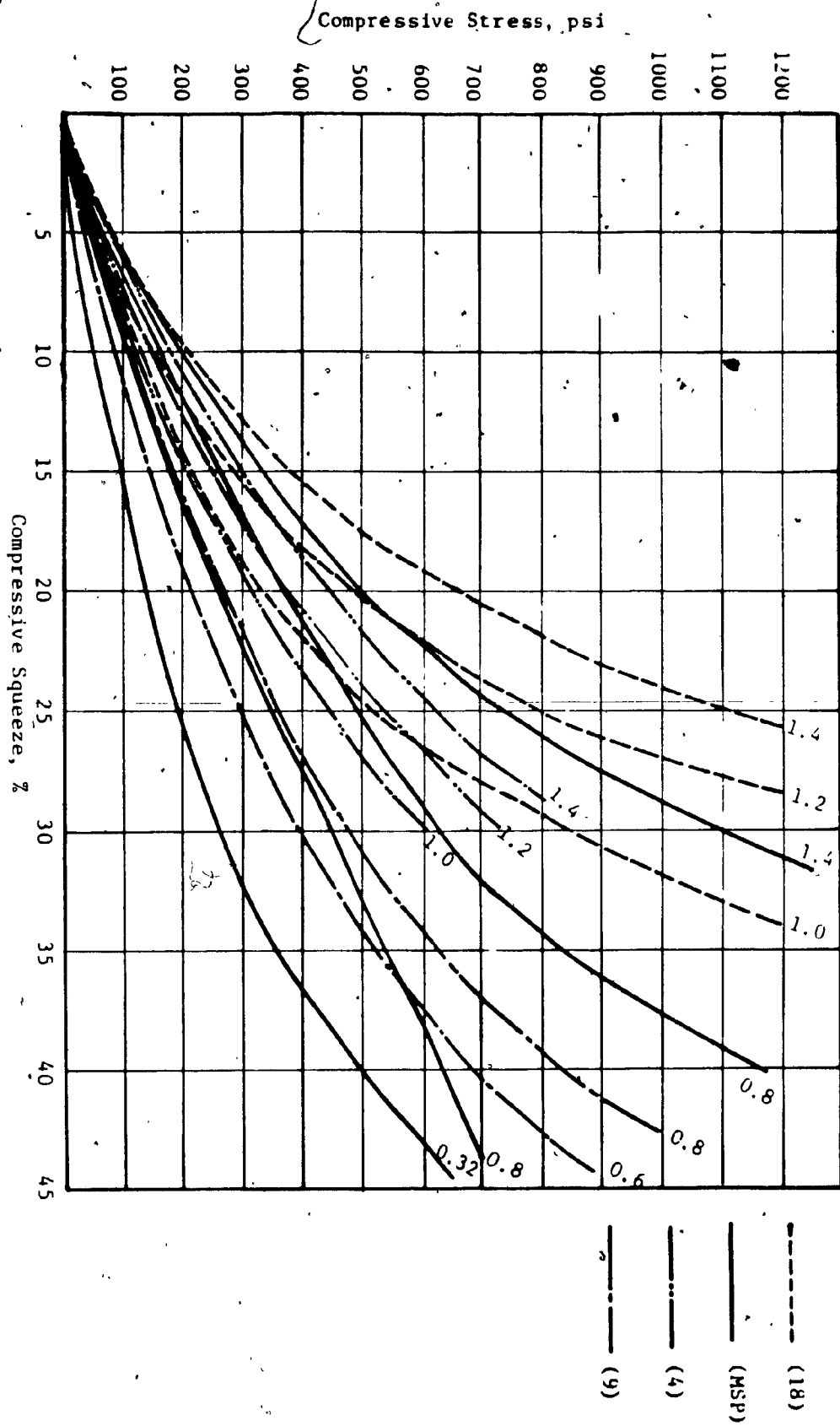


Fig. 4.16 COMPARATIVE STUDY OF COMPRESSIVE STRESS-SQUEEZE CURVES FROM EXPERIMENTAL STUDY AND THOSE AVAILABLE FROM LITERATURE [NEOPRENE 60H FOR VARYING S.F. = 0.32 TO 1.4]

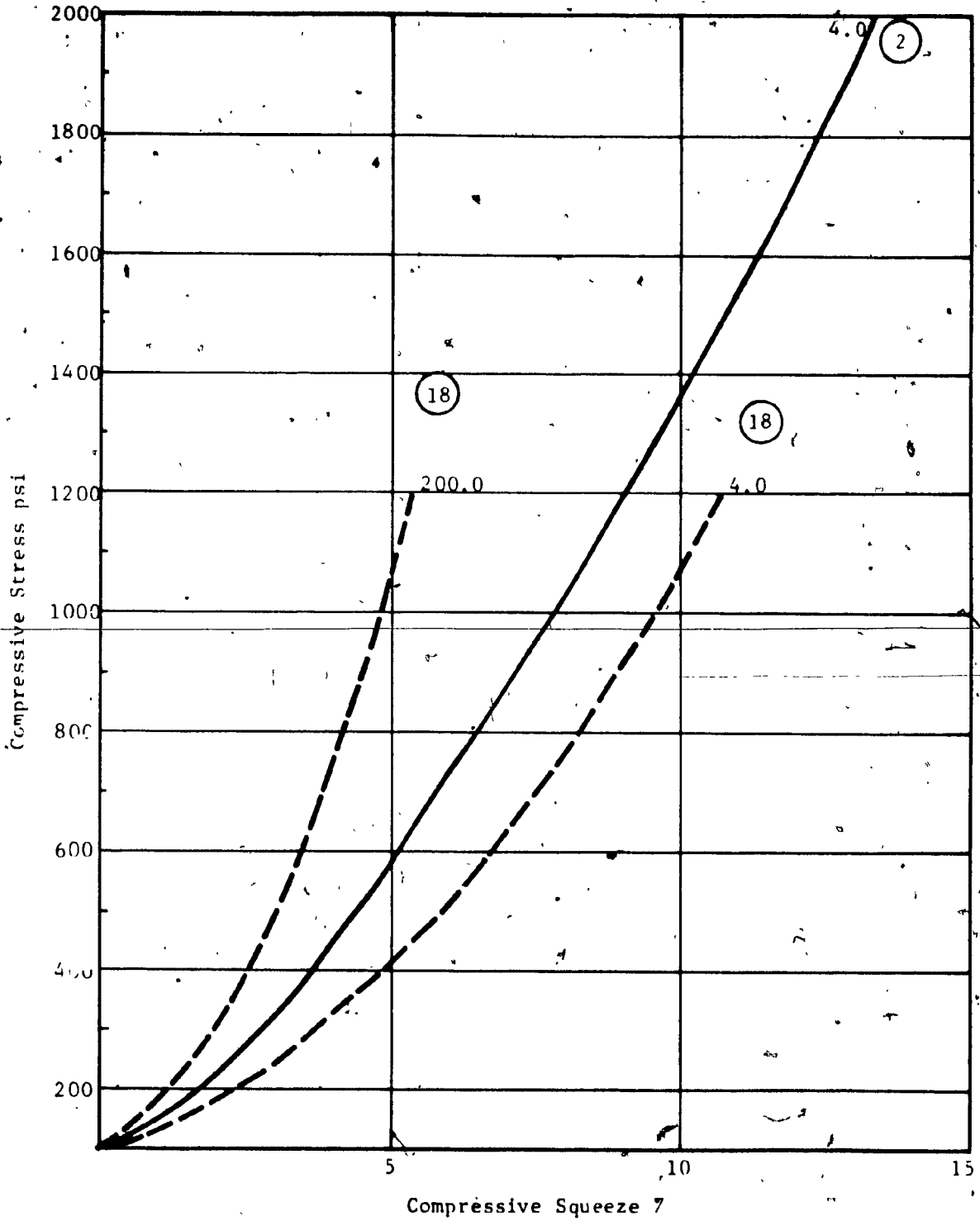
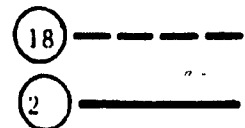
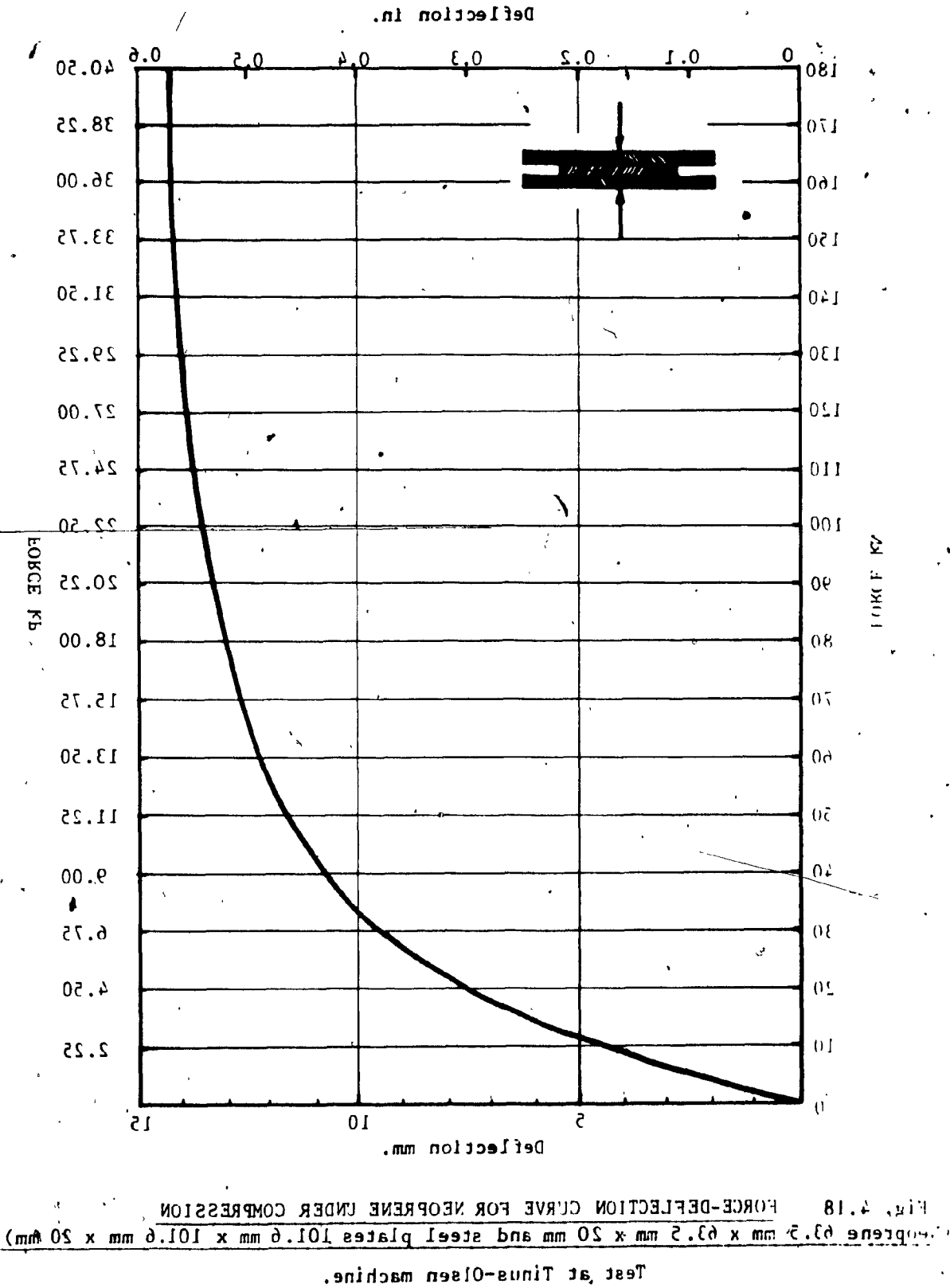


Fig. 4.17

COMPARISON OF COMPRESSIVE STRESS-SQUEEZE BEHAVIOUR OF NEOPRENE H60, S.F. = 4 AND 200 [18,12]





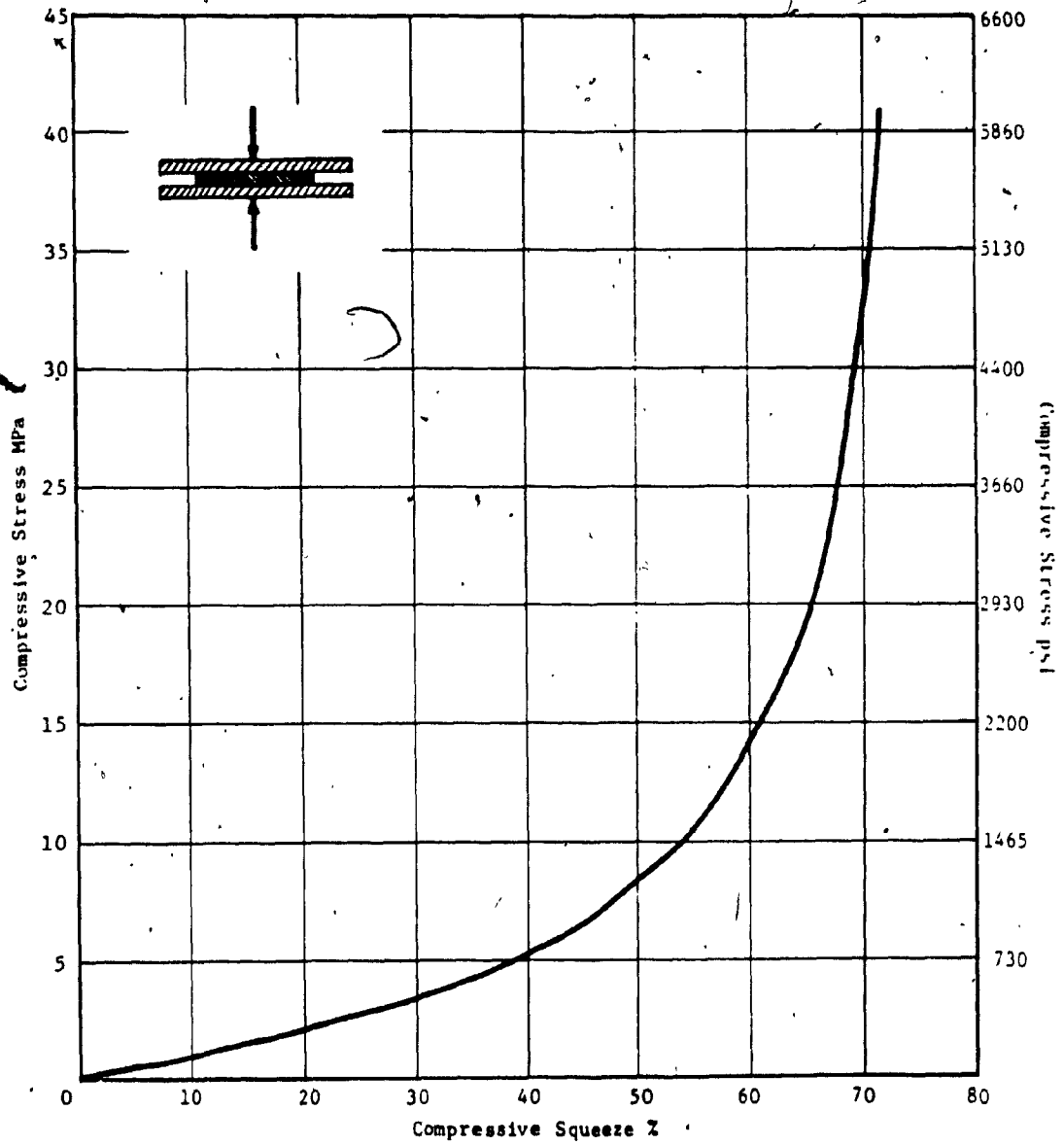


Fig. 4.19 COMPRESSIVE STRESS SQUEEZE CURVE FOR NEOPRENE (S.F. = 0.8 TINUS-OLSEN MACHINE) BASED ON Fig. 4.18.

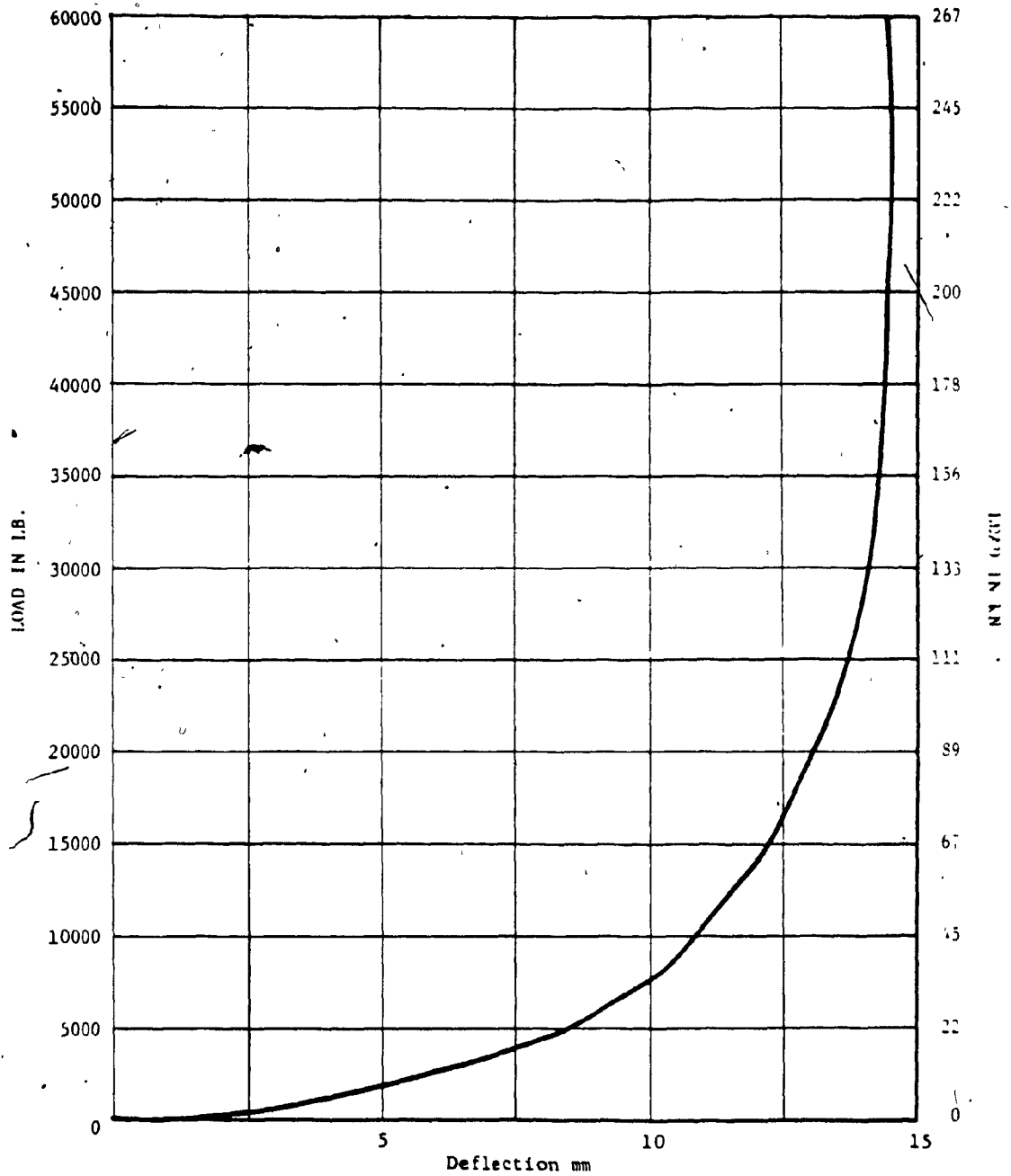


Fig. 4.20 FORCE DEFLECTION CURVE FOR NEOPRENE AT TINUS-OLSEN MACHINE

(NEOPRENE 63.5 mm x 63.5 mm x 20 mm AND STEEL PLATES 101.6 mm x 101.6 mm x 20 mm)

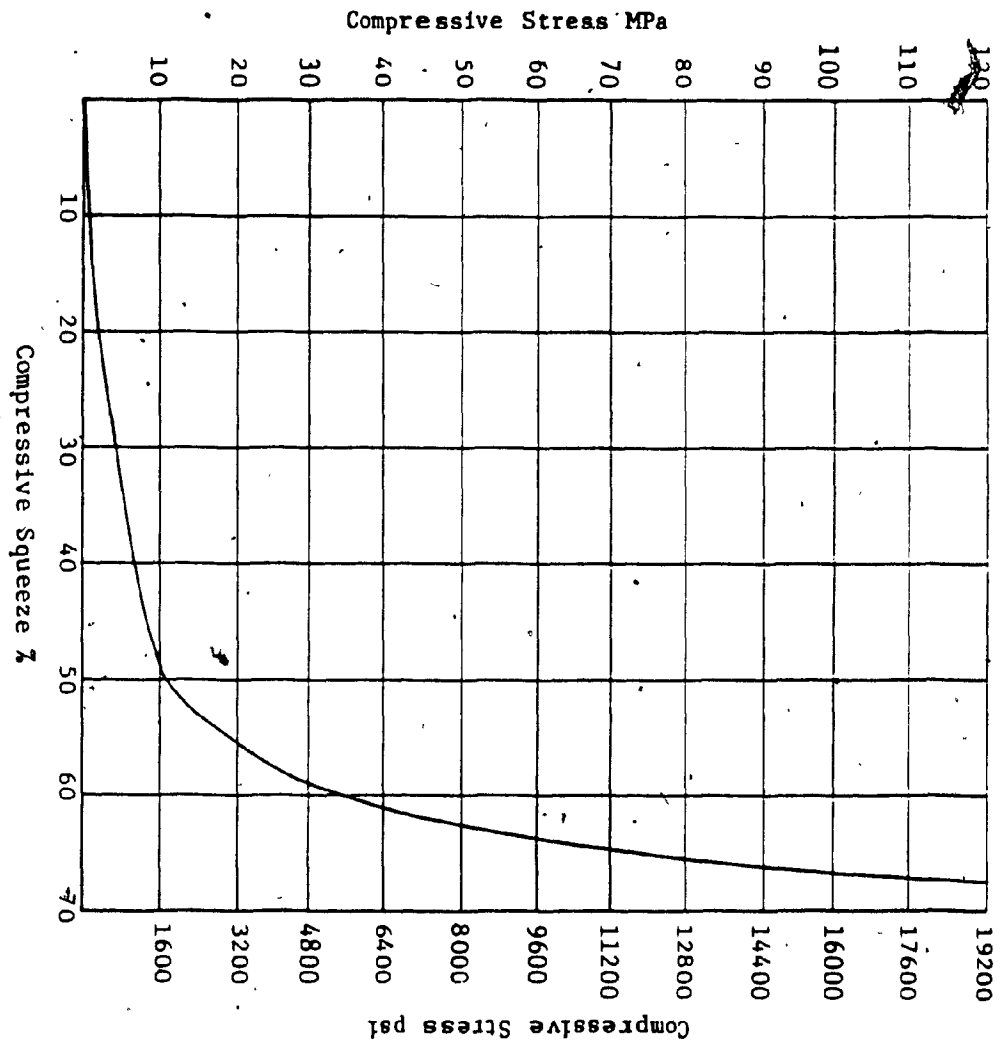
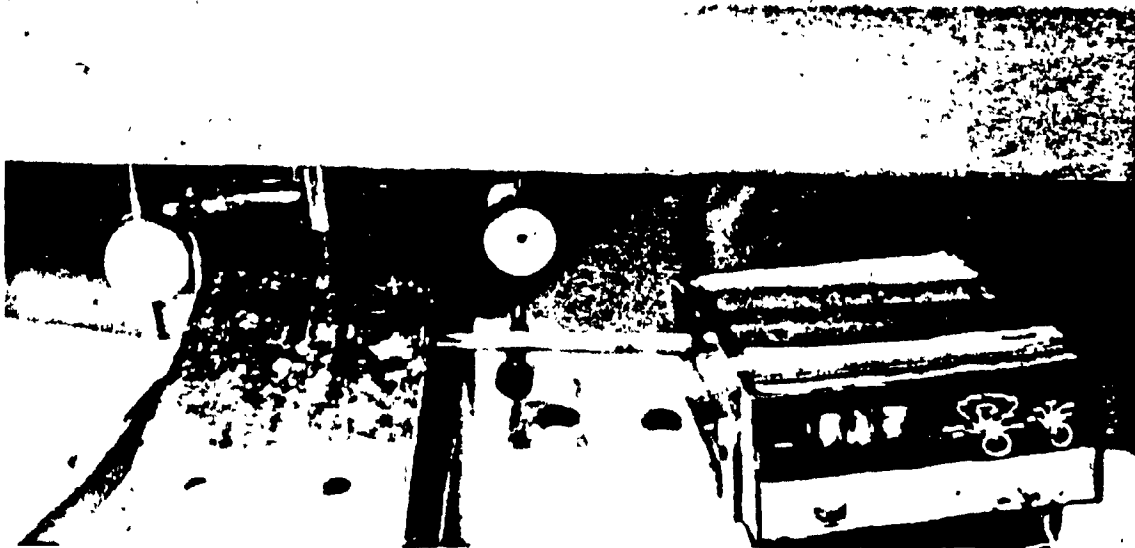
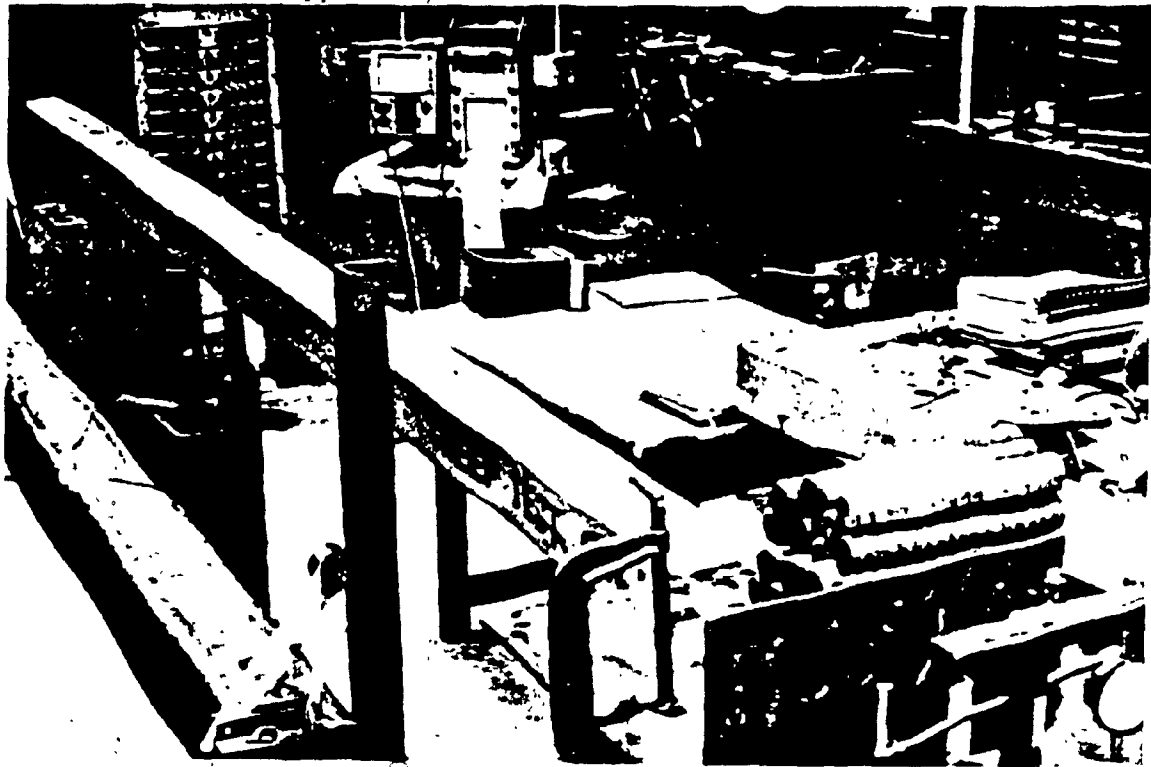


Fig. 4.21 STRESS-SQUEEZE CURVE FOR NEOPRENE UNDER COMPRESSION (TINUS OISEN), NEOPRENE AND STEEL PLATES SAME SIZE (63.5 mm x 63.5 mm x 20 mm).



C
H
A
P
T
E
R

5

CHAPTER 5

CREEP BEHAVIOR UNDER COMPRESSION

5.1. Introduction

Elastomers under constant stress show a gradual increase in deformation, occurring with a lapse of time period. The phenomenon known as creep (60, 92, 93) is exhibited due to physical and chemical processes leading to an internal reorganization of molecules within the elastomers. In the past, neoprene had reported noticeably higher rate of creep than natural rubber but this has been improved.

Measurement and exact knowledge of creep behavior of neoprene-like materials is important since it influences the space relationship between various parts of the structure. Excessive creep of the elastomer might lead to unacceptably large movements of the superstructure in relation to the foundations or adjoining structures.

Creep of elastomers varies with logarithm of time i.e. it occurs at a relatively high rate in the initial stages and then proceeds at a progressively diminishing rate. The magnitude of creep depends

on composition and structure of the elastomer, type of loading, period and intensity of stress, rate of loading, temperature and other factors.

There has been controversy over defining creep of elastomers. In rubber industries creep is defined as increase in deformation after a specified interval of time expressed as a percentage of deformation at the start of that time interval (53) whereas, many publications and industries treat creep as increase in deformation as a percentage of the original unstressed thickness of the elastomer. Thus while comparing test results provided by one researcher with another, or applying them in design, it is very difficult to find similarity of application.

5.2. Research Objectives

Whereas elastomers are used commonly to support heavy stresses (73, 94), except that the standard research tests reported by Dupont (9), Goodyear (60) and Keen (95), compressive creep of neoprene bearing pads under high stresses has never been extensively studied. Thus a thorough analysis of compressive creep of neoprene under high stresses satisfying the present need of structures is necessary. The detailed program undertaken in this respect is given in Table 5.1.

5.5. Test Program

Creep test has been defined (96, 97, 17), as change in deformation with a passage of time under constant force,

but there is considerable lack of standardised detailed procedure.

A fairly sophisticated creep apparatus for testing creep behavior of rubber materials in compression has been described by Brown et al (53).

Table 5.1 Test Program for Creep Tests on Neoprene Pads Under Different Sustained Loadings

Three specimens each of 25.4mm x 25.4mm x 20mm size were tested at following sustained stress conditions, for 10 days period. Most of the compressive creep occurs within this period.

<u>Test No.</u>	<u>Compressive Stress</u>	<u>Remarks</u>
1	500 psi.	To verify existing du-Pont curves.
2	800 psi.	To verify ASSHTO specifications.
3	1,000 psi.	To study the new proposed limits.
4	1,600 psi.	Under 200% higher stress.
5	2,400 psi.	Under 300% higher stress.
6	3,000 psi.	Equivalent to average concrete bearing strength.

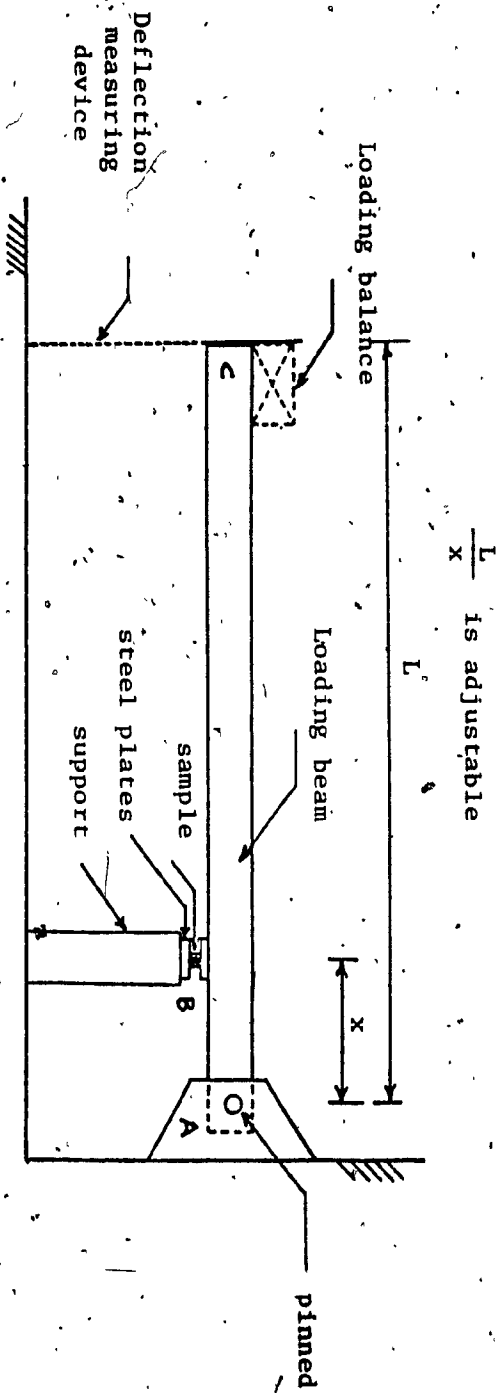


Fig. 5.1

SCHEMATIC OF SET-UP FOR CREEP TEST ON NEOPRENE

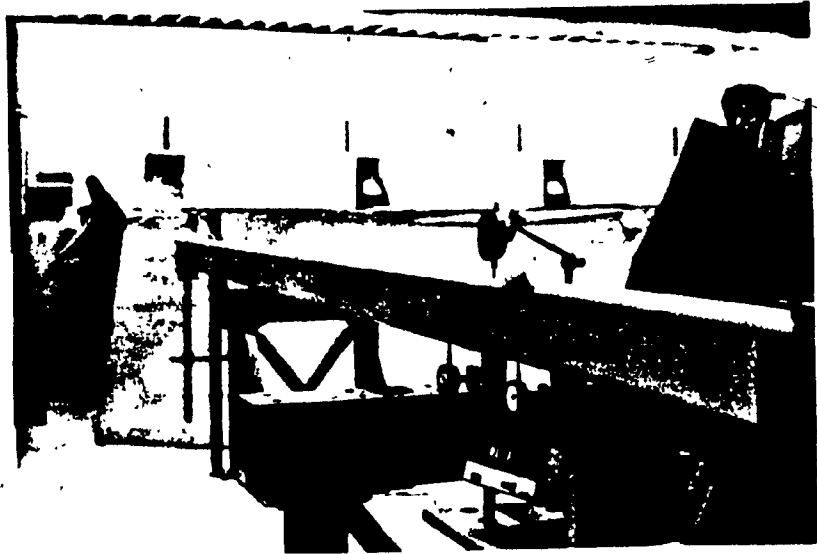
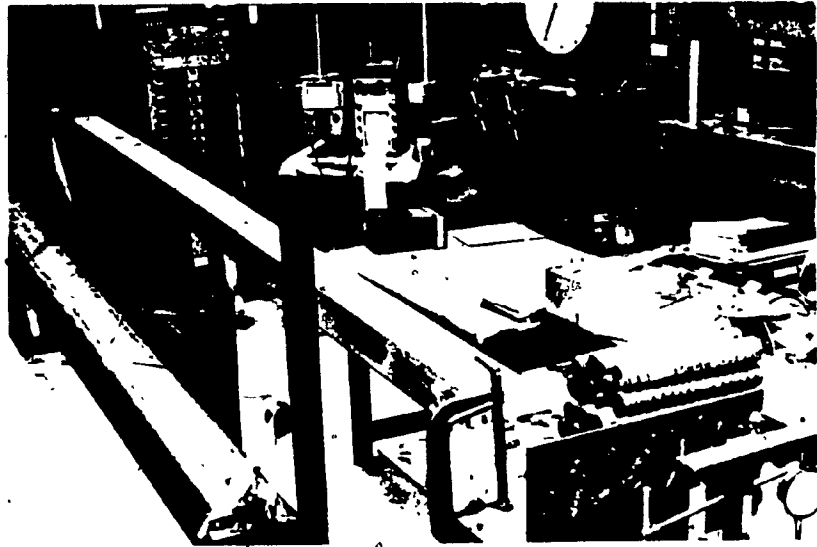


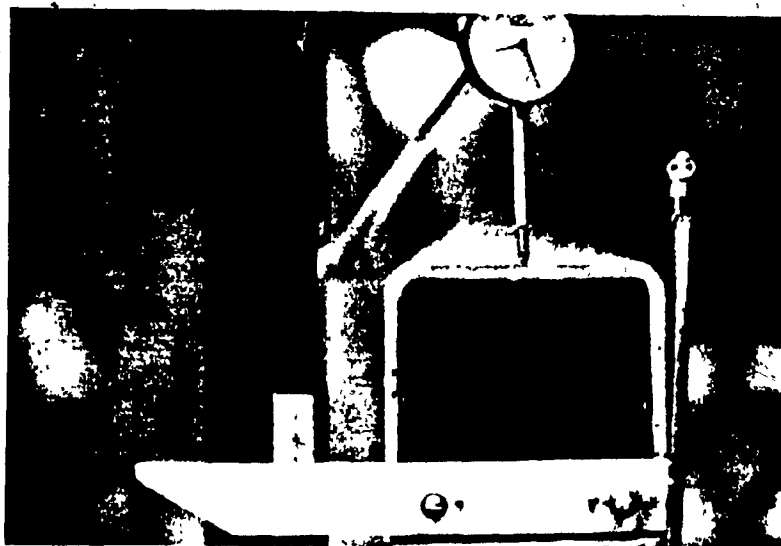
Fig. 5.2 View of testing scheme for creep tests on neoprene.



(a)



(b)



(c)

Fig. 5.3 Deflection measuring arrangement at location 'C' of the loading beam.

5.5.1. Testing Arrangement

Testing scheme developed for measurement of creep in compression is shown in Fig. 5.1, 5.2. The loading beam «AC», Fig. 5.1, pinned at end «A» is designed in such a way that a test specimen placed beneath the beam at support «B», will be loaded under compressive loading. By varying the ratio L/x and placing standard weights in the loading balance at end «C» of the beam, desired higher compressive stresses could be achieved at specimen location «B». For measuring deflections due to compressive forces, measuring devices were fixed both at location «B» and «C». The deflection measuring devices at beam end «C» include (i) a sliding pointer cum measuring rule (Fig.5.3), (ii) a dial gauge measuring nearest to 0.0001'' accuracy, (iii) a displacement potentiometer connected to strip chart recorder (pen on graph) and (iv) strain gauges with automatic recording arrangement of data acquisition system. From Fig. 5.3, it is apparent that the deflection of the specimen under compression test will be magnified at end «C» in proportion to the loading beam ratio $X:L$. The strip chart recorder, registers the deflection of the loading beam due to neoprene creep, continuously on a fixed chart paper, from the output of an LVDT. The pen movements of the recorder were controlled by voltages proportional to deflection and time speed.

Whereas at location of sample «B», deflections were measured with: (i) three dial gauges (0.001''), Fig. 5.4, (ii) microvernier, (iii) 2 strain gauges connected to the data acquisition system.

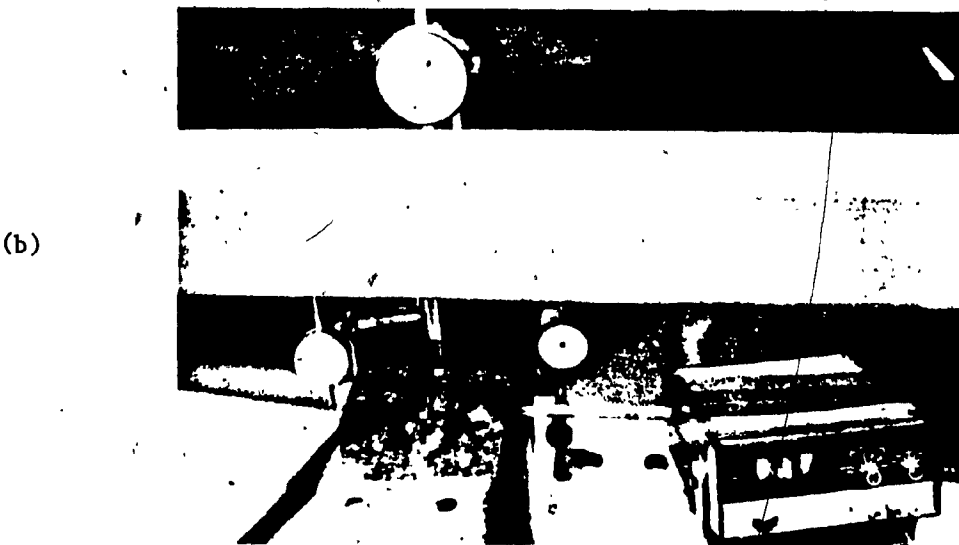
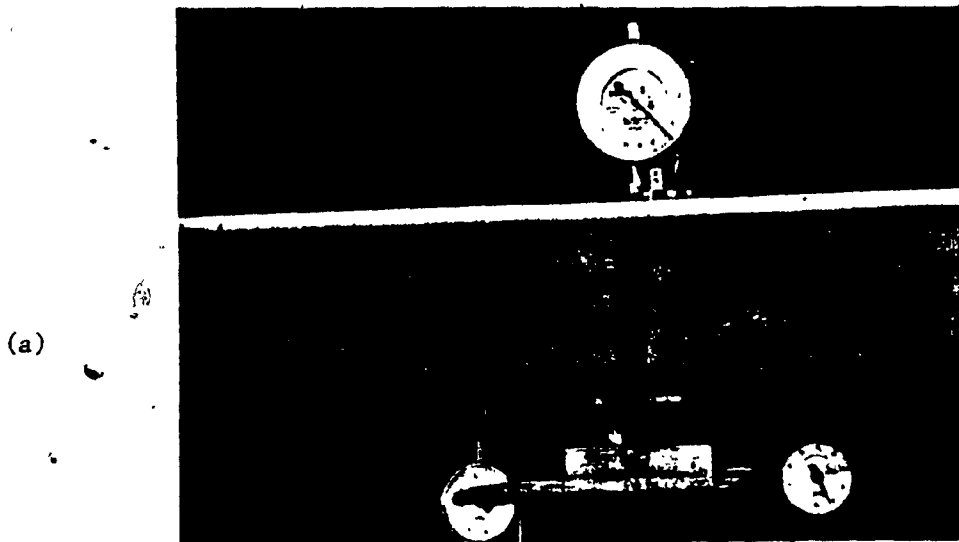


Fig. 5.4 (a) Deflection and (b) load, measuring arrangements at Location 'B' of the loading beam.

The compressive load at location «B» was sensed by means of a load cell of capacity ranging from 1,000 lbs. to 20,000 lbs. For measurement of creep in compression, the test sample was resting between two steel plates whereas 2 more plates were inserted, one between the top plate and the beam surface and the other between the load and bottom plate, so as to assure uniform compression on sample. Before loading the sample, the loading beam was resting on a mechanical screw jack and a hydraulic screw jack close to the sample location «B». The two different types of jacks were serving two different requirements: (i) while releasing the loading beam, to apply the loading smoothly and without overshoot so that the complete transfer of load is achieved in certain number of steps with pre-determined time limit (ii) to apply a sudden transfer load without an initial lapse of time.

Over a long time period of experiment there is a likely possibility of drift in the deflection measuring device and loading beam itself. To avoid the possible error due to drifting of loading beam, measurements of drifting of loading beam were conducted separately.

This particular set-up of testing arrangement was selected for the experimental study considering the range of high compressive stresses required for long periods of time. Another identical set-up, Fig. 3.3 (b), was developed, side-by-side, to verify the accuracy of results from the previous set up and also with added convenience of conducting two tests simultaneously.

5.2.2. Test Procedure

Each specimen tested for compressive creep was 25mm x 25mm x 20mm size. As used for the short term compressive tests, in the previous chapter, all samples were of 60H cut from sheet of neoprene to an accuracy of $\pm 0.0001''$. Five days prior to starting the sample testing, the loading beam itself was left resting on the screw jack so as to assure that further deflection of beam will be negligible. Measurements of beam deflection were recorded at 12 hour intervals for the first two days and at 24 hour intervals for the rest of the period.

The neoprene samples were placed between the steel plates (4'' x 4''). (Steel plates were used as readily available without any polishing or sandblasting). The completed assembly of the bearing sample was then placed between the load cell and loading beam at a position marked in advance, for desired compressive loading. Once the correct positioning is achieved, a load of 10 lbs. was applied as initial reading so as to make sure that sample is in a position to receive further loading.

Readings of all measuring devices at both location «B» and «C» were recorded corresponding to this 10 lbs. loading whereas, the strip chart recorder and data acquisition system were recording all readings continuously for the first 2 hours.

The most critical problem while loading the sample further and recording the deflection value was an uncertainty as to starting

point for measurement and plotting of creep. Above mentioned definition of creep defines creep as additional deformation under stress beyond immediate elastic deformation. The standards specify that a force shall be applied such that a strain of $20 \pm 2\%$ is realised after the time period before the first measurement is made and this first time period is recommended as 1 min. with further measurements after 10, 100, and each 1000 min. interval. Some of the existing data provides creep curves without any mention to this first measurement or rate of loading whereas, others use loading rate as 4% strain per minute until desired stress is reached.

Various ways of loading including different rate of loading to achieve the stress limit and thus corresponding time were considered (Appendix III). One of the sample strip-chart measurements is shown in (Appendix III). Due to this problem of defining initial deflection corresponding to 500 psi. stress, to verify with the available Dupont curves, tangent to the deflection curve at 2 min. time, Fig. 5.5, was decided to be the first deflection reading.

Deflection readings were recorded at intervals of every minute for the first 5 minutes and then at every five minutes interval until 30 minutes. Deflections after 15 minutes of time were slow in rate, hence, interval was increased gradually for the first 12 hours and then at after every 12 hours for the next 10 days (@ 14,200 minutes). The typical measurement record for 500 psi. and 800 psi. stress is shown in Fig. 3.2 , Appendix III. Also the typical output of strain gauge

measurements from Data Acquisition System is shown in Fig. III.3, Appendix III.

Three samples were tested for each stress condition shown in Fig. 5.10 and deflection measurements were recorded for 10 days period for each test.

Observations:

Typical test results illustrating various creep measurements and factors influencing them are given in Appendix III.

Creep test results at 500 psi. compression loading when plotted on a semi-log scale, do not show an overall good agreement with those given by du-Pont. Also, during the initial 1-day period, there is variation in creep values, which can be anticipated considering differences in recording initial deflections (Fig. 5.7.) Compression creep at the end of 10 days period also found to be just 20%, than that compared to 27%, resulted by du-Pont tests over the same period, Fig. 5.8.

Creep as deflection percentage of initial deflection corresponding to 800 psi., 1000 psi., 1600 psi., 2400 psi., and 3000 psi. compression loadings are plotted on same graph for comparison (Fig. 5.10).

Compressive creep at 3000 psi. loading is greater than that at 1000 psi. but not proportionately. At higher stresses the initial deflection

is higher and also the rate of creep. After 2 days period, the difference in creep values is almost constant for different stress values.

Thus, neoprene pads under higher compression, exhibit most of the creep during first day of loading, and the rate diminishes gradually over a period of 10 days.

The effect of normal creep of neoprene bearing pads under short term and long term compression has been reported by few researchers, Table 5.2, thus most of the creep occurs within the first 10-day period.

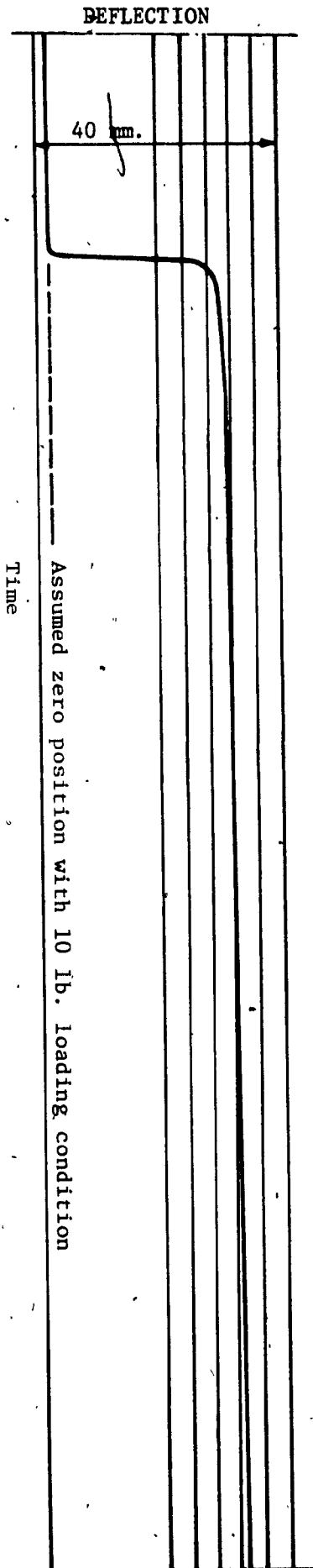


Fig. 5. TYPICAL ILLUSTRATION OF INITIAL CREEP OF NEOPRENE UNDER SUSTAINED 500 PSI. COMPRESSIVE LOADING.

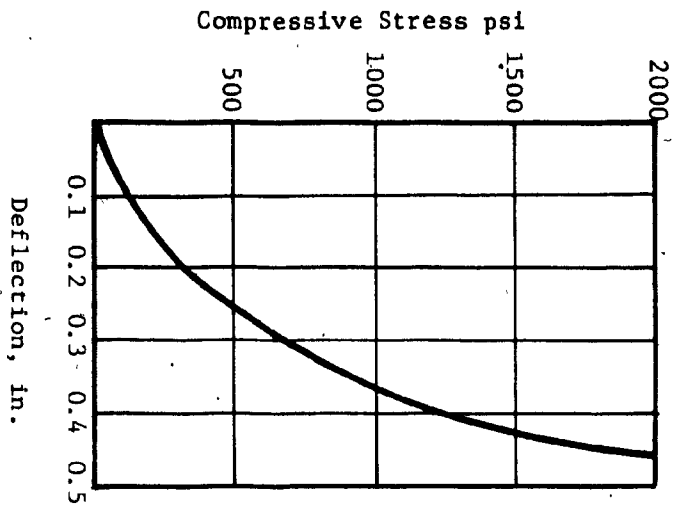
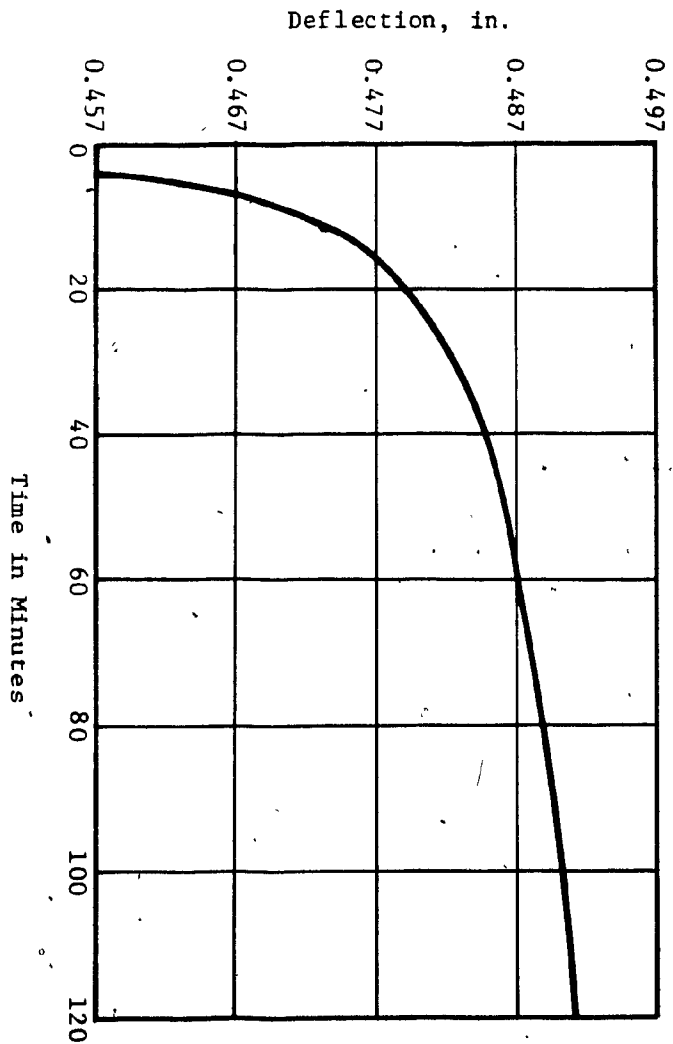


Fig. 5.6

SHORT TERM CREEP OF NEOPRENE 70H (4)



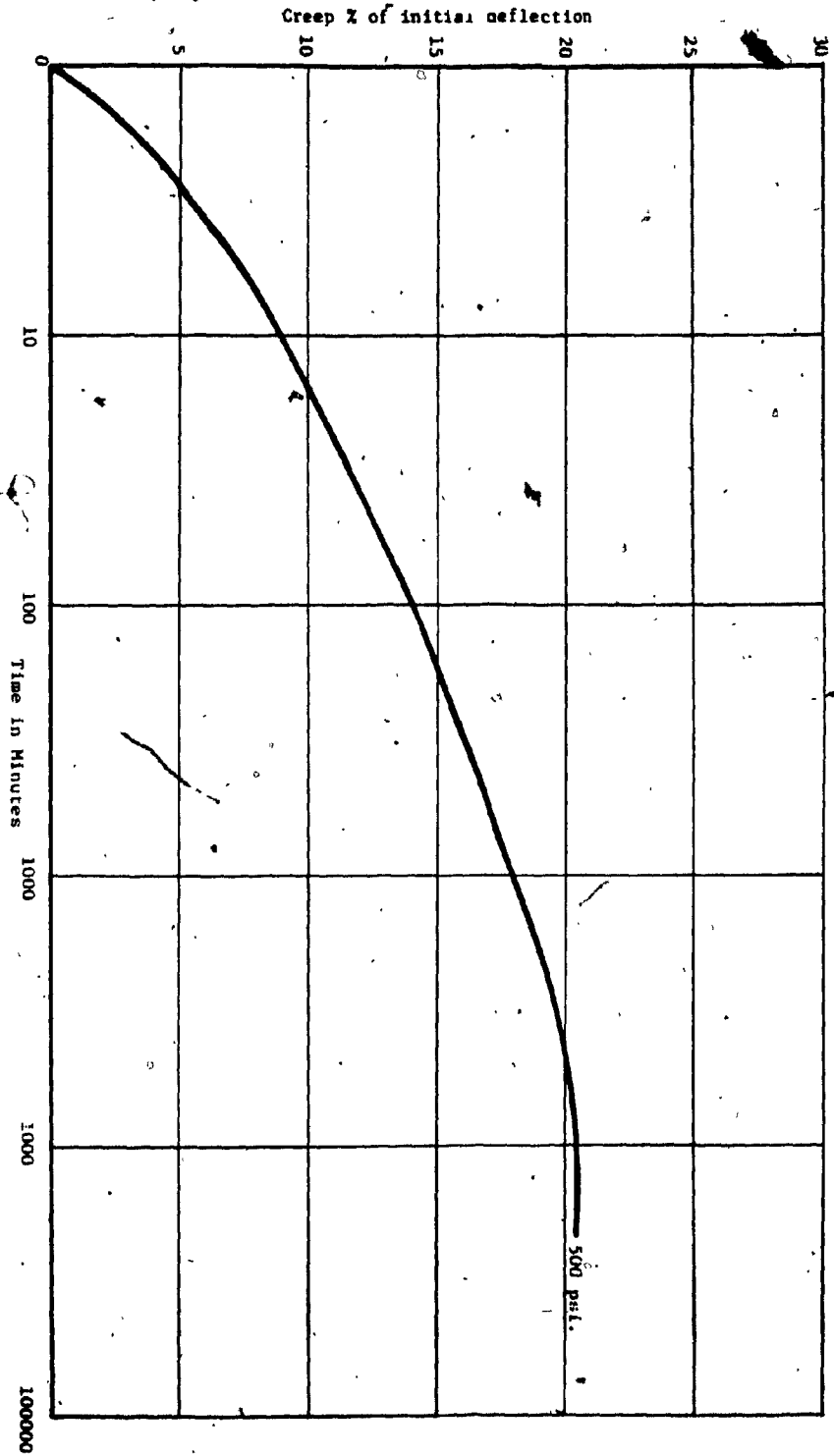


FIG. 5.7 CREEP OF NEOPRENE UNDER 500 PSI. SUSTAINED LOAD.

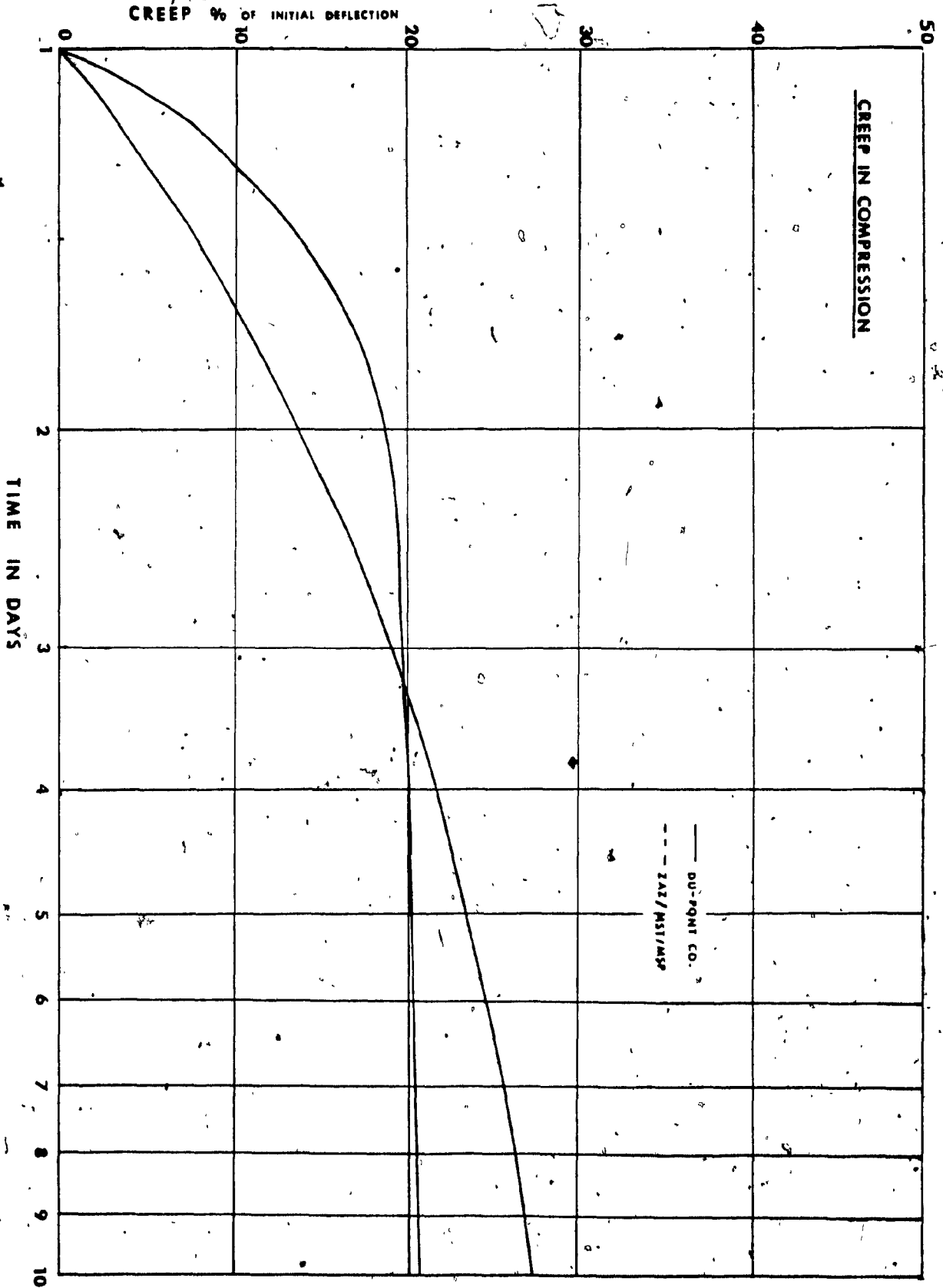


Fig. 5.8 Compressive Creep of Neoprene under 500 psi. sustained loading comparison with Dupont results.

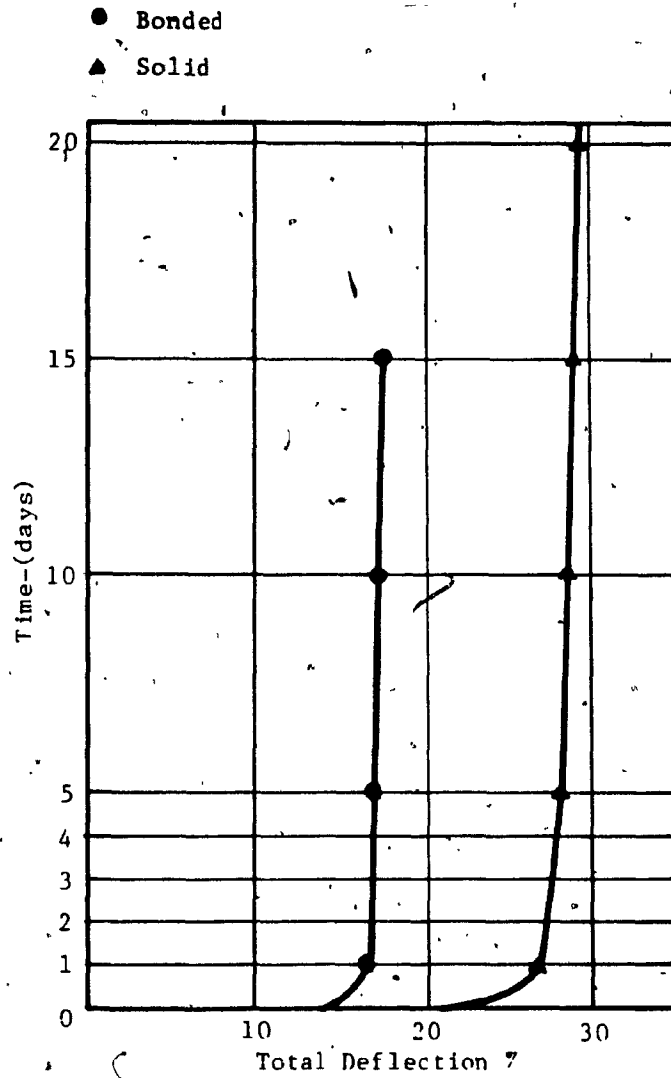


Fig. 5.9 VARIATION OF TOTAL DEFLECTION FOR SOLID AND BONDED PADS UNDER SUSTAINED STRESS OF 500 PSI. (77).

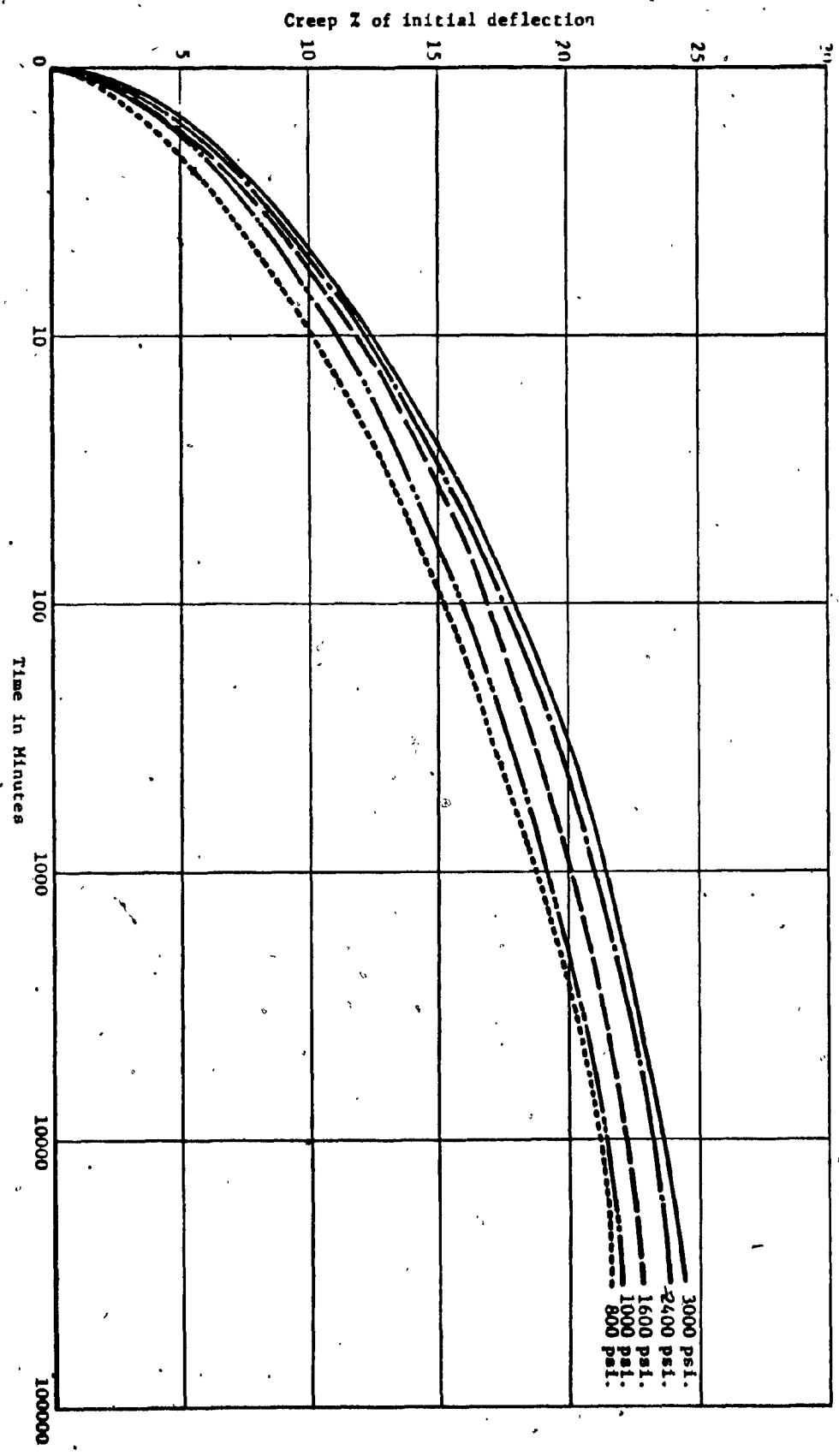
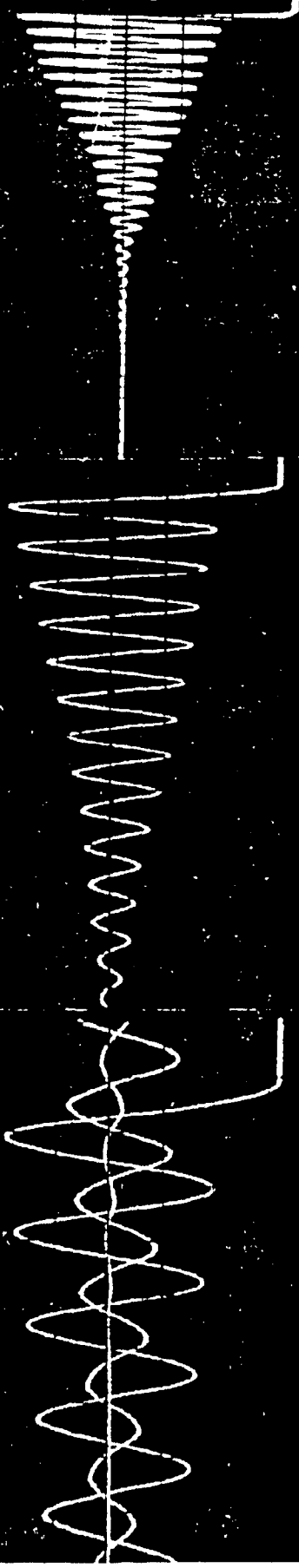
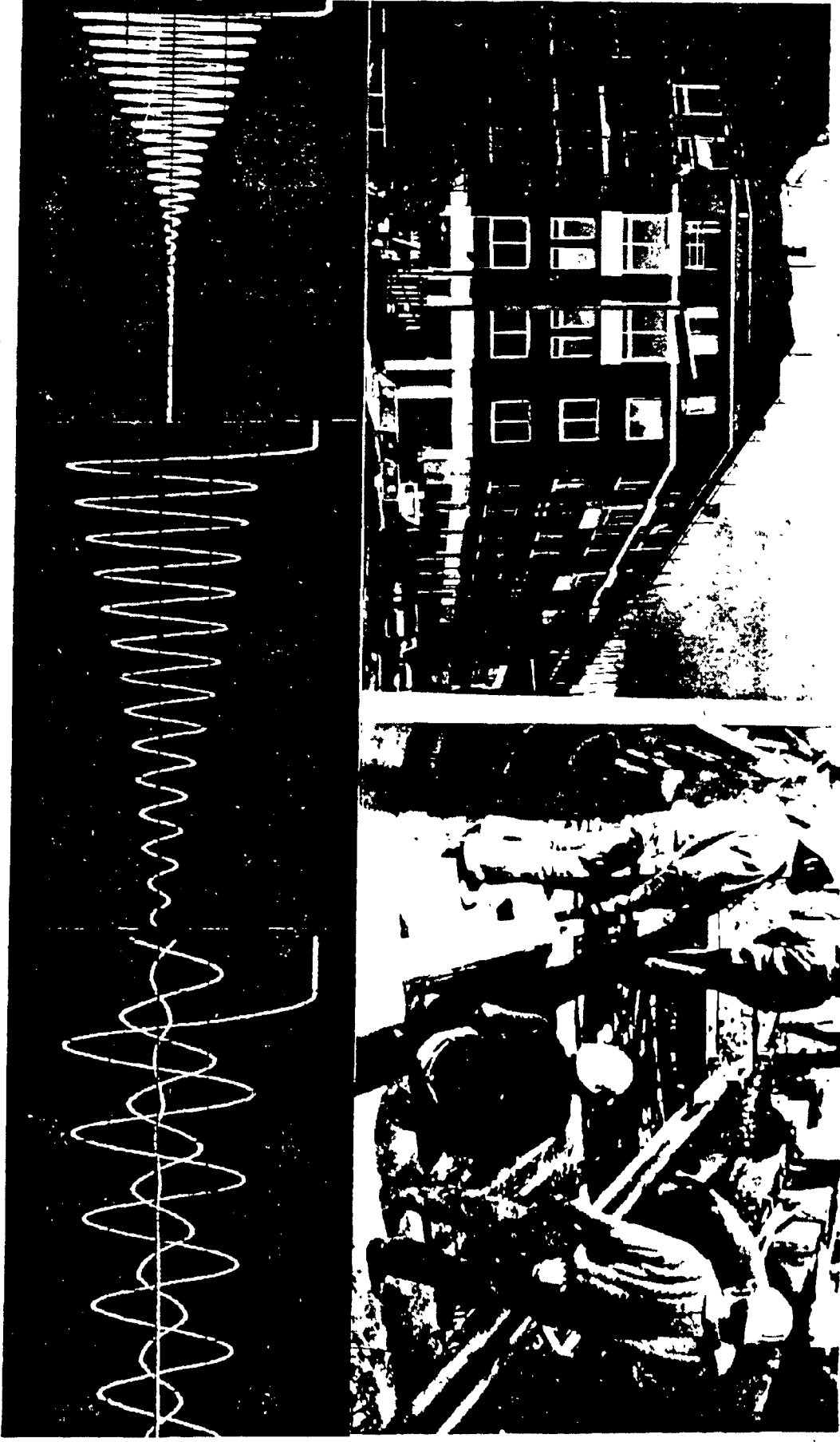


FIG. 5.10 COMPRESSIVE CREEP OF NEOPRENE UNDER VARYING SUSTAINED STRESSES (800 PSI. TO 3000 PSI).

5.5.4 Comparative study of available creep test data on neoprene
60H under sustained 500 psi. stress.

Researchers	First Period		Final Period		
	period	% of initial deflection	Period	% of initial deflection	
Du-Pont (ref. 19,20)	2 days 3 days	13.83	10 years	35%	
Crozier et al Transportation Research Record (Ref. 12)	initial	-	10 years	25%	
Long (ref. 130)	First week	25	6 months	40%	
Pare et al. Highway Research Board (ref. 5)	5 min.	2.7	Final	Additions 15% of vertical deflection	
	165 min.	6.1			
Aldridge et al. H.R.R. (ref. 7)	Solid	15 min.	20	20 days	29%
	Bonded	15 min.	12	20 days	19%
MSP				10 days	22%
Keen (Ref. 4)	initial deformation defines as deformation obtained 5 min. after loading. Fig. 5.6.				

C **H** **A** **P** **T** **E** **R**  **6**



CHAPTER 6

6. Vibration Damping and Isolation Properties

A brief description of the principles and applications of neoprene for supporting, damping and reduction of vibration effects is given. Results of an experimental study on the effectiveness of neoprene under higher compressive stresses, for damping and isolation of vibrations are studied in particular.

6.1. Summary of Previous Research

Numerous reports exist describing uses of elastomer as vibration isolation device under buildings, railway tracks, highway overpasses auditoriums, etc. A few of these references are already mentioned earlier. Description of various functions offered by neoprene have been reported by the author elsewhere (29, 87) before.

Dynamic properties of elastomers for damping and vibration isolation are discussed by Snowdon (99) and others (100, 101, 102, 103) whereas design data on damping properties of neoprene such as complex modulus, dynamic stiffness, etc., are provided by Purcell (103), Nashif (104), Kirchner (105), and others (43, 45, 94). Also, a survey on materials and systems for vibration isolation have been presented by Purcell (34), Ungar (35), Nichols (36) and others (37). Most of the literature reviewed is concentrated in

defining various degrees of damping and transmissibilities characteristics as functions of frequency and temperature.

Elastomers are mainly used for (i) static load distribution, (ii) absorption or control of vibrations and (iii) impact absorption. In all these cases the designer of these pads has to consider the (i) load deflection characteristics under varying compression loading, (ii) the long term creep behavior and (iii) the dynamic modulus and loss factor for damping capacity and force transmissibility.

6.2. Applications

A few of the examples where elastomers were provided to isolate low frequency vibrations and support heavy structures are described:

a) Next to an underground S-Bahn transit system in downtown Munich, a cultural center housing a concert house is under construction. Multilayered elastomeric mats, Fig. 6.1, were used below the S-Bahn system to reduce the vibration level at the foundation of the concert hall. The function of elastomer is to carry the heavy weight of the foundation elements and reduce vibrations by about 10 dB. Fig. 6.2 shows the installation of these mats underway.

Another example is a RHM center in London, England (39) where a 28 storey office tower is surrounded by main roads creating severe traffic noise and the new Victoria line tube tunnel was planned to



S-Bahn Tunnel during installation works.
(Courtesy of Müller - BBM GMBH, München).



Fig. 6.1 Elastomers, used for isolation of vibrations at S-Bahn system in München (Courtesy of Müller, München).



Application of elastomeric pads.



Fig. 6.2 Installation of multilayered elastomeric pads before bringing in the Ballast.

pass under the tower. Also, the dynamics of sway of the tower during strong winds became the controlling factor in the design of elastomeric pads. The 50mm thick laminated elastomer isolators were located at the top of a pile cap forming base for the main structural column. The function of neoprene isolators is to isolate the vibration induced noise and to provide uniform redistribution of stresses.

Various degrees of damping, shape, load-deflection characteristics, and transmissibility characteristics can be designed with elastomeric isolators.

6.3.1. Material Properties for Damping

When a stress is applied to elastomers, the strain always lags slightly behind the stress, and this lag can be important if the stress is varying rapidly. An important consequence of the phase difference between strain and stress is that a part of the energy put into the elastomer during increasing deformation is not returned during the recovery part of the cycle. When this force deformation relationship is plotted against each other as shown in Fig. 6.3, the large area within the hysteresis loop describes the energy loss per cycle due to damping.

The normal way of defining damping characteristics of elastomeric materials is in terms of complex modulus of elasticity E^* or complex

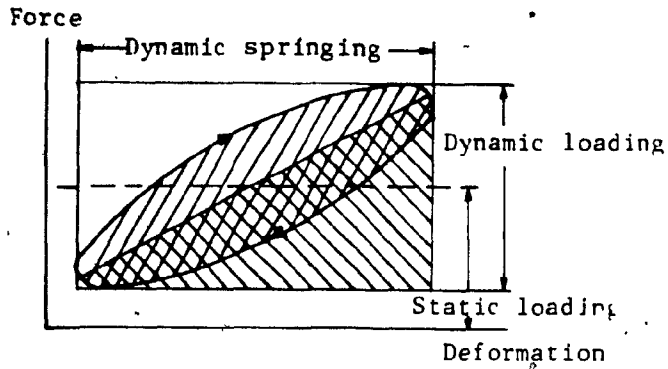


Fig. 6.3 - Schematic representation of the internal damping of rubber. The ellipse surface indicates energy loss.

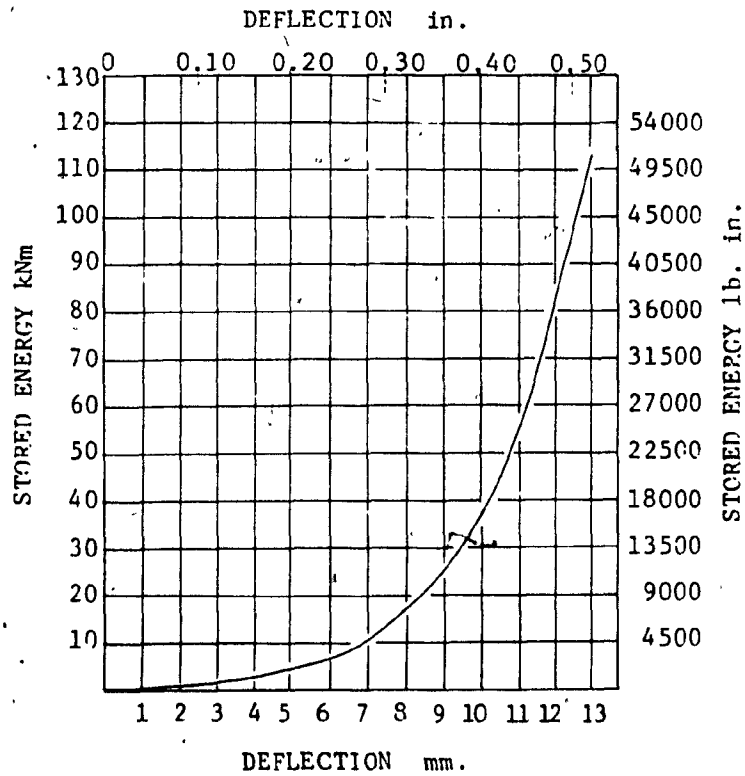


Fig. 6.4 - Energy storage in isolator which embodies neoprene in compression, determined by measuring area under curve in figure 4.10.

stiffness modulus K^* .

$$\begin{aligned} \text{where} \quad E^* &= E' + iE'' \\ \text{or} \quad &= E' (1 + i \tan \delta) \\ K^* &= K (1 + i \eta) \end{aligned}$$

where i signifies a component 90° out of phase, E' = elastic modulus, K = real part of the material stiffness, $\tan \delta$ = loss factor of material.

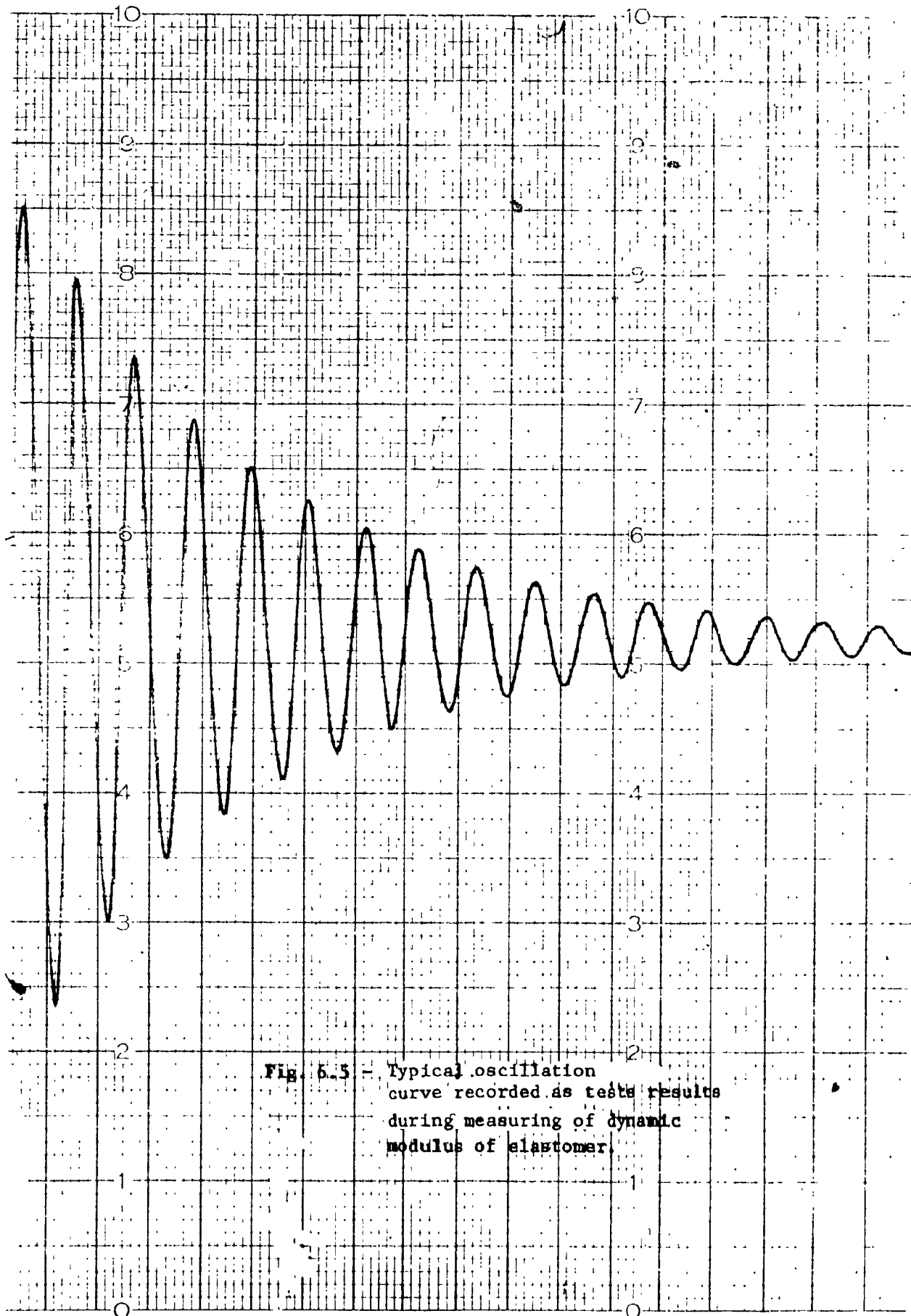
E and η are material properties and thus independent of specimen dimensions and shape. Damping effectiveness is generally expressed in terms of dimensionless number such as loss factor or damping ratio or percent of critical damping.

Tests on neoprene were conducted at McGill University on the torsional pendulum, for measurement of dynamic modulus of rubbers. Results of tests, conducted on neoprene at a temperature of 25°C , are shown in table 2.

Typical measurements recorded during the test program are shown in Fig. 6.5.

Table 6.1. Measurement of loss factor for neoprene H60 samples.

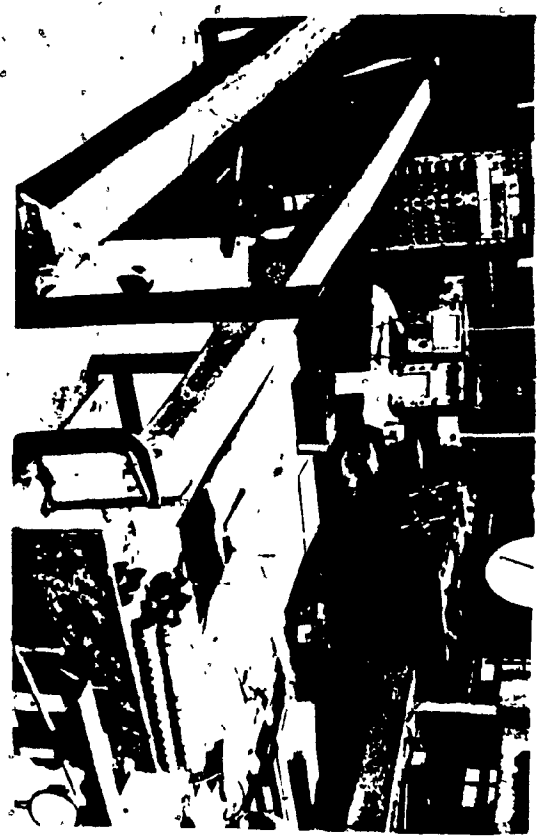
Period	Frequency	G' (SI)	G''	$\tan \delta$
2.6807	0.3720	1.980E 06	1.886E+05	0.092526
2.6834	0.3727	1.975E 06	1.913E+05	0.09690



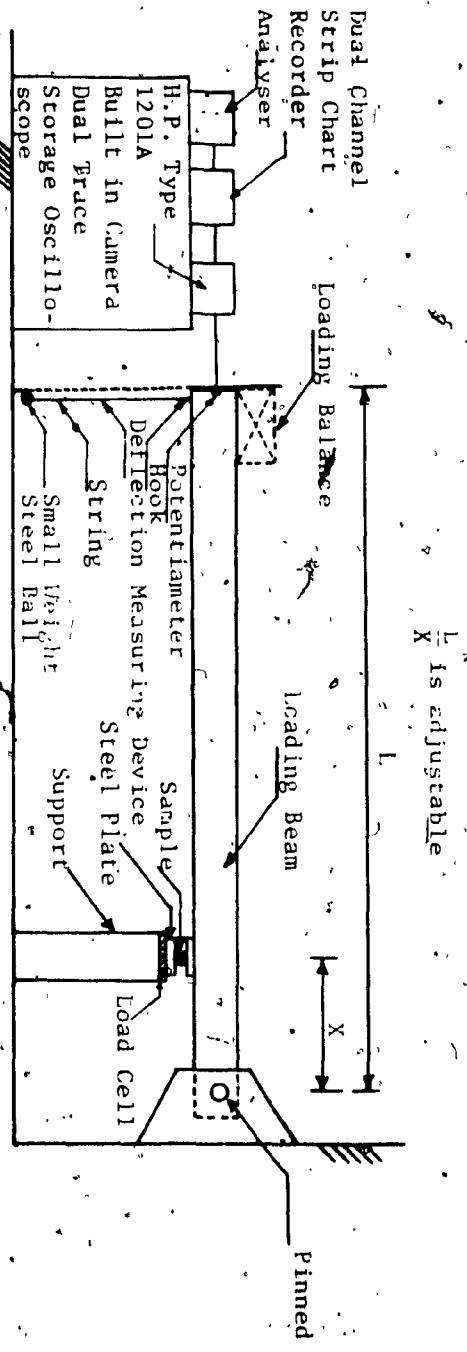
6.3.2. Damping Capacity of Neoprene

Damping is usually defined by the logarithmic decrement, where a high damping capacity material exhibits a numerically large decrement. Fig. 6.6 (a) and (b) shows the testing arrangement developed at Concordia University for measurement of the logarithmic decrement. When the loading beam is in state of free vibration, the amplitude of vibration is reduced in an exponential manner $\Delta = \log_e (x_1/x_2)$ (where x_1 and x_2 are successive amplitudes in a free vibration).

For measurement of the damping characteristics under variable higher stresses, samples were compressed by the loading beam by varying the L/x ratio and by adding required weights in the loading balance. A small mass ($m = 3.248$ kg) was hanged at the end of the beam, sudden removal of which gives the free vibration oscillations at end C. Comparable tests were conducted using neoprene or steel as bearing pads (Fig. 6.6). Test results are shown in Table 6.1. Each value of Δ , shown in the Table, is average from five repeated experiments. The discrepancy recorded was not more than 5%. Table 6.1 shows that at higher stress, the natural frequency also reduces, and both steel and neoprene pads show comparable behavior. The deviation in values of Δ calculated at 1st cycle and after 4 cycles is found to be close. At higher stress, i.e. 2500 psi (17.17 MPa), the natural frequency also decreases considerably giving very low damping



(a)

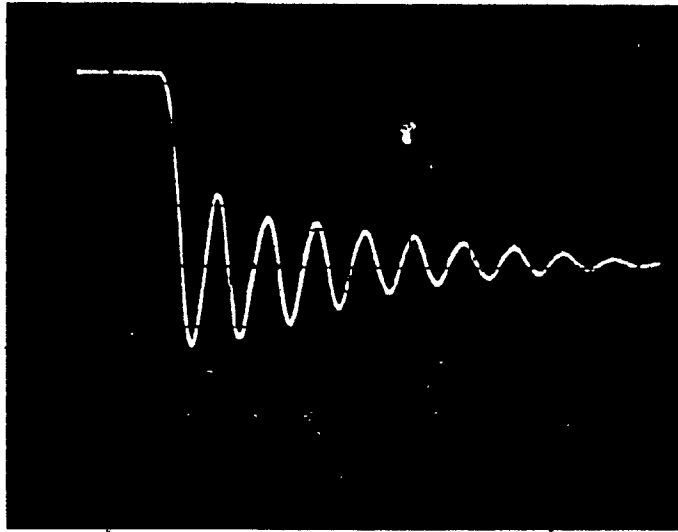


(b)

Fig. 6.6 - Set-up for measuring damping capacity of neoprene under varying high compressive stresses. (a) View of set-up (b) Schematic of set-up.

N53

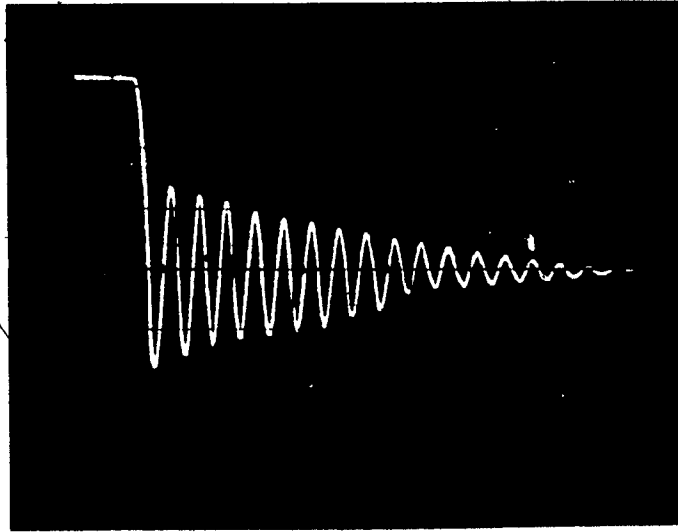
NEOPRENE 500 psi

CAL. SENS.
100 gm./Div.

Time BASE 0.2 SEC./Div.

S52

STEEL PLATE 500 psi



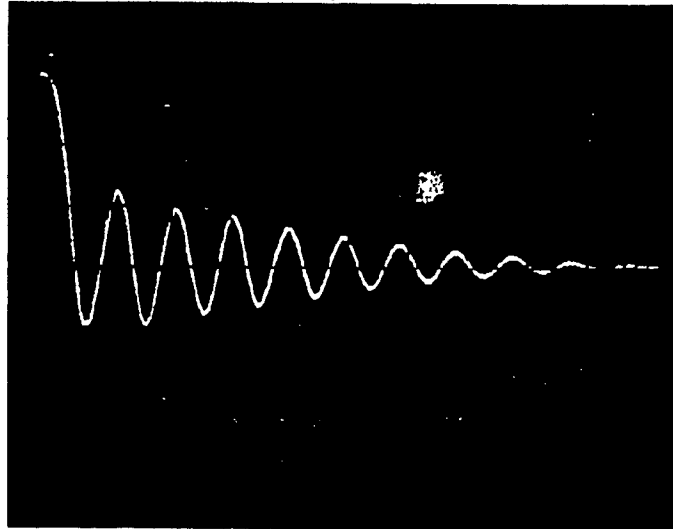
SEN. 2 MV/Div.

Time BASE 0.2 SEC./Div.

Fig. 6.7 - Free vibration oscillations for neoprene and steel pads under 500 psi. stress.

N 81

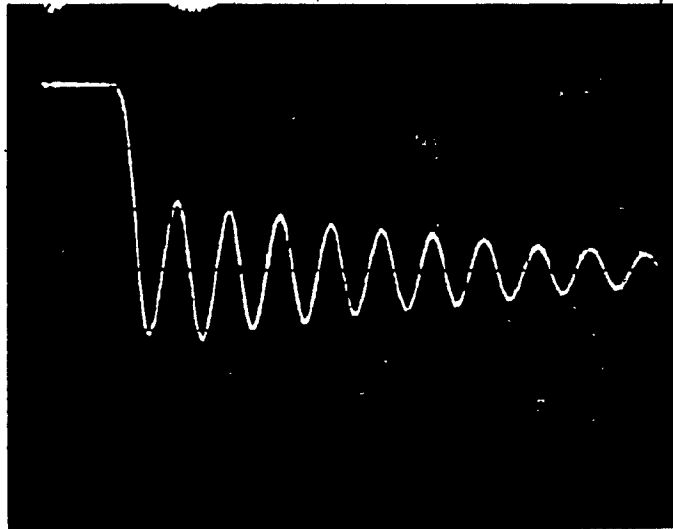
NEOPRENE 800 psi.



TIME BASE 0.2 SEC./DIV.

S 82

STEEL PLATE 800 psi.

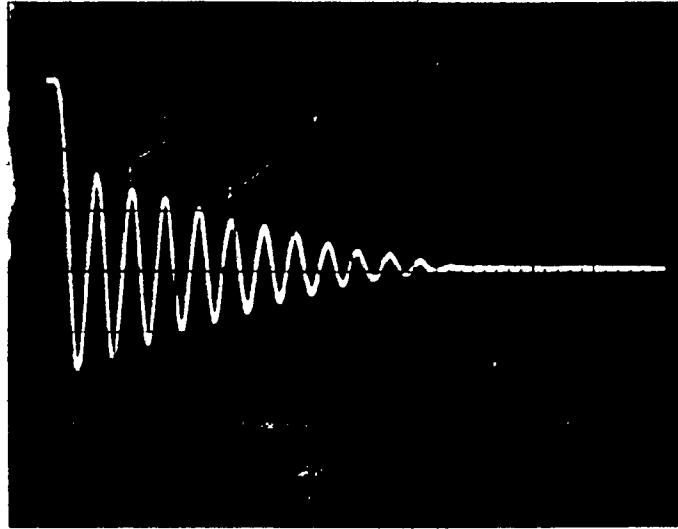


TIME BASE 0.2 SEC./DIV.

Fig. 6.7 - Free vibration oscillations for neoprene and steel pads under 800 psi. stress.

N152

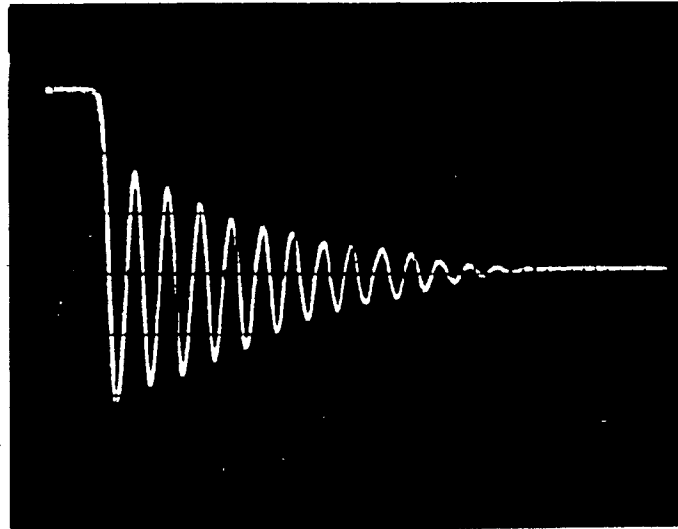
NEOPRENE 1500 psi.



TIME BASE 0.5 sec./Div.

S152

STEEL PLATE 1500 psi.

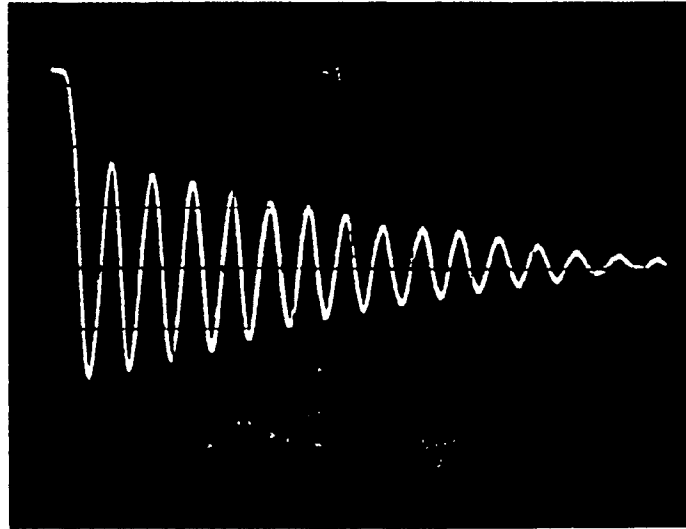


TIME BASE 0.5 sec./Div.

Fig. 6.7 - Free vibration oscillations for neoprene and steel pads under 1500 psi. stress.

N201

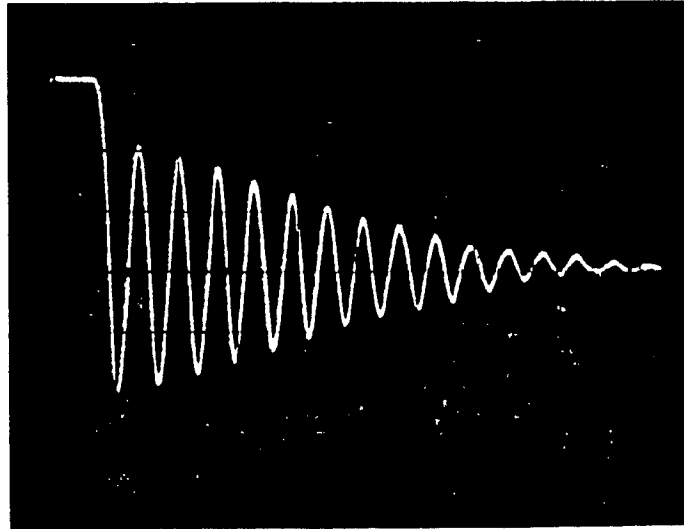
NEOPRENE 2000 psi.



TIME BASE 0.5 Sec./Div.

S201

STEEL PLATE 2000 psi.

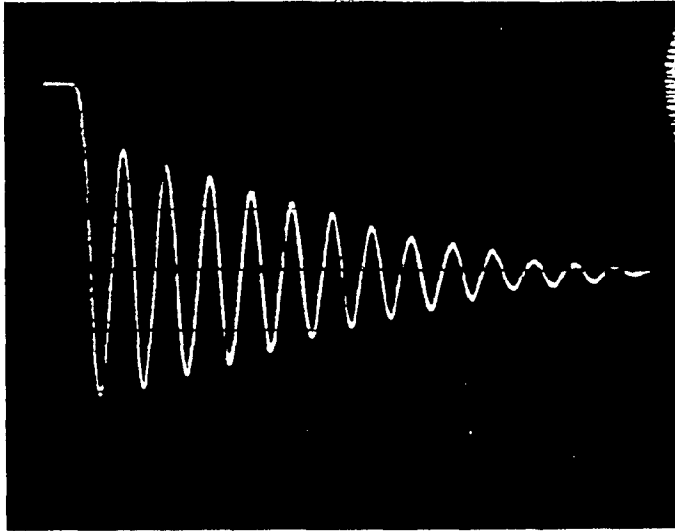


TIME BASE 0.5 Sec./Div.

Fig. 6.7 - Free vibration oscillations for neoprene and steel pads under 2000 psi. stress.

N 253

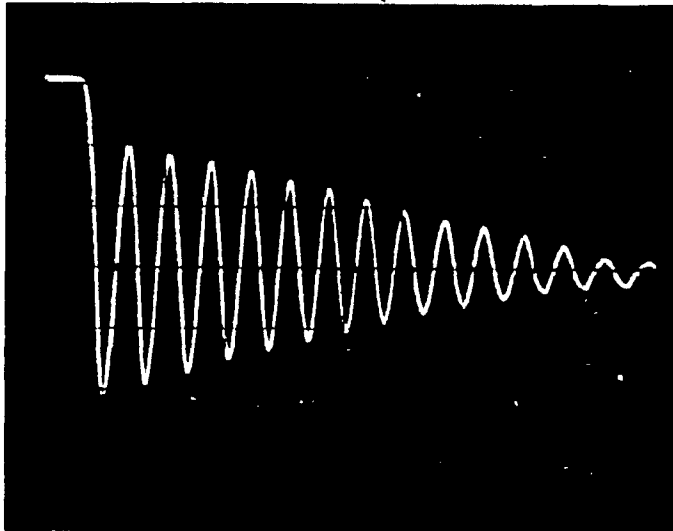
NEOPRENE 2500 psi.



TIME BASE 0.5 Sec./Div.

S 252

STEEL PLATE 2500 psi.



TIME BASE 0.5 Sec./Div.

Fig. 6.7 - Free vibration oscillations for neoprene and steel pads under 2500 psi. stress.

Table 6.1 Experimental results for measurement of damping characteristics of Neoprene under varying compressive stresses.

Photo No.	Stress* psi MPa	Material***	Frequency Hz	$\log \frac{x_1}{x_2}$ **	$\frac{1}{4} \log \frac{x_1}{x_5}$ **	Δ ****	Notes
N53	500	3.43 Neoprene	6.25	0.29	0.275	0.283	Indicates good
S52	500	3.43 Steel	12.5	0.12	0.103	0.112	energy transfer
N81	800	5.5 Neoprene	5.46	0.25	0.240	0.245	Present stress
S82	800	5.5 Steel	5.55	0.154	0.134	0.144	limit
N152	1500	10.3 Neoprene	3.57	0.174	0.167	0.171	
S152	1500	10.3 Steel	3.84	0.128	0.164	0.146	
N201	2000	13.74 Neoprene	3.25	0.121	0.117	0.119	Neoprene is set
S202	2000	13.74 Steel	3.13	0.101	0.128	0.114	in compression
N253	2500	17.17 Neoprene	2.5	0.118	0.133	0.125	Neoprene is inefficient in transferring energy
S252	2500	17.17 Steel	2.94	0.09	0.101	0.100	

*Stress measured on the sample resting on the load cell

**Calculated values of logarithmic decrement are taken from average of five experiments

***Both neoprene pad and steel plate are of same size (25.4 mm x 25.4 mm x 20 mm)

****2% - 5% error is obtained due to end connection of the beam and oscilloscope time base sensitivity

effect. Neoprene is almost set in compression with very low dissipation of energy. It can be expected that layered pads will be more efficient due to shear contribution.

6.4. Vibration Isolation

An effective means of reducing structure borne noise and vibrations is to separate physically the structure and interpose elastomers between them.

Whereas the detailed description of elastomeric properties and techniques used for isolation is beyond the scope of this study, the discussion is limited to damping and transmissibility effectiveness at varying higher stresses.

The transmissibility, through mounting in one direction, neglecting motions in other directions, is given by

$$T_R = \frac{1}{\sqrt{1 + \eta^2 / (1 - \Omega^2 / \omega^2)^2 + \eta^2}}$$

where Ω = input frequency in Hz, ω = mounting frequency Hz and η = loss factor.

Corresponding to $\eta = 0.095$ as recorded (see Table 2), the transmissibility of vibration curve is shown in Fig. 10 (Davey 1964).

As seen in Fig. 6.8, reduction in transmission (force,

acceleration, etc.) can be obtained only for values greater than $\sqrt{2}$ of the frequency ratio. Below this frequency, the isolator is no longer effective for isolation.

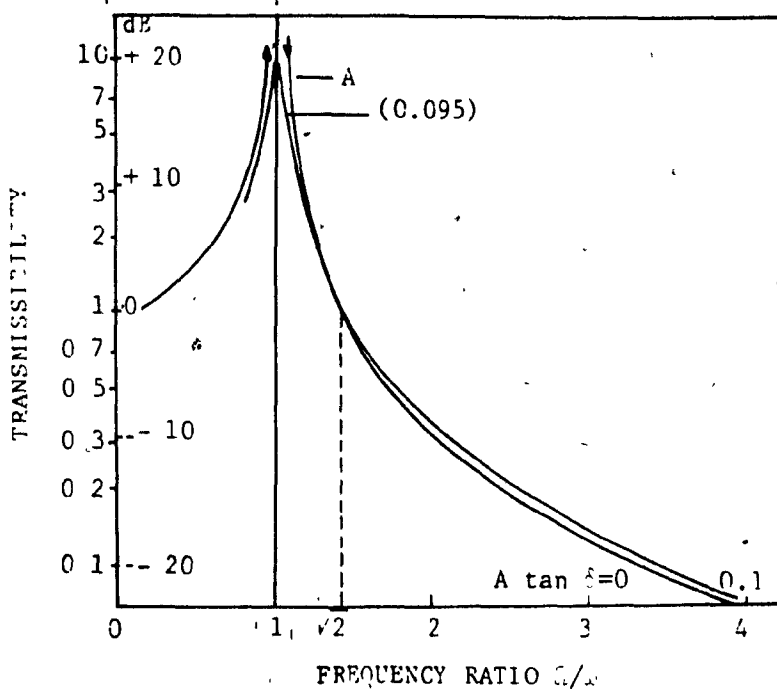


Fig.6.8- Unidirectional transmissibility of a mounting as a function of frequency ratio for experimentally found loss factor. For neoprene ($\tan \delta$) = 0.095. Curve A is for zero damping and the transmissibility goes to infinity at $\Omega/\omega = 1$.

C H A P T E R 7



CHAPTER 7

7. NEOPRENE BEHAVIOR UNDER EXCESSIVE COMPRESSION

Behavior of neoprene bearing pad under excessive compressive stresses is described in this chapter. Based on experimental results and available test data an attempt is made to define the ultimate strength or excessive load carrying capacity for these pads. Potential causes and criteria of failure are discussed. Expected life period of elastomers predicted by various authorities based on experience is also given in comparative form.

7.1. Excessive Compressive Stresses

From the compression deflection curves described in Chapter 4, it has been observed that after approaching certain loading, corresponding increase in deflection is almost negligible. Neoprene is no more capable for serving its required functions such as to provide necessary horizontal, vertical, or rotational movements.

Thereby, it can be stated that under higher compressive stresses of the order 10,000 to 20,000 psi., neoprene pads is squeezed out, and remains as bearing film. Researchers (130), based on experience, have proposed maximum permissible stress for neoprene of 10 tons/in² but not more than the permissible pressure on the support material.

(steel or concrete). However, the maximum permissible stress for neoprene is yet disputable.

7.2. Ultimate Strength

From the experimental findings it can be stated that neoprene bearings can be loaded satisfactorily for stresses more than 4000 psi. and further they can withstand stresses as high as 16,000-18,000 psi. However, it has been proved that rubber material can support a stress of 10,000 psi. without affecting adversely, and it has been stressed up to 40,000 psi., safety signs (69).

Recent tests on neoprene (du Pont 1981,20) have demonstrated 5,000 psi. (34.5 MPa) as safe load bearing capacity with extended ability to withstand stresses up to 10,000 psi. (69 MPa), whereas other tests (12), conducted on Full-size 55 H neoprene bearings have exhibited ultimate strength of 1,600 psi. (11.0 MPa).

7.3. Failure Criteria and Causes

Failure of elastomeric pads is hard to define both experimentally as well as theoretically (110). Kuhn (U.S.S.R.) has proposed a mechanism for the failure of elastomers under higher stress based on a statistical model of the network of non-Gaussian chains, how-



Fig. 7.2

Splitting along lateral surfaces.



Fig. 7.1 Permanent distortion of neoprene pad tested at compressive stress 18000 psi (Prindipal tear at an angle of 45°).

ever, recent studies in Poland (95) have concluded different failure region than that expected theoretically.

During the experimental tests conducted by the author, at compressive stress of 20,000 psi (140 MPa), and long term compressive creep under 3,000 psi., it has been observed after unloading the test sample has slight tears at an angle of 45° , Fig. 7.1, or along the lateral surface, Fig. 7.2, appears. This is due to excessive bulging of free sides of elastomers, Fig. 7.3. Thus, the so-called failure expects to be of slow progressive nature due to deterioration or excessive deformation. These observations confirm the test results provided by others (2, 6, 7) on similar pads (Fig. 7.4).

Few of the possible causes of elastomeric failure can be summarized as:

- (i) From the short term compressive tests conducted by Grote (German rules (70)) concluded that failure of elastomeric bearings always occurs by rupture of steel plates, Fig. 8.1.
- (ii) Due to excessive bulging, elastomers tend to flow laterally under higher compression. Thus, the friction between structural elements and elastomers produces splitting forces (70) proportional to stress and elastomer thickness which are large enough to destroy concrete, Fig. 2.4.
- (iii) An uneven seating can cause breakdown of bond between elastomer and steel plates. Disintegration of bearing seatings has been stated as the most common cause (BE 5400, Part 9) of bearing

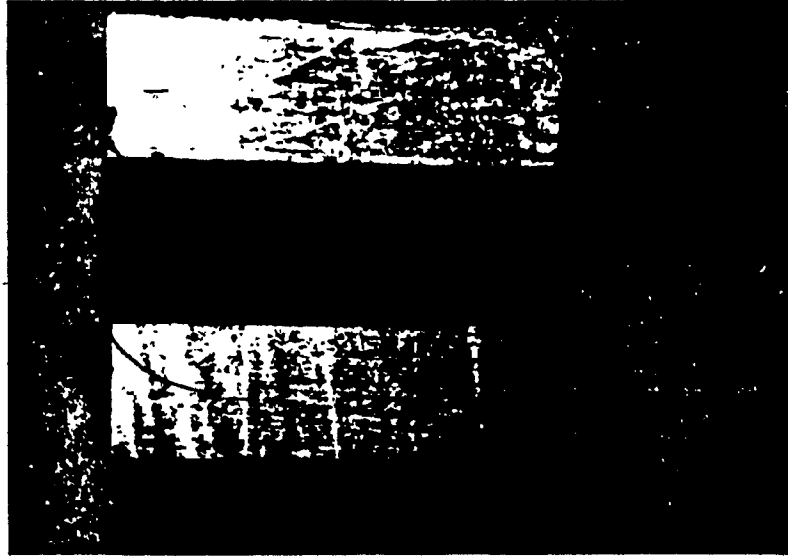


Fig. 7.3 Bulging along line EF under compression:
Tension along points E and F (free sides of pad).

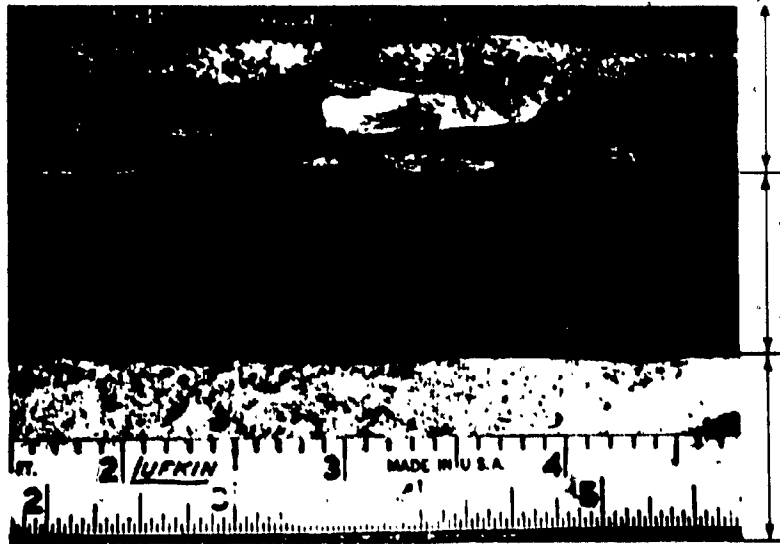


Fig. 7.4 Typical splitting failure due to repeated loading.
(N.R.C. Washington, D.C.)

failure and has recently been highlighted at the Greavelly Hill Motorway, Birmingham, England.

(iv). The greatest cause of bearing malfunction is being reported

(56) because of inadequate or improper installation.

7.4 Predicted Life of Elastomeric Bearings:

AUTHORITIES Ref. No.	PREDICTED LIFE
1 Lindley (58)	<ul style="list-style-type: none"> Well formulated material in well designed bearings under compressive stress lives in excess of <u>100 years</u>
2 BS 5400 : 9A Lee (56)	<ul style="list-style-type: none"> Expected 100 years but cautious Facilities for replacement and measures for correcting the effects of differential settlements, movements should be provided
3 Long (101)	<ul style="list-style-type: none"> Limited life of 45-80 years Replacement provisions be made while designing the structure
4 NRPRA ()	<ul style="list-style-type: none"> 100 years for natural rubber
5 Dupont (19, 20)	<ul style="list-style-type: none"> 50 years or more for neoprene
6 Brielmater (10)	<ul style="list-style-type: none"> Live load and low temperature over a long period in case of bridges reduces the effectiveness of neoprene bearing pads gradually
7 Marsh (106) Henderson (107) Steffens (108)	<ul style="list-style-type: none"> With reasonable tolerances elastomers can perform satisfactorily for the life of the building With proper maintenance, life of structure For <u>reasonable life</u>, design <u>compressive stress</u> should be <u>less</u>



C

H

A

P

T

E

R



8

CHAPTER 8

GENERAL CONCLUSIONS AND RECOMMENDATIONS

The test program in this research study was limited in scope, mainly to study the behavior of neoprene pads under excessive stresses due to overloading of structures. Variables such as shape factor, thickness, hardness, etc. and influence of temperature variation have not been included in these studies.

In general, it can be concluded that properly designed and installed elastomeric bearings can be subjected to stresses in excesses of current design limitations. The acceptance of excessive stress value, however, depends on various factors (partially described in Chapter 2,4,5).

The compression-deflection curves established in our test results indicate that compressive deflections decrease with increasing shape factor and restriction of bulging effect by means of steel plates. By allowing less free area for expansion, the compression squeeze reduces by almost 25-30% for same shape factor; rate and time of loading.

It has been observed that at higher compressive stresses, further increase in deflection for a corresponding increase in load is reduced and neoprene has reduced capacity of serving such functions as to provide necessary horizontal, vertical or rotational movements. Thus at stresses in the range of 10,000 to 20,000 psi., considering various influencing parameters, neoprene pads shall be treated simply as bearing pad improving surface

contact between support and supported structure. When the pad is larger than or equal to the bearing area, bulging along edges produces combined stresses that may cause the pad to split or tear. Pads under sustained high compressive stresses exhibit slight tears on the unloaded surface (surface at 90° to the loading direction) and splitting along the lateral surface (along loading direction). The failure occurring in this form were of a relatively slow progressive nature and not rapid.

In some instances it may be important to consider creep deformation which may be more than 30% of initial deflection. Creep deflection as a percentage of initial deflection based on our tests is shown in Fig. 5.10. Existing du-Pont standard compressive creep curves are prepared for 500 psi. stress. From our creep test results for higher range of stresses 500 psi. to 3000 psi., it can be observed that under higher stress creep curves are different.

The size of pad also influences significantly the behavior of neoprene pad (Fig. 4.17). It must be considered while establishing the performance of neoprene pads in service.

Further research should include developing of an analytical model describing the strength and behavior of neoprene based on elastoplastic behavior and considering molecular structure and rheological aspects.

REFERENCES

1. Lindley P.B., 'The stiffness of rubber springs', in 'Use of rubber in engineering', edited by Allen P.W., Lindley P.B. and Payne A.R., Maclaren & Sons Ltd. London 1967, p. 1-23.
2. Lindley, P.B., 'Natural rubber structural bearings', World Congress on Joint Sealing and Bearing Systems for Concrete Structures ACI Publication, SP-70, p. 353-377.
3. Rejcha C., 'Design of elastomeric bearings', PCI Journal Vol. 9, No. 5, Oct. 1964, p. 62-78.
4. Pare R.L. and Keiner E.P., Charles A. Maguire Associates, 'Elastomeric Bridge Bearings', Highway Research Board Bulletin 242, July 1960, p. 1-19.
5. Crozier W.F.; Stoker J.R.; Martin V.C. and Nordlin E.F., 'Laboratory Evaluation of full size elastomeric bridge bearing pads, Transportation Research Board no. 547, 1976, p. 55-58.
6. Nordlin E.F.; Stoker J.R.; and Trimble R.R., 'Laboratory and field performance of elastomeric bridge bearing pads', Highway Research Record #253, 1967, p. 84-96.
7. E.I. Du Pont de Nemours and Co., 'Elastomeric Bulletin no. 3A Sept. 1981, Wilmington, Delaware 19898.
8. Spitz I., 'The design and behavior of elastomeric bearing pads' Die Siviele Ingenieur in Sud Afrika Vol. 20, n.9, Sept. 1978, p. 219-229.
9. E.I. du Pont de Neumours and Co., 'Design of Neoprene Bridge Bearing Pads', Nov. 1959, Wilmington, Delaware, p. 25.

10. Proposed ASTM Specifications D 4014, 'Standard Specification for Plain and Steel-laminated elastomeric bearings for Bridges', April 1981.
11. Ministry of Transport, 'Provisional Rules for the Use of Rubber in Highway Bridges', M.O.T. Memorandum no. 802, H.M.S.O. London, Jan. 1963, p. 3-19.
12. Bell L.W.; Shloss A.L.; and Subramanian N.S., 'Additional Design Data Based on Full-Size Bearing Pads of Neoprene', World Congress on Joint Sealing and Bearing Systems for Concrete Structures, ACI Publication SP-70, p. 1087-1099.
13. Leonhardt Fritz, 'From past achievements to new challenges for Joints and Bearings', World Congress on Joint Sealing and Bearing Systems for Concrete Structures, ACI Publication SP-70, p. 735-760.
14. Eggert H., 'Lager Feur Bruecken Und Hochbauter', (Bearings for bridges and tall buildings), Bauingenieur, Vol. 53, n.5, May 1978, p. 161-168 (In German).
15. Joe J.A., 'Bridge Bearings; The influence of research', Highway and Public Works, Vol. 48, n. 1847, Oct. 1980, p. 14, 16, 18-19.
16. Lee D.J., 'The theory and practice of bearings and expansion joints for bridges', Cement and Concrete Association, 1971.
17. Davey A.B. and Payne A. R., 'Rubber in Engineering Practice', Maclaren & Sons Ltd, London 1964, p. 25.
18. National Cooperative Highway Research Program Synthesis of Highway Practice, 'Bridge Bearings', no. 41, 1977, p. 30-48.
19. Rubber Bearings on Thames River, Civil Engineering (U.S.), Jan. 1982, p. 12-13.

20. Stranaghan G., 'Rubber Bearings for Economical Bridge Design', World Congress on Joint Sealing and Bearing Pads of Neoprene' p. 187-195.
21. Torr R.P., 'Bridge Bearings' in 'Use of rubber in Engineering' edited by Allen P.W. et al, Maclaren and Sons, London, 1967, p. 146-157.
22. Beyer E. and Wintergerst L., 'New Bridge Bearings: New types of support', Der Bauingenieur, Vol. 35, No. 6, p. 227-230.
23. Topaloff B., 'Rubber Bearings for Bridges: Calculation and Application', Der Bauingenieur, Vol. 39, No. 2, 1964, p. 50-64.
24. Gent A.N., 'Rubber Bearings for Bridges', Rubber Journal and International Plastics, Oct. 17, 1959, p. 2-4.
25. Graves J.R., 'Rubber Seats for Prestressed Beams', Engineering News Record, May 16, 1957, p. 67.
26. Anon, 'Girder rest on elastomeric pads', Engineering News Record, April 2, 1964, p. 101.
27. Brandt A.M., 'Nowe Roswiazania Lozysk Mostowych' (New Solutions for the Bridge Bearing Design), Inx Budowinctwo, Vol. 32, No. 8-9, August-Sept. 1975, p. 392-396. (In Polish).
28. Derek H., 'Bridge Bearings', Civil Engineering (London), Oct. 1976, p. 44-45, 48.
29. Zielinski Z.A.; Troitsky M.S. and Pimprikar M.S., 'Elastomers for Vibration Control in Construction Engineering', Proc. International Conference on Construction Practices and Instrumentation in Geotechnical Engineering, Surat, Dec. 20-23, 1978, p. 373-379.
30. Hirshfield C.F. and Piron E.H., 'Rubber Cushioning Devices', ASME Trans. Vol. 59, 1937, PRO-59-5, p. 482-485.

31. Snowdon J.C., 'Vibration Isolation: Use and characterization', Rubber and Chemistry Technology Vol. 53, p. 1041-1087.
32. Gent A.N., 'Elastic Stability of Compression Springs', J. of Mechanical Engineering Science, Vol. 6, no. 4, p. 318-326.
33. Hull E.H., 'The use of rubber in vibration isolation', Trans. ASME J. of App. Mechanics, Vol. 59, 1937, p. A109-A114.
34. Purcell W.E., 'Materials for Noise and Vibration Control', S/V, Sound and Vibration, 11(7), July 1977, p. 4-29.
35. Ungar E.E. et al, 'Prediction and Control of Vibrations in Buildings', Shock and Vibration Dig., 8(9), Sept. 1976, p. 13-24.
36. Nichols J.F., 'Case Histories of Practical Noise Attenuation of Construction Plant and Equipment', Proceedings Vibration and Noise Control Engineering, Sydney, Australia, Oct. 11-12, 1976, p. 137-138.
37. Northwood T. D., 'Isolation of Building Structures from Ground Vibration', ASME Design Engineering Technical Conf. on Isolation of Mechanical Vibrations; Impact; and Noise, Cincinnati, Ohio, 1973, p. 87-100.
38. Reed A.J., 'Sound and Vibration Isolation of Large Structures', in 'Use of Rubber in Engineering' edited by Allen P.W.; Lindley P.B. and Payne A.R., Maclaren and Sons, London, 1967, p. 197-203.
39. Crocker R.J., 'Construction of the RHM Centre on Resilient Mountings', Insulation, July 1972, p. 173-178.
40. Grootenhuis P., 'Resilient Mountings of Large Structures', in Elastomers: Criteria for Engineering Design', edited by Hepburn C.; and Reynolds R.J.W., Applied Science Publishers Ltd. London, Chap. 13, p. 219-240.

41. Liquorish A.D.; Director TICO Manufacturing Ltd., Surrey, London, 'Neoprene Bearings in Structural Applications', Personal Correspondence, March - April 1983.
42. Newland D.E.; Professor of Engineering, University of Cambridge, London, 'Engineering Applications of Resilient Materials', March 22, 1983.
43. Brondson R. and Remington P., 'Resilient Rail Fasteners and the Control of Elevated Structure Noise', Inter-Noise 80, Miami, Florida, p. 403.
44. Müller H.A.; Opits U. and Volberg G., 'Structureborne Sound Transmission from the Tubes of a Subway into a Building for a Concert Hall', Inter-Noise 80, Miami, Florida, Dec. 8-10, p. 715-718.
45. Towers D.A., 'Estimation and Control of Ground Vibrations from Trains on Concrete Elevated Structures', Inter-Noise Miami, Florida, Dec. 8-10, 1980, p. 399-402.
46. Derham, C.J. and Walker R.A., 'Luxury without Rumble', The Consulting Engineer, Vol. 39, July 1975, p. 49-53.
47. Clayden K.J.C., 'Noise and Vibration Attenuation in the Barbican Scheme, in 'Use of the Rubber in Engineering', by Allen P.W. et al, Maclaren & Sons, London, 1967, p. 204-212.
48. Muller H.A., Muller-BBm; GMBH Schalltechnisches Beratungsburo, 'Elastomers for Vibration Isolation: in Munich', Personal correspondence, March 3, 1983.
49. Derham C.J.; Thomas A.G.; Eidinger J.M. and Kelly J.M., 'Natural Rubber Foundation Bearings for Earthquake Protection: Experimental Results', Rubber Chemistry and Technology, Vol. 53, no. 1, March-April, 1980, p. 186-209.

50. Kelly J.M., 'Aeismoc Base Isolation: Its History and Prospects' World Congress on Joint Sealing and Bearing Systems for Concrete Structures, ACI Publication SP-70, Vol. I, p. 549-586.
51. Mckeel W.T. Jr. and Kinnier H.L., 'Dynamic Stress Study of Composite - Span Bridge with Conventional and Elastomeric Bearings', Highway Research Record no. 354, 1971, p. 13-26.
52. Grote Jupp, 'Over 20 years of Elastomeric Bearings without trouble: A Scheme for Safety and Reliability', ACI Publication SP-70, 1982, Vol. II, p. 865-886.
53. Brown R.P., 'Physical Testing of Rubbers', Applied Science Publishers Ltd., London, 1979, p. 82-84; 140-143; 200-211.
54. Zielinski Z.A.; Troitsky M.S.; Pimprikar M.S., 'Bearing Pad Performance Under High Stress', Proc. Society of Engineering Science Annual Meeting, University of Missouri-Rolla, Rolla, Oct. 27-29, 1982, p. 181.
55. Gent A.N., 'Load-deflection Relations and Surface Strain Distributions for Flat Rubber Pads', Proc. of the Rubber in Engineering Conference held at the Institution of Electrical Engineers London, W.C.2, Sept. 26, 1956, p. 25-42.
56. Gent A.N. and Lindley P.B., 'The Compression of Bonded Rubber Blocks', Proc. Inst. Mech. Engrs., Vol. 173, no. 3, p. 111-122.
57. Lindley P.B. 'Engineering Design with Natural Rubber', The Malaysian Rubber Producer's Research Association, Brickendobury, England, 1978.
58. Eggert H.V., 'Vorlesungen über Lager im Bauwesen', Verlag Von Wilhelm Ernst and Sohn Berlin, München, 1980, (In German).

59. Minor J.C. and Egen R.A., 'Elastomeric Bearing Research', National Cooperative Highway Reserach Program Report 109, 1970, p. 2-53.
60. Kimmich E.G., 'General Engineering Properties of Rubber', Chap. 4 in 'Engineering Uses of Rubber', edited by McPherson A.T. and Klemin A., Reinhold Publishing Co. New York, N.Y. 1956, p. 63.
62. Long J.E., 'Bearings in Structural Engineering', Butterworth and Co., Durban, 1974.
63. Lee D.J. 'Recent Experience in the Specification, Design, Installation, and Maintenance of Bridge Bearings', ACI Publication SP-70, Vol. 1, p. 161-175.
64. Union International des Chemins de Fer, 'U.I.C. Code 772R': Code for the Use of Rubber Bearings for Rail Bridges', Jan. 1969.
65. BS DD 47: 1975, 'Draft for Development: Vibration Isolation of Structures by Elastomeric Mountings', British Standards Institution, London.
66. British Standards 5400 (Draft 1982): Steel, Concrete and Composite Bridges: Part 9A - Code of Practice for Design of Bearings: Part 9B - Specifications for Materials, Manufacture and Installation of Bearings', London, 1982.
67. Department of the Environmental, Highways Directorate', Design Requirements for Elastomeric Bridge Bearings', Technical Memorandum (Bridges) No. BE 1/76, Feb. 1976, London.
68. American Association of State Highway and Transportation Officials, 'Standard Specifications for Highway Bridges', 12th edition, Washington, D.C., 1979.

69. American Association of State Highway and Transportation Officials, 'Standard Specification for Laminated Bridge Bearings', AASHTO M251-74, Standard Specifications for Transportation Materials and Methods of Sampling and Testing', 12th edition, Washington, D.C. 1978.
70. Standards Association of Australia, 'Elastomeric Bearings for use in Structures', Australian Standard 1523-1976, Sydney, N.S.W., Australia, 1976.
71. Federal Ministry of Interior, Switzerland, 'Swiss National Roads, Standard Bridge Designs, Section 341 Bearings', Switzerland, 1973.
72. Approval Notices issued by the Institute of Civil Engineering, Berlin, 1975-77.
73. Institut für Bautechnik, Richtlinien für die Zulassungsprüfung von Bewehrten Elastomerlagern, Berlin (1980), (Rules for approval tests for laminated elastomeric bearings), (In German).
74. The Ministry of Shipping and Transport, (Road Wing), Govt. of India, New Delhi, 1978, 'Specifications for Roads and Bridge Works'.
75. Lucas J.W., Federal Department of Public Works, 'Report on Laminated Bridge Bearings', Public Works in Canada, Ottawa, Feb. 1960.
76. Aldridge W.W.; Sestak J.J. and Fears F.K., 'Tests on Five Elastomeric Bridge Bearing Materials', Highway Research Record No. 253, 1967, p. 72-83.
77. Treloar L.R.G., 'The Physics of Rubber Elasticity', Oxford University Press, Oxford, 2nd edition 1958.
78. Lindley P.B., 'A finite - element programme for the plane - strain analysis of rubber', J. of Strain Analysis, Vol. 10, no. 1, 1975, p. 25-31.

79. Salmons J.R., 'Research Needs of the Precast Prestressed Concrete Industry', PCI Journal Vol. 26, no. 6, Nov.-Dec. 1981, p. 2-10.
80. Rivlin R.S. and Saunders D. W., 'Cylindrical Shear Mountings', Trans. Instn. Rubber Indus., 1949, Vol. 24, p. 296.
81. Nachtrab W.B. and Davidson R.L., 'Behavior of Elastomeric Bearing Pads under Simultaneous Compression and Shear Loads', Highway Research Board no. 76, 1964, p. 83-101.
82. Purkiss C.W., 'New Design Parameters for Elastomeric Bridge Bearings: What They Mean in Terms of Performance', World Congress on Joint Sealing and Bearing Systems for Concrete Structures, Niagara Falls, Sept. 1981, p. 379-387.
83. Bartenev G.M. and Zuyev Yu. S., 'Strength and Failure of Visco-elastic Materials', Pergamon Press Ltd., 1968, p. 105-209.
84. Price A.R., 'Abnormal and Eccentric Forces on Elastomeric Bridge Bearings', Transp. Road Research Lab. TRRL Rep. no. 708, 1976, p. 1-33.
85. The Goodyear Tire and Rubber Company, 'Handbook of Molded and Extruded Rubber', Akron, 1959.
86. Roeder, University of Washington, Seattle, 'Design of Elastomeric Bridge Bearings', Personal Report, Sept. 1981, p. 10.
87. Zielinski Z.A.; Troitsky M.S. and Pimprikar M.S., 'Elastomers for Vibration Control in Construction Engineering, Discussion', Proc. Construction Practices and Instrumentation in Geotechnical Engineering, Surat., India, Dec. 20-23, 1982, Vol. 2, p. 1-3.
88. Chaudhari P.R. and Garg A.K., 'Acceptance Criterion for Shear Modulus of Elastomeric Bearings', Indian Concrete Journal, April, 1981, p. 108-111.

89. Newland D.E. and Liquorish A.D., 'Engineering Applications of Resilient Materials', Chap. 12 in 'Elastomers: Criteria for Engineering Design', Edited by Hepburn and Reynolds, Applied Science Publishers Ltd., London, 1979, p. 189-214.
90. Liquorish A.D., 'Structural Resilient Seatings', Soc. Envir. Eng., Symposium on Developments in Resilient Mountings of Civil Engineering Structures, London, 1976. p. 2.
91. Keen W.N., 'Creep of Neoprene in Shear Under Static Conditions; Ten Years', Trans. ASME, Vol. 75, July 1953, p. 891-893.
92. Keen W.N., 'Creep of Neoprene in Shear Under Static Conditions', Trans. ASME Vol. 68, April, 1946, p.237-240.
93. Freakley P.K. and Payne A.R., 'Theory and Practice of Engineering with Rubber', Applied Science Publishers, London, 1978, p. 8-10, 113-119.
94. SAE Draft J952 and U.S. Environmental Protection Agency, Washington, D.C., 'Noise from Construction Equipment', March, 1974.
95. ASTM D575-69, Committee D-11.10, 'Rubber Properties in Compression', 1969.
96. BS 903 Part A15, 1958 (Draft in revision), 'Determination of Creep and Stress Relaxation'.
97. BS 903 Part 4A, 1973, 'Determination of Compression Stress-Strain'.
98. Snowdon J.C., 'Dynamic Mechanical Properties of Rubberlike Materials', Applied Research Laboratory Seminar on Vibration of Damped Structures, Sept. 22-26, 1975, p. 2-7.
99. O'Keefe Edmund, 'Evaluation of Viscoelastic Properties for Use in the Design of Structural Damping', Noise-CON 1979, Indiana 1979, p. 147-152.

100. Kirschner F., 'Noise Reduction at the Source with new Vibration Damping Materials', Noise-CON 73, Washington D.C., Oct. 15-17, 1973, p. 405-407.
101. Jones D.I.G., 'Damping in Noise and Vibration Control', Proc. of the Tecynical Program Noisexpo, National Noise and Vibration Control Conf. Chicago, Illinois, March 14-17, 1977, p. 82-87.
102. Purcell W.E., 'Materials for Noise and Vibration Control', Sound and Vibration, Materials Reference Issue, July 1977, p. 4, 27-28.
103. Nashif A.D., 'Materials for Vibration Control in Engineering', The shock and Vibration Bulletin Part 4, & Bulletin 43, June 1973, Naval Research Laboratory, Washington, D/C/ p. 145-147.
104. Kirschner A., 'Materials for Vibration Damping Control', Inter-Noise 75, Sendai, August 27-29, 1975, p. 499-505.
105. Kyczynska M., 'ODKSZTALCALNOSC GUMOWYCH LOZYSK MOSTOWYCH, (Deformability of Rubber Bridge Bearings)', Arch Inz Ladowej, Vol. 20, No. 4, 1974, p. 729-740.
106. Marsh S.W., 'The Use of Rubber in Heavy Engineering', in Proc. of Rubber in Engineering Conf. London, Sept. 26, 1956, p. 87-90.
107. Henderson A.B., 'Rubber in Heavy Engineering', in Ref. 107.
108. Steffens R.J. 'Discussion on, The use of rubber in heavy engineering, ref. 107, p. 114-115.
109. Bouilly G.K. and Kinder D.F., 'Compressive Behavior of Elastomeric Bridge Bearings', Plastics Rubber Process Appl. Vol. 1, no. 3, Sept. 1981, p. 277-285.

APPENDIX I

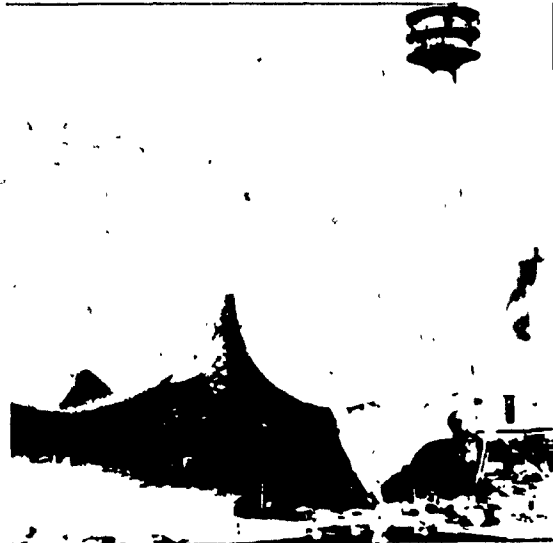
NEOPRENE BEARINGS AT THE BASE OF TOWER STRUCTURE
OLYMPIC STADIUM MONTREAL

1. Description of Structure
2. Function of Neoprene
3. Properties of Neoprene and Details
4. Problems Encountered
5. Research Requirements
6. Recommendations

1. Description of Structure

The Montreal Olympic structure, one of the largest sculptures in the world, Fig. 1, is a huge elliptical bowl married to a triangular based 50-storey 55' high tower leaning almost 175 feet over the stadium field that straddles the swimming pool and diving hall. During 1976 Olympic Games, the stadium seated 59,000 and provided 14,000 standing. Construction of the olympic stadium complex is not just costly, Fig. 2, it is also an experimental laboratory of architectural designs, structural calculations, and material and construction techniques, Fig. 3.

The estimated cost of the Complex, designed by French architect Roger Taillibert, was \$175 million in October 1972, whereas after spending \$825 million the stadium is still roofless and the tower is unfinished. The stadium measures 1580' along the long axis and 580' between supports. The retractable roof of the stadium has the task of covering 18,000 sq. m. The spectacular tower, sloped at a 60 degree angle out over the stadium playing field, meant to be 18 storeys high topped off with a heliport for three helicopters. The tower will have two functions - to support & storage space for the 2mm thick 200 ton Kevlar based fabric woven roof (made in West Germany) over the stadium from a series of 17 cables, and to house several floors of gymnasiums, administrative offices and a tower top revolving restaurant. Considering the huge roof, it was inevitable that the tower had to be very tall, over 522'. Moreover, the top of the tower had to be above the roof as much as possible, so that the opening in the stadium roof was offset from the centre



Design of Olympic Stadium tower in Montreal based on similar concept of Olympic Structure in Munich. (Courtesy of Southam Communications Ltd.).

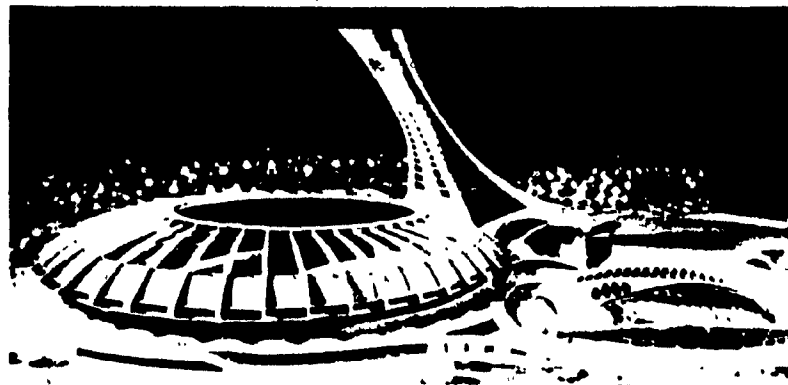


Fig. A1 Model of Olympic Complex (Courtesy of Southam Communications Ltd.).

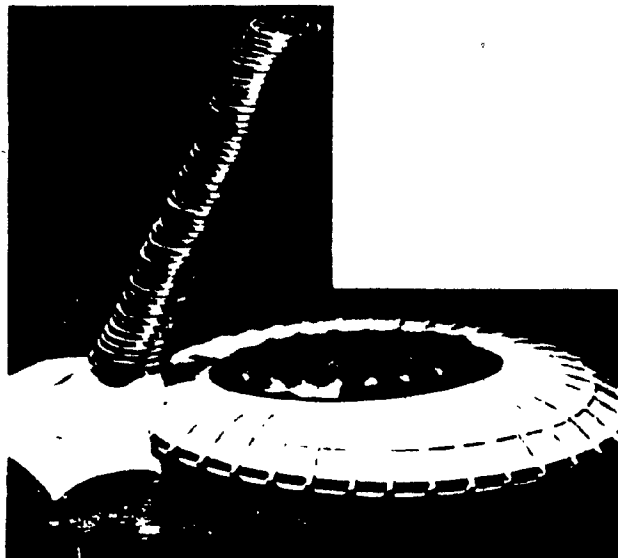


Fig. A2 A photograph showing tower model made of coins (money).

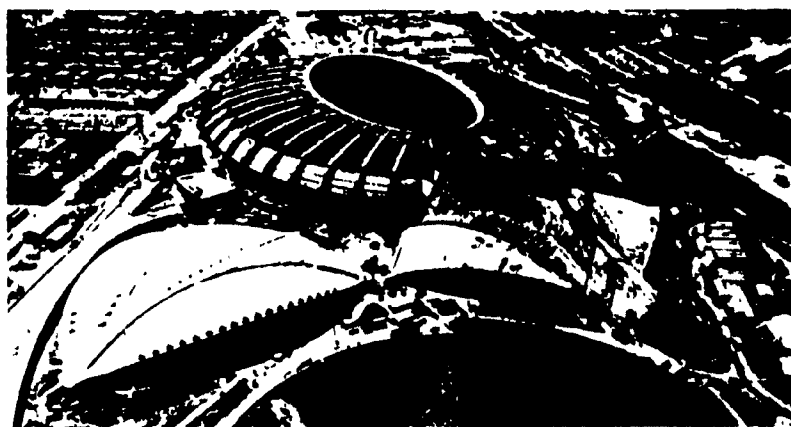


Fig. A3 The Olympic Stadium and tower structure on April 30, 1976.
(Courtesy of Southam Communications Ltd.).

towards the tower while the tower was made to lean towards the opening.

Offsetting the opening makes the stadium asymmetrical and the structural frames at one end different from those at the other. The 60° inclination of the tower requires more steel and concrete merely to hold up the dead weight of the structure. The retractable roof and tower were seen as best choice for climate control for Montreal's future major league games.

The rear leg of the tower is anchored into bedrock by post-tensioning cables whereas the two front legs are resting on neoprene pads. A funicular elevator will ride the tension leg of the tower to a top level restaurant and observation floor at the top. The silhouette of the tower with its lateral shells, give appearance of a modern airplane taking off.

2. Function of Neoprene Bearing Pads

Required Functions

For the prestressed concrete tower structure neoprene bearing pads should be able to permit both the initial prestressing movements and long term movements which could be in the form of translation, rotation or compression. The heavy loads cause high bearing stresses and relatively large rotations and movements at the bearings. Thus, an acceptable neoprene bearing must (1) provide a smooth and uniform transfer of load from tower to substructure (2) permit tower rotation

at the bearing due to deflection of the tower under load (3) allow lateral and longitudinal movements due to thermal and other factors (such as prestressing forces or high concentration of stresses). (Movement between the base of front walls due to emp. shrinkage, other forces is expected to 2 1/2') (4) also, it should be durable, economical and maintenance free.

3. Properties of Neoprene and Details

The neoprene bearings at the base of the tower structure, designed by Dr. Tupallof and fabricated by 'Gummiverk Krabung', are steel laminated types, Fig. 3.1. Details of its installation and arrangement of location are shown in Fig. 3.2.

Properties of Neoprene

Neoprene hardness 60H

size 900 x 900 x 18.5 mm
(Nos. 2 x 36)

E_n = 136500 psi. short-term

= 102300 psi. long-term

G_n = 170 psi. short-term

= 128 psi. long-term

Ultimate strength of neoprene bearings in compression

= 28,000 psi. (2000 kg/cm²)

Present compression stress - 4700 psi.

Maximum compression stress expected - 7000 psi.

4. Problems Encountered

The OIB (Olympic Installation Board), controlled by the Quebec Government, took over construction of the structure in November 1975 when doubts appeared about the completion of the construction work. On October 21, 1977, architect and chairman of Government appointed committee, Mr. Jean-Claude Marsen recommended leaving off the tower and installing an unspecified type of fixed or movable roof or leaving off the roof and the tower, to installing the Taillibert roof with a skeleton tower. Again, during February 1978 and May 1979 schedules and plans were prepared for the tentative completion by Summer 1981. Construction of the first stage five-storey section was underway, while in November 1979 it was reported by OIB president Robert Nelson that the unfinished concrete tower has sunk (settled) by 4'' in the past 3 years because the structure is not rigid enough to be stable without its upper sections. He stated, the mast will be much stronger when it is finished similar to 'in any building, the addition of extra floors stabilizes the structures'. Further, he assured the problem has been solved by installing extra steel cables under tension in the base of the tower.

The construction of the tower was followed till level 283' @ 306' (Feb. 1980), 2355' (Oct. 1980), @ 372' (Dec. 1980), whereas on June 7, 1980 the Minister Responsible for Olympic Installations made a statement that, 'the tower and retractable roof of the Olympic Stadium may never be finished because of serious doubts about the further capability of tower to support further weight'. He said

because of shoddy workmanship and shifting of concrete, the tower will not be able to support the curving tower which Taillibert designed to house sport and office space and to support the retractable parachute roof. This shifting of concrete can change the stress and weight distribution originally calculated by planners.

The work was stopped in December 1980, after engineers noticed hair-line cracks in the tower's concrete base.

The engineers worried that the base might be too weak to support the full weight of the 622' structure and prestressed concrete of the tower.

In August, 1981 Mr. Saulnier, President of the OIB reported the major flaw in the Stadium's tower. The flaw is due to the neoprene pads under the front two legs of the tower, which absorb vibrations and tremors. The pads are under excessive compressive stresses and 'an excessive effort' is being required of the pads according to most of the international codes dealing with neoprene. The tower is currently under a compression of 4700 psi. (French and German codes specify max. pr. of 2140 spi and U.S. specifies 800 psi.).

If no correction measures are taken, the maximum pressure expected when the tower is completed would be 7000 psi, according to a study prepared by consultants with JBEC (James Bay Energy Corporation). A recent inspection of the foundation found that 'the pads have bulges at the observable edges which indicate overstress or ruptures in the neoprene.

TABLE AI TOTAL LOADINGS AT TOWER BASE AT VARIOUS CONSTRUCTION STAGES

Tower Const. Stage	Elevation ft.	Loading Elevation		Reactions at front legs R_1 Fig. 4	From Tower R Fig. 4	At Fixed R_2 Fig. 4
		D.L.	L.L.			
Feb. 1980	322'	322'	-	2 x 5500 k	not available	
Present	411'	411'	-	2-x 82300 k	174900 k	10300 k
Complete (estimated)	622'	622'	237'- + 622' moveable roof	L x 122200 k	321900 k	77500 k

The JBEC study reported that 'the Olympic Stadium will become a short-term disaster unless work is undertaken to strengthen the overall structure of the stadium. The neoprene pads along the base of the tower can no longer adequately distribute the weight above them.

Though there is no immediate danger of a collapse, the tower cannot be left as it is. The consultants estimate \$21 million to correct the engineering faults discovered so far.

As superior Court Judge Albert Malouf concluded in an enquiry in 1980, Taillibert's Stadium 'was extremely complex both from points of view. of design and from that of construction'.

The research was initiated at the structure's laboratory of Concordia University to study the behavior of neoprene pads under excessive compressive stresses exceeding North American and European engineering norms.

Suggested Alternatives & Recommendations

- (1) Feasibility of building a permanent roof made of light-weight metal or some type of membrane.
- (2) A central pillar to be constructed at a cost of \$4.5 million to correct the tower problem.
- (3) The base could be strengthened by stretching steel cables underneath the internal shifting of concrete poured in 1976. The building supposed to go on top should be scrapped.
- (4) OIB's plans & analysis revealed (after double checking) that rather than one or two cables capable of holding 7000 tons as OIB had planned to use, what was needed was a single 'mega-cable' able to hold 23,000 tons - and there was nowhere to put it.
- (5) Providing an exterior support in the form of elevator leading up to an observation deck and a roof top restaurant.
- (6) Reinforcing the tower front wall either by
 - (a) means of prestressing
 - (b) providing an extra support for the front wall, Fig. 4.

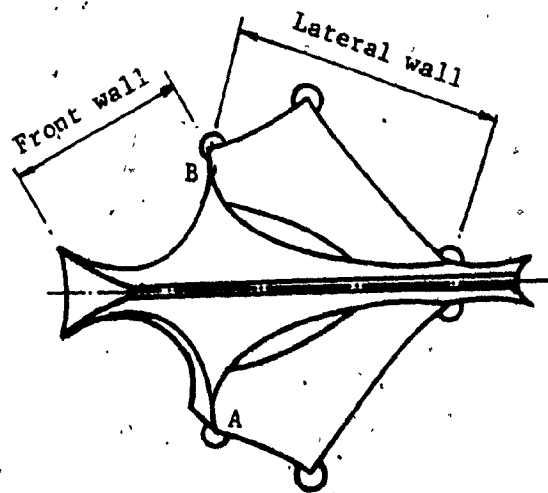
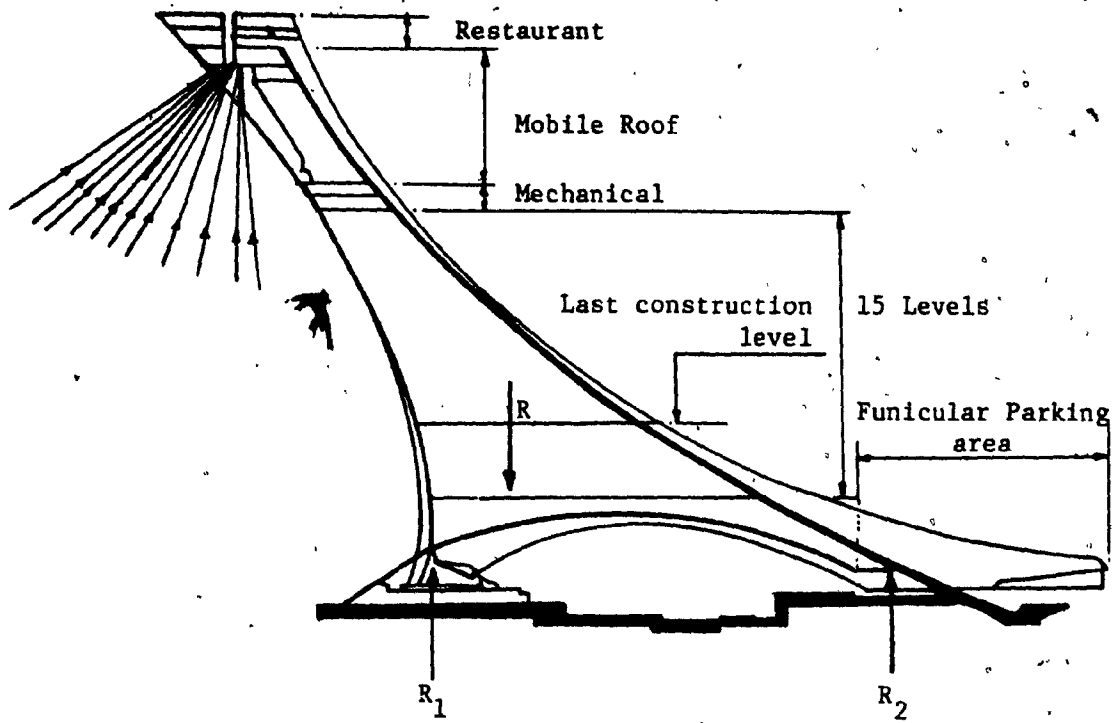


Fig. A4 Plan and cross-sectional view of tower with loadings and reactions.

REFERENCES (APPENDIX I)

1. Malouf, 'Raport de la Commission d'enquête sur le cout de la 21^e Olympiade, Vol. 1, 2, 3, 4, 1980.
2. Harris L., 'Big 'O' needs repairs costing \$21 million: Expert', the Montreal Gazette, Octo. 28, 1981, p. 4.
3. Anon., 'What to to about cursed Olympic Stadium', Toronto Star, Oct. 24, 1981, p. B1.
4. Gerard W., 'A tilt to Folly, Macleans, Vol. 94, August 24, 1981, p. 18.
5. Malarek V., 'Major Flaw in Tower Undermines OlympicRoof', The Globe & Mail, August 7, 1981, p. 2.
6. Anon., 'Hopes for Stadium roof dim as new flaws found', The Montreal Gazette, June 13, 1981, p. 3.
7. Anon., 'Insurance Cancelled on Big 'O' Tower', The Montreal Gazette, Apr. 3, 1981, p. 3.
8. Anon., 'Saulnier wants tower, roof put on Stadium as planned', The Montreal Gazette, Feb. 2, 1981, p. 3.
9. Laughlin A., 'Big O may stay roofless', The Montreal Gazette, June 7, 1980, p. 1-2.
10. OIB, 'Stadium mast sinks 4 inches: It's common, Officials say', The Montreal Gazette, Nov. 3, 1982, p. 1.
11. Anon., 'Roof to go ahead at Olympic Stadium', The Globe and Mail, June 21, 1979, p. A9.
12. Low R., 'Olympic roof on the way', The Montreal Star, May 5, 1979, p. A1.

13. Anon., 'Stadium roof delayed a year', The Montreal Star, Feb. 11, 1978, p. A1.
14. Low R., 'Committee Split on Original Design...', The Montreal Star, Oct. 22, 1977, p. A3.
15. Anon., 'Olympic Stadium roof issue bounces back to OIB...', The Montreal Star, Oct. 21, 1977, p. A1.
16. Dunsen M.V., 'Stadium, Velodrome cast in Concrete', The Financial Post, Vol. 70, May 15, 1976, p. S12.
17. Sandori P., 'Olympic Complex: Structural Development', The Canadian Architect, Sept. 1976, p. 56-60.
18. Flaga K. and Bogoria S.J., 'Genese et developpement de la conception de installations sprotives projetées jeux Olympiques de Montreal par Roger Taillibert', Proc. IASS World Congress on Space Enclosures, July 4-9, 1976, Concordia University, Montreal, p. 1037-1047.
19. Stueren D.L.G. and Wardle M.W., 'Advanced High Specific Strength Materials for Space Enclosures', Proc. IASS World Congress on Space Enclosures, Montreal, July 4-9, 1976, p. 955-960.
20. Hix John, 'Olympic Complex...' The Canadian Architect, Sept. 1976, p. 45-55.

APPENDIX IIStiffness and Critical Load

The load deflection behavior of elastomers under high compression where deviations from linearity of load-comp. curves are observed (or strains greater than 10%) is given by (128)

$$F = AE_0 \left[\ln \frac{1}{(1-e)} + KS^2 \left(\frac{1}{(1-e)} - 1 \right) \right]$$

The compressive stiffness of an elastomeric bearing is

$$K_c = \frac{F_c}{\delta_c}$$

the shear stiffness

$$K_s = \frac{F_s}{\delta_s}$$

and rotation stiffness

$$K_r = \frac{M}{\alpha}$$

Thus, the vertical stiffness

$$\frac{1}{K_v} = \frac{\delta_v}{V} = \sum \frac{1}{K_c}$$

The critical load at which buckling occurs is (58)

$$V_{cr} = \frac{K_s \beta}{2\eta} \left[\sqrt{1 + \frac{4\pi^2}{t\beta^2} \frac{K_r}{K_s}} - 1 \right]$$

and corresponding deflection at

$$\text{buckling } \frac{V_{cr}}{K_v}$$

the complete basic design formulae are given in Ref. (82).

Fig. III.1 (a) Typical Stepped type loading by means of releasing screw jack (Neoprene under 800 psi.).

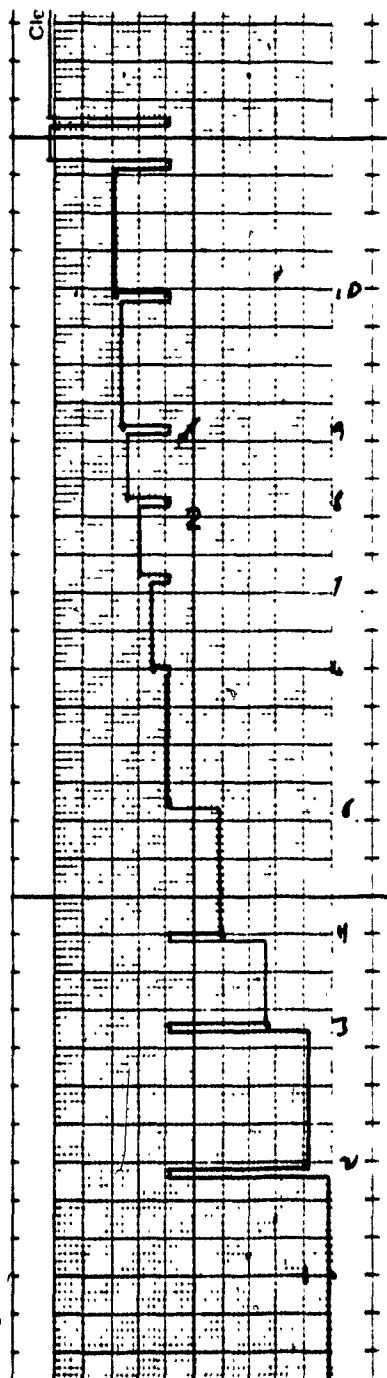


Fig. III.1 (b) Typical Stepped type loading by means of releasing screw jack. (Neoprene under 800 psi.) (Less loading time).

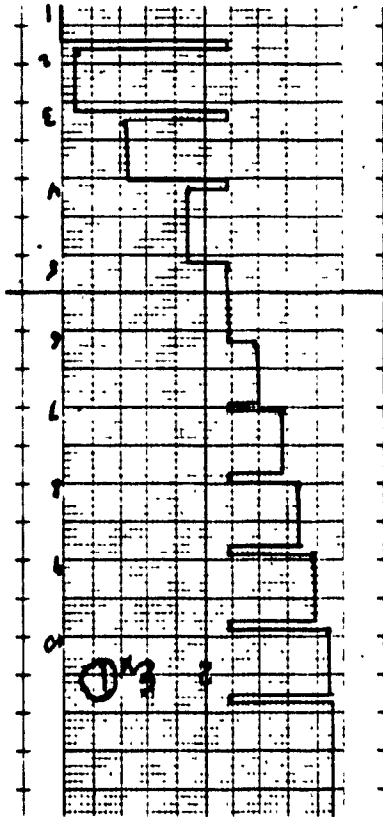
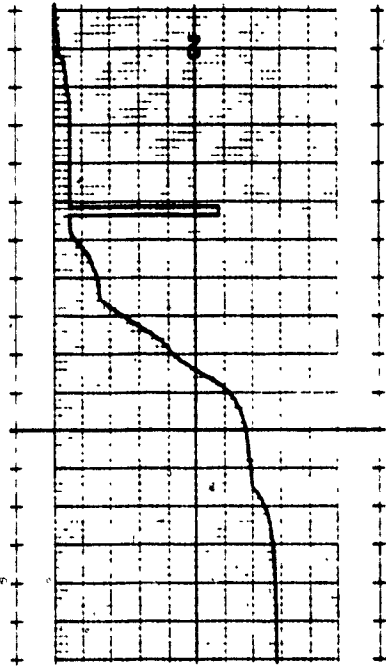


Fig. III.1 (c) Impact loading by means of releasing hydraulic jack. (Suddenly). (Neoprene under 100 psi).



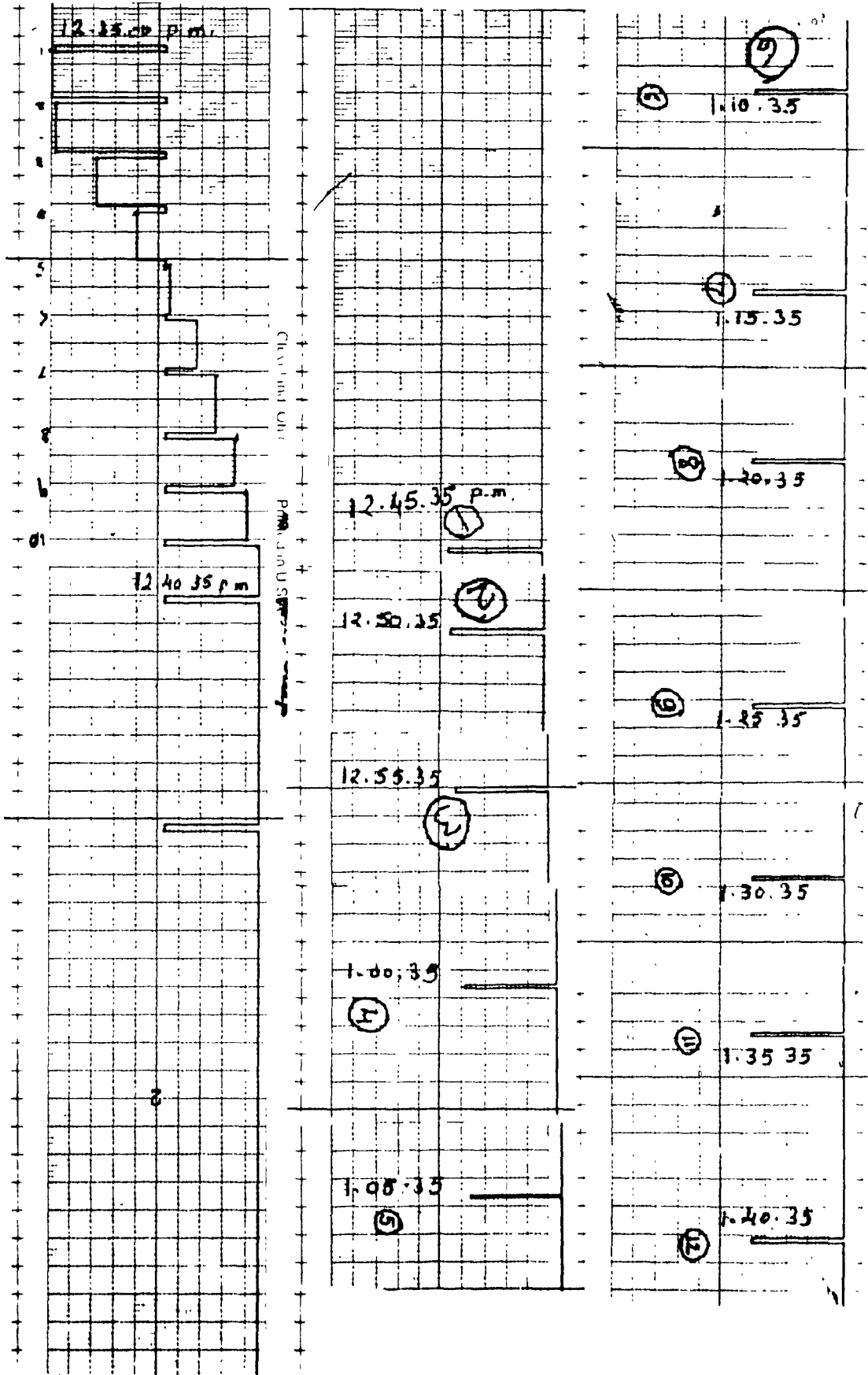


Fig. III.2 Typical compressive creep measurement for first 5 minutes and one hour [Neoprene under 800 psi].

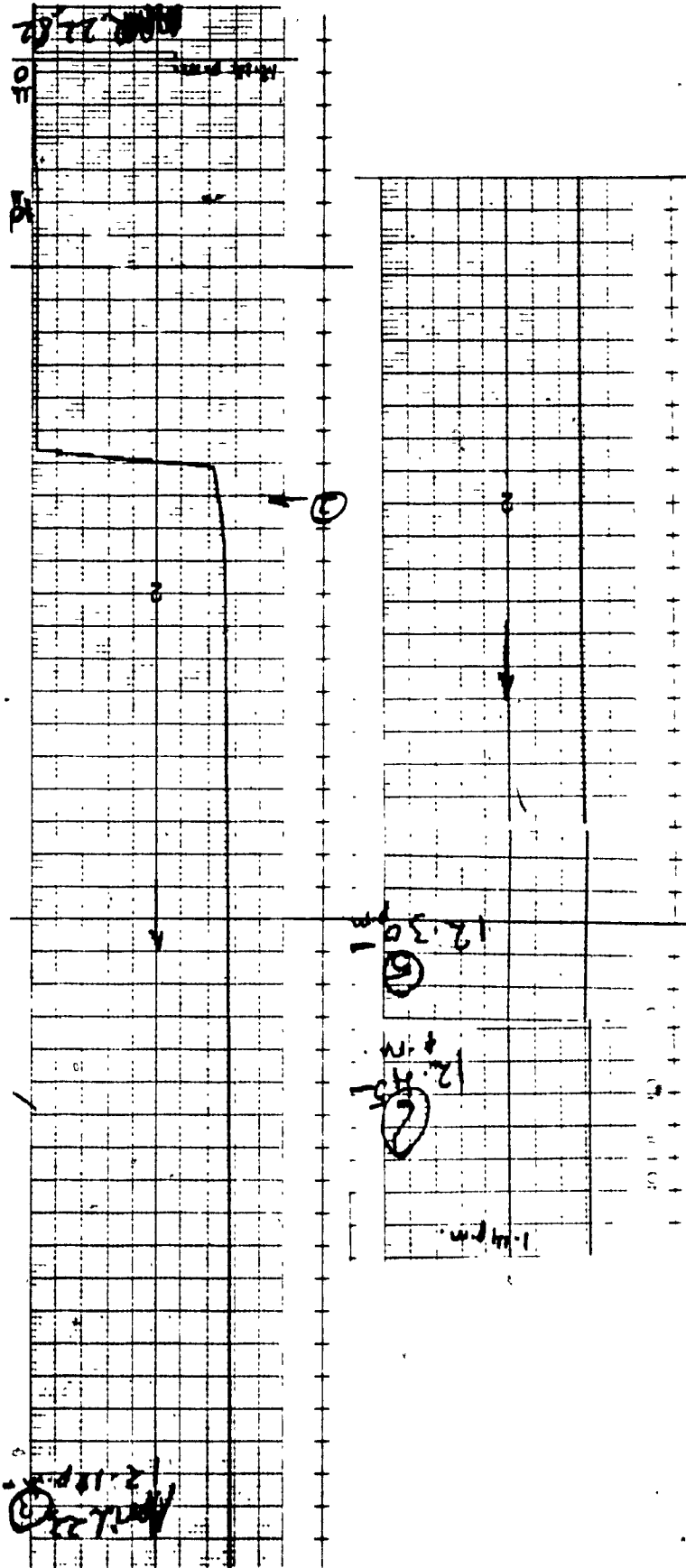


Fig. III.2 Typical compressive creep measurement for first 5 minutes and one hour period (500 psi).

Fig. III.3 Typical output of strain gage measurements from data acquisition system (Neoprene under 800 psi).

1933	05	-4225	4		
1933	04	-4224	4		
1938	03	+1634	4		
1938	02	+1628	4		
1938	01	-0021	0	6	
1938	00	-0351	0		
1938	09	-4223	4		
1938	08	-4223	4		
1938	07	-4223	4		
1938	06	-4224	4		
1938	05	-4224	4		
1938	04	-4223	4		
1938	03	+1634	4		
1938	02	+1623	4		
1940	01	-0019	0	5	
1938	00	-0293	0		
1937	09	-4225	4		
1937	08	-4225	4		
1937	07	-4225	4		
1937	06	-4225	4		
1937	05	-4225	4		
1937	04	-4225	4		
1937	03	+1635	4		
1937	02	+1630	4	4	
1937	01	-0019	0		
1937	00	-0208	0		
1936	09	-4223	4		
1936	08	-4223	4		
1936	07	-4223	4		
1936	06	-4224	4		
1936	05	-4224	4		
1936	04	-4224	4		
1936	03	+1634	4		
1936	02	+1630	4		
1936	01	-0020	0	3	
1936	00	-0115	0		
1935	09	-4225	4		
1935	08	-4225	4		
1935	07	-4225	4		
1935	06	-4225	4		
1935	05	-4226	4		
1935	04	-4225	4		
1935	03	+1635	4		
1935	02	+1631	4		
1935	01	-0019	0	2	
1935	00	-0018	0		
1934	09	-4226	4		
1934	08	-4226	4		
1934	07	-4226	4		
1934	06	-4226	4		
1934	05	-4226	4		
1934	04	-4226	4		
1934	03	+1637	4		
1934	02	+1633	4		
1934	01	-0019	0		
1934	00	-0010	0		
1941	09	-4225	4		
1941	08	-4225	4		
1941	07	-4225	4		
1941	06	-4225	4		
1941	05	-4225	4		
1941	04	-4225	4		
1941	03	+1633	4		
1941	02	+1629	4		
1941	01	-0020	0	10	
1941	00	-0483	0		
1940	09	-4225	4		
1940	08	-4225	4		
1940	07	-4225	4		
1940	06	-4226	4		
1940	05	-4226	4		
1940	04	-4226	4		
1940	03	+1634	4		
1940	02	+1630	4		
1940	01	-0020	0	9	
1940	00	-0456	0		
1940	09	-4224	4		
1940	08	-4225	4		
1940	07	-4225	4		
1940	06	-4224	4		
1940	05	-4225	4		
1940	04	-4224	4		
1940	03	+1633	4		
1940	02	+1629	4		
1940	01	-0019	0	8	
1940	00	-0482	0		
1939	09	-4224	4		
1939	08	-4224	4		
1939	07	-4224	4		
1939	06	-4224	4		
1939	05	-4224	4		
1939	04	-4223	4		
1939	03	+1633	4		
1939	02	+1623	4		
1939	01	-0019	0	7	
1939	00	-0394	0		
1938	09	-4225	4		
1938	08	-4225	4		
1938	07	-4225	4		
1938	06	-4224	4		

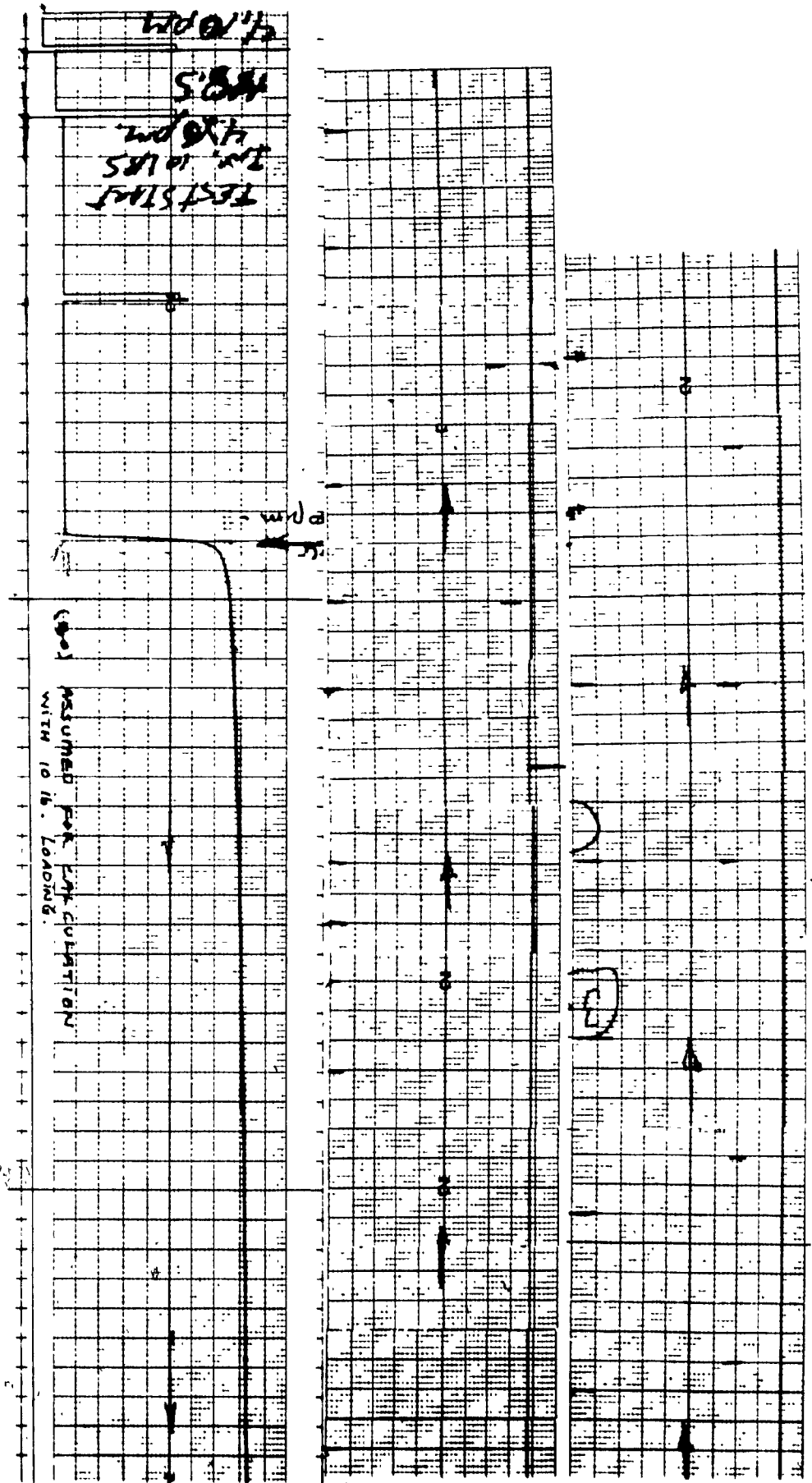


Fig. III. 4 Illustration of assumed initial deflection with a typical creep record for 5 days of test period to verify existing du-Pont curve (500 psi).